Antal Kerpely Doctoral School of Materials Science and Technology

Compatibility and Structure-Property Relationships in Poly(vinyl chloride), Thermoplastic Polyurethane, and Bio-Plasticizer Blend Systems

PhD Dissertation

By

Yitbarek Firew Minale

Supervisors:

Prof. Dr. Kálmán Marossy

Prof. Dr. Major Andrea

Head of the Doctoral School

Prof. Dr. Valéria Mertinger, DSc

Institute of Energy, Ceramics, and Polymer Technology

Faculty of Materials and Chemical Engineering

University of Miskolc

Hungary, 2026

"Through faith we understand that the worlds were framed by the word of God, so that things which are seen were not made of things which do appear."

Hebrews 11:3

Acknowledgment

I would like to express my sincere and heartfelt gratitude to my supervisor, Prof. Dr. Kálmán Marossy, for his intellectual and scientific guidance, continuous encouragement, kindness, and unwavering support throughout my PhD journey. His extensive experience, cooperative nature, and thoughtful mentorship greatly contributed to this research work. Beyond being a supervisor, he has been a truly kind and supportive mentor whose guidance made this journey smoother and more meaningful. I am also grateful to my co-supervisor, Prof. Dr. Andrea Major, for her support, encouragement, and valuable guidance throughout this research. My special thanks also go to Assoc. Prof. Dr. Tamás Szabó for his continuous support, technical guidance, encouragement, and cooperation throughout my study. His valuable assistance, insightful discussions, and mentorship greatly contributed to both this research work and my academic development.

I would like to thank the staff and members of the Department of Polymer Engineering, especially Dr. Anna Sycheva, Annamaria Polyákné Kovács, and Ildiko Tasnadi, for their kindness, technical assistance, and the supportive working environment they provided throughout my study. I would also like to express my sincere appreciation to Assoc. Prof. Dr. Mariann Kollár for her constructive feedback and valuable comments during my semester research seminars throughout the study period. I am sincerely grateful to Assoc. Prof. Dr. Ivan Gajdos from the Technical University of Kosice, Slovakia, for hosting me several times as a visiting PhD student through exchange and mobility programs, during which thermogravimetric and some mechanical measurements were conducted. His support and collaboration are highly appreciated. I would also like to thank Solczi Ágnes, Stumpf Éva, and Ledniczky Virág for their kindness, administrative assistance, and help throughout my studies. My sincere appreciation also goes to Prof. Dr. Helga Kovács and Prof. Dr. Péter Baumli for their support during my study, especially in facilitating mobility opportunities that significantly contributed to this research experience.

Finally, I would like to express my deepest gratitude and love to my family for their prayers, unconditional love, encouragement, patience, and unwavering support throughout my academic journey.

Yitbarek Firew Minale

Miskolc, 2026

Supervisor's Recommendation

As supervisor, I would like to introduce Mr. Yitbarek Firew Minale in detail and recommend him with the greatest professional conviction for the purpose of obtaining his doctoral degree. Mr. Yitbarek Firew Minale obtained his MSc degree at the University of Miskolc and stood out for his wide-ranging interests.

His doctoral research focuses on ternary polymer blends, which are a novel, dynamically developing group of materials in polymer technology. However, the development of these materials is largely based on experience.

He developed his research plan in a complex and logical manner, in which the investigation of structure-property-processing relationships was given a prominent role.

He mastered several testing techniques and conducted his own tests. He often assisted with other departmental tasks to improve his knowledge. I must emphasize that he contributed to the teaching activities of the department and established a particularly good relationship with MSc and PhD students.

Mr. Yitbarek Firew Minale is able to prepare scientific articles independently and efficiently. He has exceeded the doctoral school's requirements and demonstrated a strong ability to publish scientific results in peer-reviewed journals.

I find it particularly valuable that he easily found potential cooperation partners and independently built research relationships, even across national borders. These relationships also resulted in valuable publications.

Based on his personality, professional preparation, and work ethic, I am convinced that he will continue to be of significant value in both academia and industry after obtaining his doctoral degree. His scientific and teaching career could be decisive in the field of polymer technology and materials science in the long term.

In all, his overall achievements can be highly valued; he has met the requirements of the Antal Kerpely Doctoral School of Materials Science and Technology. I wish him to achieve his goals for both the successful completion of his doctoral studies and the realization of his dreams in his future scientific and personal life.

Dr. Kálmán Marossy

Professor Emeritus

Miskolc, 14th June 2026

Declaration

During the preparation of the thesis, I did not use the services of artificial intelligence, except for grammatical and stylistic corrections.

Yitbarek Firew Minale

Contents

List of Figures

List of tables

List of Abbreviations

CED	Cohesive Energy Density
DMA	Dynamic Mechanical Analysis
DSC	Differential Scanning Calorimetry
DTG	Derivative Thermogravimetry
DIDP	Diisodecyl phthalate
DEHP	Di(2-ethylhexyl) phthalate
FTIR	Fourier Transform Infrared Spectroscopy
HCl	Hydrogen Chloride
PVC	Poly(vinyl chloride)
SEM	Scanning Electron Microscopy
TGA	Thermogravimetric Analysis
T_g	Glass Transition Temperature
TPU	Thermoplastic Polyurethane
TSD	Thermally Stimulated Discharge
WCO	Waste Cooking Oil
$\Delta\delta$	Difference in Solubility Parameter
ΔE_v	Molar Energy of Vaporization
ΔG	Gibbs Free Energy of Mixing
ΔH	Enthalpy of Mixing
ΔS	Entropy of Mixing
δ	Solubility Parameter
ϕ	Volume Fraction
T	Absolute Temperature

1. Introduction and Literature Review

1.1. Introduction

Polymer blending has become one of the most widely adopted approaches for developing materials with tailored and enhanced properties by combining existing polymers with complementary properties [1, 2]. Compared with synthesizing entirely new polymers, blending offers a more cost-effective and time-efficient strategy while utilizing already established processing technologies and industrial infrastructure [3-5]. Through appropriate selection of blend components and composition, polymer blends can provide improved combinations of mechanical strength, flexibility, toughness, thermal stability, chemical resistance, and processability that are often difficult to achieve using a single polymer alone. Consequently, polymer blends have gained considerable importance in applications such as automotive components, construction materials, packaging, medical devices, smart textiles, and consumer products [6-9].

Among commercially important thermoplastics, poly(vinyl chloride) (PVC) remains one of the most extensively used polymers because of its low cost, chemical resistance, flame retardancy, mechanical strength, and processing versatility [10, 11]. However, despite these advantages, PVC exhibits inherent rigidity, brittleness, and limited thermal stability, which restrict its application in products requiring flexibility and elasticity [12]. For this reason, PVC is commonly modified through plasticization or blending with more flexible polymers [10, 13].

Conventional plasticization of PVC relies predominantly on phthalate-based plasticizers because of their high efficiency and low cost [14, 15]. Nevertheless, increasing concern regarding the migration, toxicity, and environmental impact of phthalates has intensified the search for safer and more sustainable alternatives. In recent years, bio-based plasticizers derived from renewable or waste resources have emerged as promising candidates for replacing conventional petroleum-based plasticizers while reducing environmental impact [16].

Thermoplastic polyurethane (TPU), on the other hand, is an elastomeric thermoplastic polymer characterized by excellent elasticity, toughness, abrasion resistance, and favourable thermal performance [17, 18]. Due to its segmented structure consisting of soft and hard domains, TPU exhibits a unique combination of elasticity and mechanical durability [18, 19]. However, TPU is substantially more expensive than PVC, which limits its use in high-volume and cost-sensitive

applications [20]. Blending PVC with TPU therefore offers a practical route for combining the rigidity and cost-effectiveness of PVC with the elasticity and toughness of TPU, thereby enabling the development of materials with balanced properties while reducing reliance on higher-cost elastomeric systems.

At the same time, increasing environmental concerns and sustainability requirements have stimulated growing interest in bio-based additives derived from renewable or waste feedstocks [21]. Among these, glycerol diacetate monolaurate derived from waste cooking oil (WCO) represents a particularly attractive alternative because it simultaneously addresses plasticizer sustainability and waste valorisation within a circular-economy framework [22].

Despite the promising potential of PVC/TPU/bio-plasticizer systems, the final performance of these polymer blends depends strongly on compatibility between the constituent components. Compatibility governs intermolecular interactions, molecular mobility, phase morphology, stress transfer, and ultimately the mechanical and thermal behaviour of the material [23]. Since most polymer systems are thermodynamically immiscible, predicting and evaluating compatibility remains one of the central challenges in polymer blend design [24].

Thermodynamic compatibility can be estimated using solubility parameter concepts, while swelling-based analysis provides an effective indirect approach for predicting compatibility prior to processing [25]. However, thermodynamic prediction alone cannot fully guarantee compatibility in polymer systems, making complementary post-processing analyses necessary for evaluating intermolecular interactions, molecular mobility, relaxation behaviour, and phase morphology. Among the available characterization techniques, thermally stimulated discharge (TSD) analysis offers high sensitivity toward localized molecular mobility and dipolar relaxation processes, making it particularly useful for investigating intermolecular interactions and phase heterogeneity in polymer blends [26, 27].

Although previous studies have separately investigated PVC/plasticizer, PVC/polyurethane blends, and bio-based plasticizers, comprehensive investigation of ternary PVC, TPU, and bio-plasticizer systems remains limited. In particular, the integration of thermodynamic compatibility prediction using swelling-based solubility parameter analysis with complementary post-processing relaxation, spectroscopic, morphological, mechanical, and thermal analyses has not been comprehensively investigated. Furthermore, limited attention has been given to glycerol diacetate

monolaurate derived from waste cooking oil as a sustainable plasticizer in PVC/TPU blend systems.

Therefore, this study focuses on the development and investigation of sustainable PVC/TPU/bio-plasticizer blend systems using glycerol diacetate monolaurate derived from waste cooking oil. The study integrates thermodynamic compatibility prediction with comprehensive experimental validation in order to establish relationships among intermolecular interactions, molecular mobility, phase morphology, mechanical behaviour, and thermal stability. By combining the complementary properties of PVC and TPU while reducing dependence on conventional phthalate plasticizers, this study aims to contribute toward the development of flexible, thermally balanced, and more sustainable PVC-based polymer systems.

1.2.Polymer Blends

Polymer blending is a widely used approach for designing and producing materials with tailored and enhanced properties through the combination of existing polymers [28, 29]. In recent decades, polymer research has increasingly focused on blending strategies rather than the synthesis of entirely new polymers, owing to the ability of polymer blends to efficiently satisfy technological requirements while reducing development time, production cost, and financial risk. Furthermore, polymer blending utilizes already established processing technologies and industrial infrastructure, making it an economically attractive route for the development of advanced polymeric materials [1, 30, 31].

Polymer blends can provide combinations of properties that are difficult to achieve using individual polymers alone. By controlling blend composition, intermolecular interactions, and phase morphology, materials with improved mechanical strength, elasticity, flexibility, thermal stability, and chemical resistance can be produced. Consequently, polymer blends have found widespread applications in automotive, construction, packaging, medical, electrical, and textile industries [6-9].

Despite these advantages, the major challenge in polymer blending is the inherently low miscibility of most polymer systems [24]. Because high-molecular-weight polymers possess very low entropy of mixing, many blends undergo partial or complete phase separation, resulting in heterogeneous morphologies that strongly influence molecular mobility, mechanical performance, thermal

behaviour, and long-term stability [32, 33]. Therefore, understanding and controlling compatibility is essential for establishing desirable structure-property relationships in polymer blends, since compatibility directly governs intermolecular interactions, phase morphology, and stress transfer between blend components [34, 35].

1.3. General Properties of PVC, TPU, and Plasticizers

1.3.1. Poly(vinyl chloride) (PVC)

Poly(vinyl chloride) (PVC) is one of the most widely used thermoplastic polymers due to its versatility, chemical resistance, flame retardancy, ease of processing, and relatively low cost [10, 11]. Structurally, PVC consists of repeating chlorinated hydrocarbon units, where the presence of polar carbon–chlorine bonds strongly influences its intermolecular interactions, molecular mobility, and physical properties (Figure 1). Industrially produced PVC is predominantly atactic, although it typically contains a few percent of syndiotactic sequences of varying length. The stereochemical arrangement of the chlorine substituents influences chain packing and intermolecular interactions and contributes to the characteristic structural organization of PVC. In addition to its chemical structure, PVC exhibits a unique supramolecular structure arising from strong dipole-dipole interactions between the polar C–Cl groups. These interactions promote local ordering and the formation of supramolecular associations, which significantly influence the molecular mobility, relaxation behaviour, thermal transitions, plasticization behaviour, and mechanical properties of PVC. Consequently, PVC exhibits high mechanical strength, rigidity, dimensional stability, and resistance to acids, oils, and many chemicals, making it widely utilized in construction, transportation, electrical insulation, flooring, piping, and numerous industrial applications [10, 36-38].

Despite these advantages, unplasticized PVC is inherently rigid and brittle, exhibiting limited elasticity, poor impact resistance, and relatively low thermal stability [12, 39]. Upon heating, PVC undergoes dehydrochlorination, resulting in the release of hydrogen chloride and the formation of conjugated polyene sequences that accelerate thermal degradation [40-42]. These limitations restrict its direct use in applications requiring flexibility, toughness, or prolonged thermal resistance [43, 44]. Consequently, plasticizers are commonly incorporated to increase chain mobility and improve flexibility and processability, thereby transforming rigid PVC into soft and

flexible materials suitable for films, tubing, cable insulation, medical devices, and flexible coatings [45, 46].

The broad tunability of PVC through formulation and plasticization also makes it an important matrix polymer for polymer blending systems. In particular, polymer blending provides an effective strategy for improving flexibility, toughness, and thermal/mechanical performance while retaining the advantageous properties of PVC. Due to its polarity, processability, and formulation versatility, PVC has become an important base polymer for the development of flexible and functional blend systems [10, 47].

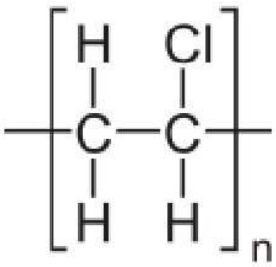

Figure 1. Repeating unit structure of poly(vinyl chloride) (PVC).

1.3.2. Thermoplastic Polyurethane (TPU)

Thermoplastic polyurethane (TPU) is an elastomeric engineering thermoplastic widely used due to its high elasticity, toughness, abrasion resistance, chemical resistance, and favourable thermal performance [48, 49]. TPU is typically synthesized through the reaction of diisocyanates with polyols in the presence of chain extenders, producing linear polymers containing repeating urethane linkages together with ester, ether, or urea groups depending on the formulation. To obtain linear thermoplastic polyurethanes, the reactants must be predominantly bifunctional; the use of polyfunctional isocyanates or polyols can lead to branching and crosslinking, resulting in thermoset rather than thermoplastic polyurethane structures [50, 51].

TPU has a segmented block-copolymer structure consisting of alternating soft and hard segments covalently bonded within the polymer chain. The soft segments are generally long, flexible, and relatively low in polarity, contributing elasticity and chain mobility, whereas the shorter hard segments are more polar and provide mechanical strength, rigidity, and thermal resistance aa [48, 49]. Due to the polarity difference between these segments, TPU commonly exhibits microphase-

separated morphologies stabilized by intermolecular interactions, particularly hydrogen bonding between urethane groups [18, 19].

The unique combination of elasticity and mechanical strength makes TPU attractive for applications including coatings, films, cables, medical devices, automotive components, and flexible engineering materials [52]. In polymer blending systems, TPU is frequently incorporated to improve flexibility, toughness, and impact resistance [34]. However, the segmented structure and phase behaviour of TPU strongly influence its compatibility with other polymers, making intermolecular interactions, molecular mobility, and phase morphology critical factors governing the final properties of TPU-containing blends [35].

1.3.3. Plasticization and Conventional Plasticizers

Plasticizers are additives used to improve the flexibility, softness, toughness, and processability of polymers, particularly rigid polymers such as PVC. Plasticization occurs through the reduction of intermolecular forces within the polymer matrix, resulting in increased chain mobility and reduced glass transition temperature (T_g). Consequently, the polymer becomes softer, more flexible, and easier to process under thermal and mechanical conditions [53, 54]. During this process, plasticizer molecules position themselves between polymer chains, increasing intermolecular spacing and reducing chain-chain interactions [46, 55, 56].

In polymer blend systems, plasticizers may also contribute to improved compatibility by reducing interfacial tension and facilitating intermolecular interactions between blend components. This effect is particularly important in PVC-based blends, where differences in molecular structure and polarity may promote phase separation and poor dispersion. Therefore, plasticization influences not only flexibility and processability but also phase morphology, molecular mobility, and overall blend integrity [57].

1.3.4. Environmental and Health Risks of Phthalates

Despite their high plasticization efficiency and widespread industrial use, phthalate-based plasticizers have become a major environmental and public health concern [58, 59]. Since phthalates are physically incorporated rather than chemically bonded to the polymer matrix, they can migrate or leach from plastic products during service conditions, particularly under heat, pressure, or mechanical stress [15, 60-62]. This behaviour is especially problematic in applications

such as food packaging, medical devices, toys, flooring, and other consumer products associated with frequent human exposure [63, 64].

Several commonly used phthalates, including di(2-ethylhexyl) phthalate (DEHP), dibutyl phthalate (DBP), and benzyl butyl phthalate (BBP), have been identified as endocrine-disrupting chemicals (EDCs) and have been associated with reproductive toxicity, hormonal imbalance, liver damage, and other adverse health effects [65-67]. In addition, the release of phthalates into the environment contributes to long-term contamination of soil, water, and ecosystems due to their widespread use and limited biodegradability. These concerns have resulted in increasing regulatory restrictions on high-risk phthalates by organizations such as the European Union through REACH regulations and the United States Environmental Protection Agency (EPA) [68, 69].

Although phthalates continue to dominate the plasticizer market because of their low cost and high plasticization efficiency, growing concern regarding their environmental persistence and potential toxicity has intensified the search for safer and more sustainable plasticizer alternatives [14, 70].

1.3.5. Bio-Based Plasticizers and Glycerol Diacetate Monolaurate

In response to the environmental and health concerns associated with conventional phthalate plasticizers, increasing attention has been directed toward bio-based plasticizers derived from renewable, biodegradable, and waste-based resources. These materials aim to provide the flexibility and processing advantages of conventional plasticizers while reducing toxicity, migration, and environmental impact [53, 71, 72].

Among the various renewable feedstocks investigated, waste cooking oil (WCO) has emerged as a particularly attractive raw material due to its abundance and limited current utilization. Globally, approximately 15 million tons of WCO are generated annually, with more than 60% of which is improperly discarded, contributing to environmental pollution and ecological damage [73-75]. The utilization of WCO for the production of bio-based plasticizers therefore aligns with circular economy principles by simultaneously addressing waste management challenges and reducing dependence on non-renewable petrochemical resources [76, 77].

One promising bio-based plasticizer derived from WCO is glycerol diacetate monolaurate, which is synthesized through a transesterification process [22]. The molecular structure of glycerol

diacetate monolaurate is shown in Figure 2. Similar to conventional plasticizers, glycerol diacetate monolaurate functions by positioning itself between polymer chains, thereby increasing free volume and molecular mobility while reducing intermolecular interactions and glass transition temperature [78].

Compared with conventional phthalates, glycerol diacetate monolaurate exhibits lower migration tendency together with improved environmental and toxicological characteristics, making it a promising candidate for applications involving medical devices, food-contact materials, and environmentally friendly polymer products. In addition to its functional performance, the use of WCO-derived plasticizers contributes to sustainable materials development through valorisation of waste resources and reduction of environmental burden [22]. While they offer advantages in terms of reduced toxicity and environmental impact, their performance depends strongly on their compatibility with the base polymer [79, 80].

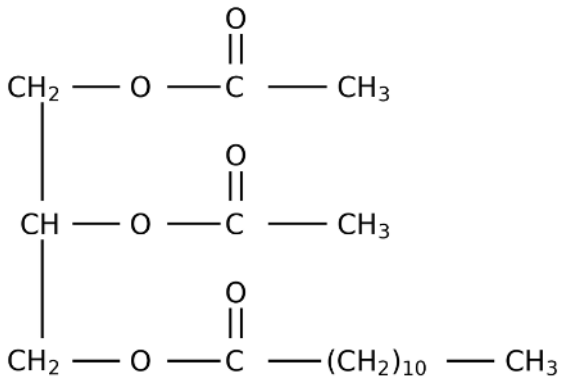

Figure 2. Molecular structure of glycerol diacetate monolaurate.

1.4. Why PVC, TPU, and Glycerol Diacetate Monolaurate?

The selection of suitable components is a critical factor in designing polymer blends with balanced and enhanced properties. In this research, PVC and TPU were selected as the base polymers, while glycerol diacetate monolaurate was chosen as a bio-based plasticizer due to their complementary properties. PVC provides good mechanical strength, flame retardancy, chemical resistance, ease of processing, and low cost; however, its inherent rigidity, brittleness, limited elasticity, and relatively low thermal stability restrict its use in flexible applications [81, 82]. In contrast, TPU exhibits high elasticity, toughness, and better thermal performance, properties that can compensate for several limitations of PVC [48, 49, 52].

Blending PVC with TPU therefore offers a practical approach for developing materials with balanced rigidity and flexibility while reducing reliance on higher-cost elastomeric materials. However, since the final performance of polymer blends strongly depends on intermolecular interactions and phase behaviour, compatibility between the blend components becomes a key consideration [34, 35].

Glycerol diacetate monolaurate was selected as a bio-based plasticizer due to its renewable origin and plasticization efficiency. In addition to its renewable origin, glycerol diacetate monolaurate is derived from abundant and largely underutilized waste cooking oil streams, which positions it as as a highly sustainable option [73, 75]. The use of a waste cooking oil-derived plasticizer therefore contributes not only to the development of flexible polymer systems but also to the utilization of renewable resources and reduction of dependence on conventional phthalate plasticizers.

1.5. Thermodynamic and Technological Compatibility

The concept of polymer blend miscibility originates from the mixing behaviour of simple liquids, where miscible systems form homogeneous single-phase mixtures [83]. However, polymer blending differs significantly from liquid mixing because polymers have high molecular weights, limited chain mobility, and very low entropy of mixing. Consequently, achieving complete molecular-level mixing in polymer blends is thermodynamically difficult, and most polymer systems exhibit partial or complete phase separation [24].

In polymer blends, miscibility generally describes the extent to which one polymer is molecularly dispersed within another and how closely the system approaches homogeneous single-phase behaviour. The degree of compatibility between blend components strongly influences phase morphology, intermolecular interactions, molecular mobility, and ultimately the final properties and performance of the material [23].

From a thermodynamic perspective, a polymer blend is considered compatible when favourable intermolecular interactions produce a negative free energy of mixing and relatively homogeneous phase behaviour. Such systems commonly exhibit single or unified relaxation and transition behaviour, indicating significant molecular-level interaction between the blend components [84]. In contrast, thermodynamically incompatible blends tend to exhibit distinct transition temperatures

corresponding to their parent polymers, reflecting phase separation, weak interfacial adhesion, and limited intermolecular interaction [25, 85].

Beyond thermodynamic considerations, technological compatibility represents a more practical concept associated with processability and macroscopic homogeneity. A polymer blend may therefore be considered technologically compatible when the components can be processed into uniform materials without severe phase separation or structural defects while maintaining useful and application-relevant properties [86].

1.6. Factors Affecting Miscibility of Polymer Blends

The compatibility of polymer blends is influenced by several factors, including blend composition, polarity, intermolecular interactions, molecular weight, and temperature. Since most polymer systems possess very low entropy of mixing, even small variations in these parameters can significantly affect phase behaviour, intermolecular interaction, and blend morphology [32, 33].

Blend composition plays an important role in determining compatibility. In some systems, limited amounts of one polymer may be dispersed within the matrix of another polymer, whereas blends containing nearly equal proportions of both components often exhibit greater phase separation due to reduced thermodynamic stability [87]. The polarity of the constituent polymers is also critical, since polymers possessing similar polarity or chemical structure generally exhibit stronger intermolecular affinity and improved miscibility, while large polarity differences tend to promote immiscibility [88].

Specific intermolecular interactions such as hydrogen bonding, dipole-dipole interaction, and ion-dipole interaction can further enhance compatibility between otherwise immiscible polymers. The presence of functional groups capable of forming such interactions may significantly improve molecular-level mixing and interfacial cohesion [89]. In addition, molecular weight strongly influences blend miscibility because increasing chain length further reduces entropy of mixing, making high-molecular-weight polymer systems generally more susceptible to phase separation [90, 91].

Temperature also strongly affects polymer blend miscibility and phase behaviour. Depending on the polymer pair, increasing temperature may either enhance or reduce miscibility, resulting in upper critical solution temperature (UCST) or lower critical solution temperature (LCST)

behaviour. Consequently, polymer compatibility may vary considerably with processing and service temperatures [1, 92].

The influence of composition and intermolecular interactions has also been reported in PVC/TPU systems. Jeong et al. [93] investigated PVC blends containing segmented TPU and reported that PVC exhibited miscibility with the polycaprolactone soft segment of TPU, where the glass transition behaviour varied systematically with blend composition. The study further demonstrated that the mechanical response and deformation behaviour of the blends were strongly dependent on composition and phase interaction.

1.7. Thermodynamic Compatibility and the Necessity of Swelling Experiments

The compatibility of polymer blends is fundamentally governed by thermodynamic considerations. For a polymer blend to be thermodynamically miscible, the Gibbs free energy of mixing (ΔG) must be negative [35]:

$$\Delta G = \Delta H - T\Delta S \qquad (1)$$

where ΔH and ΔS represent the enthalpy and entropy changes associated with mixing at temperature T, respectively. In polymer systems, the entropy of mixing is extremely small because of the high molecular weight and limited mobility of polymer chains. Consequently, the enthalpic contribution becomes the dominant factor controlling miscibility [94]. Under these conditions, favourable intermolecular interactions such as hydrogen bonding, dipole-dipole interaction, or donor-acceptor interaction are often necessary to reduce ΔH and promote compatibility between polymer components [95].

The enthalpy of mixing can be estimated using the Scatchard–Hildebrand relationship:

$$\Delta H = V\phi_1\phi_2(\delta_1 - \delta_2)^2 \qquad (2)$$

where V is the total volume of the mixture, ϕ represents the volume fraction of each component, and δ is the solubility parameter of the material. According to this relationship, compatibility is favoured when the difference between the solubility parameters of the components is small. When $\delta_1 = \delta_2$, the enthalpy of mixing approaches zero, promoting molecular-level mixing and homogeneous phase behaviour. In contrast, large differences in solubility parameter generally lead to phase separation and thermodynamic incompatibility [96, 97].

The solubility parameter is related to the cohesive energy density (CED) of a material and is expressed as:

$$\delta = (CED)^{1/2} = \left(\frac{\Delta E_v}{v}\right)^{1/2} \qquad (3)$$

where ΔE_v is the molar energy of vaporization and v is the molar volume. The solubility parameter therefore reflects the intermolecular cohesive forces within a material and provides a useful basis for predicting polymer–polymer and polymer–solvent interactions [98].

For low-molecular-weight liquids, solubility parameters can be determined from vaporization measurements. However, direct determination for polymers is impractical because polymers typically degrade before reaching their vaporization temperatures [25, 98]. Consequently, swelling experiments in solvents with known solubility parameters provide an important indirect method for estimating polymer compatibility. In this approach, the polymer is immersed in a series of solvents, and the solvent producing maximum swelling is considered to possess a solubility parameter close to that of the polymer [96, 97]. The swelling percentage can be determined using:

$$\%S = \frac{w_2 - w_1}{w_1} \times 100 \qquad (4)$$

where w_1 and w_2 represent the sample weights before and after swelling, respectively [99]. Because swelling behaviour reflects intermolecular affinity between the polymer and solvent, this method provides a practical experimental approach for estimating polymer solubility parameters and predicting blend compatibility prior to processing [96]. Accordingly, swelling-based solubility parameter analysis was employed in the present study to evaluate the thermodynamic compatibility of the investigated polymer systems.

1.8. Need for Complementary Compatibility Evaluation Beyond Swelling-Based Prediction

In this research, the compatibility of PVC, TPU, and bio-plasticizer systems was initially predicted using swelling experiments based on solubility parameter analysis, where smaller differences in solubility parameter values ($\Delta\delta$) indicate closer intermolecular affinity and more favourable thermodynamic compatibility [96]. Although a negative Gibbs free energy of mixing is a necessary condition for compatibility, thermodynamic prediction alone cannot fully guarantee compatibility in polymer systems from kinetic and mechanical perspectives [91].

From a kinetic perspective, the high viscosity of polymer melts restricts chain diffusion and limits molecular-level homogenization during processing. Even under elevated temperature and mechanical mixing conditions, long-range diffusion of macromolecular chains remains inherently slow because of the large molecular size and restricted chain mobility of polymers [24]. In addition, from a mechanical standpoint, mixing occurs primarily between clusters and entangled regions of polymer chains rather than completely disentangled individual molecules, which further limits homogeneous intermolecular interaction within the blend system [32, 33].

Consequently, the final compatibility behaviour of polymer blends may not always correspond completely with predictions based solely on thermodynamic considerations of the individual components [100]. Therefore, compatibility prediction based on swelling and solubility parameter analysis should be complemented by techniques capable of probing post-processing molecular mobility, intermolecular interaction, relaxation behaviour, and phase morphology.

Thermal relaxation analyses such as DMA and TSD provide important information regarding segmental dynamics and intermolecular interactions developed within the blend system after processing, while morphological characterization reveals the degree of phase homogeneity and interfacial structure [26, 47, 101]. Consequently, combining thermodynamic prediction with relaxation and morphological analyses provides a more reliable and comprehensive evaluation of compatibility behaviour in polymer blend systems.

1.9. Characterization of Compatibility in Polymer Blends

Evaluating compatibility in polymer blends requires the use of multiple characterization techniques because compatibility influences several interconnected factors, including molecular mobility, intermolecular interactions, thermal transitions, and phase morphology [102]. No single analytical method can fully describe the compatibility behaviour of polymer systems, particularly in partially compatible blends where phase interactions may occur at different structural scales [88]. Consequently, a combination of thermal, relaxation, spectroscopic, and morphological analyses is commonly employed to obtain a more reliable understanding of polymer blend compatibility.

Dynamic mechanical analysis (DMA) is one of the most widely used techniques for evaluating compatibility in polymer blends. In DMA, compatibility is commonly assessed through the

relaxation behaviour associated with the glass transition of the blend components [103]. Completely compatible blends typically exhibit a single relaxation transition or a broad intermediate transition resulting from cooperative molecular mobility and homogeneous mixing at the molecular level (Figure 3e). In contrast, incompatible blends generally display two distinct relaxation transitions corresponding to the glass transitions of the parent polymers, reflecting phase separation and limited intermolecular interaction (Figure 3b). Depending on the extent of phase interaction and heterogeneity, intermediate behaviours may also occur. Micro heterogeneous incompatible systems may exhibit broadened or partially overlapping transitions while still retaining two distinct relaxation processes (Figure 3c), whereas heterogeneous blends with stronger intermolecular interactions may exhibit substantial transition broadening and partial merging of the relaxation peaks (Figure 3d). Figure 3a represents the typical DMA response of a single homopolymer for comparison [25, 85]. Typical DMA responses for homopolymers and polymer blends exhibiting different degrees of compatibility are illustrated in Figure 3. Compared with conventional thermal analysis techniques, DMA exhibits high sensitivity toward subtle changes in molecular mobility, relaxation behaviour, and phase interactions.

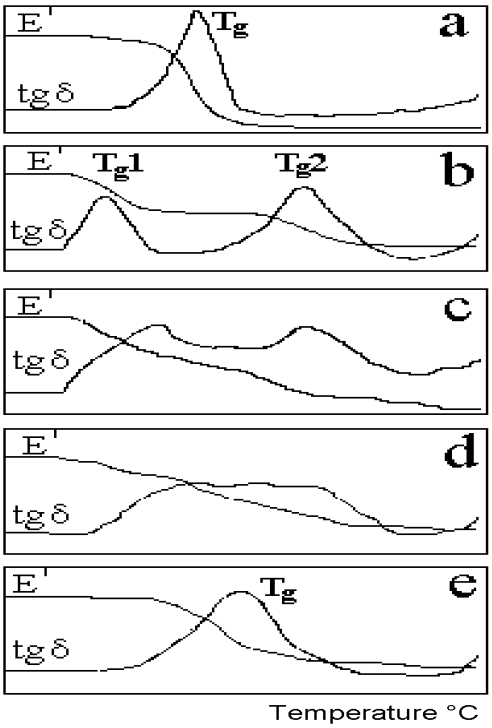

Figure 3. Typical DMA responses of compatible, partially compatible, and incompatible polymer blends [104].

Differential scanning calorimetry (DSC) is another widely used technique for evaluating polymer compatibility through glass transition behaviour. A compatible blend typically exhibits a single glass transition temperature (T_g), whereas incompatible systems display two distinct glass transitions corresponding to the individual blend components [105]. However, DSC has relatively limited resolving power for partially compatible systems, particularly when the T_g values of the components are close or when one phase exists in low concentration. Consequently, subtle phase interactions may not always be clearly distinguished using DSC alone.

Thermally stimulated discharge (TSD) analysis has emerged as a highly sensitive technique for investigating molecular mobility and compatibility in polymer systems. Unlike DSC, which primarily detects thermal transitions, TSD measures dipolar relaxation processes by monitoring depolarization currents during controlled heating following electrical polarization. Because TSD directly probes localized dipolar molecular motions, it is particularly sensitive to intermolecular interactions, interfacial effects, and subtle changes in segmental mobility [26, 106]. Compatible polymer blends commonly exhibit unified or strongly interacting relaxation behaviour, whereas incompatible systems tend to show multiple distinct relaxation processes associated with phase-separated domains [86].

Morphological characterization using microscopy techniques such as scanning electron microscopy (SEM) provides direct information regarding phase structure, dispersion, and interfacial adhesion in polymer blends. Compatible systems generally exhibit more homogeneous morphologies with reduced interfacial separation, while incompatible blends often display distinct dispersed domains, voids, or coarse phase-separated structures [107]. SEM observations therefore provide important complementary evidence for interpreting compatibility behaviour obtained from thermal and relaxation analyses.

Several studies have demonstrated the importance of combining multiple characterization methods when evaluating compatibility in polymer blends. Wei Wu et al. [108] investigated segmented polyurethane/chlorinated PVC blends using DSC and FTIR analyses. Their study demonstrated that the thermal transition behaviour and intermolecular interactions of polyurethane/CPVC blends were strongly influenced by the chemical structure of the polyurethane soft segments. The DSC results revealed different glass transition behaviours among the investigated systems, while FTIR

analysis indicated variations in intermolecular interaction within the blends. Representative DSC curves for the investigated systems are shown in Figures 4 and 5.

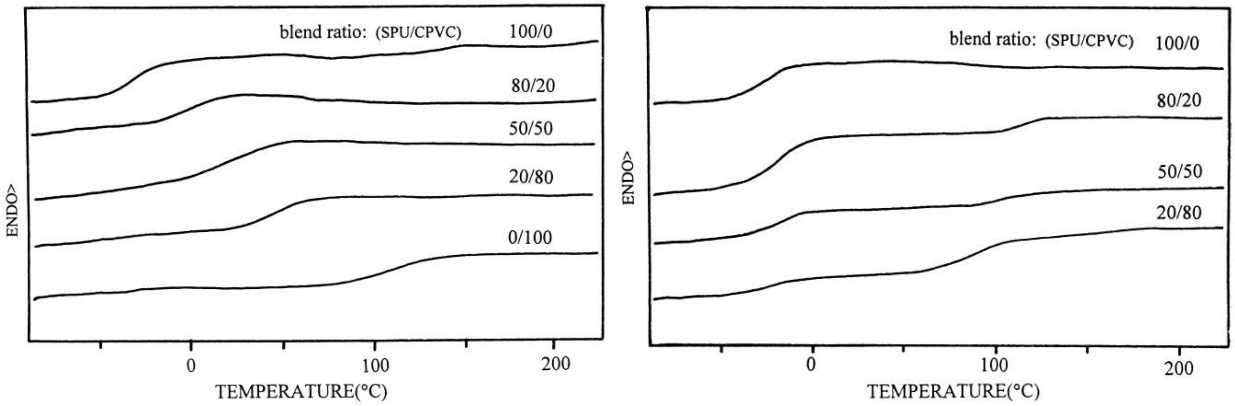

Figure 4. DSC curves of PCL/CPVC blends. Figure 5 DSC curves of PPO/CPVC blends.

Similarly, Tourta et al. [109] investigated the morphology of PS/PVC blends using SEM and reported that increasing phase separation was associated with the appearance of aggregated dispersed domains and microvoids resulting from weak interfacial adhesion. Their results demonstrated that morphological observations provide direct evidence of compatibility behaviour and phase interaction within polymer blend systems.

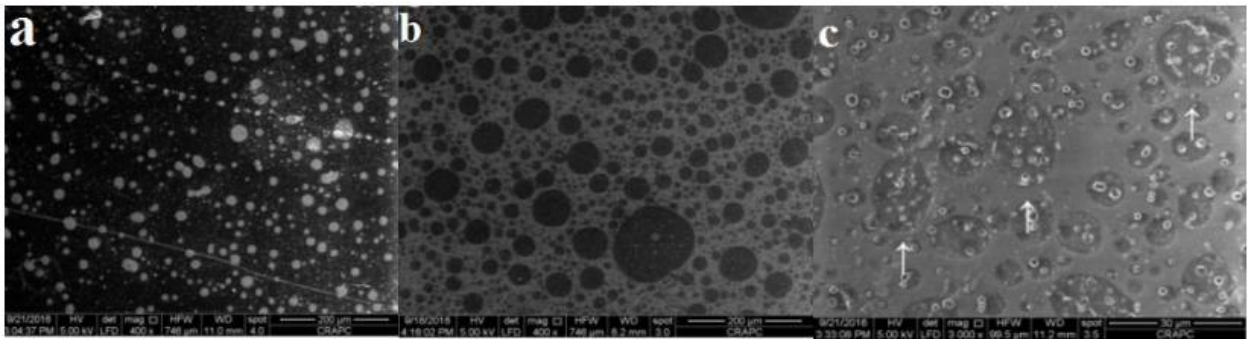

Figure 6. SEM micrographs of PS/PVC blends with varying compositions [109].

Overall, different characterization techniques probe compatibility at different structural and molecular scales. DSC primarily detects bulk thermal transitions and may exhibit limited sensitivity toward phase interactions or partially compatible systems [110]. In contrast, DMA provides greater sensitivity toward cooperative viscoelastic relaxation behaviour, while TSD is highly sensitive to localized dipolar molecular motions and intermolecular interactions [111]. Consequently, combining relaxation-based techniques with morphological analysis provides a

more reliable and comprehensive evaluation of compatibility behaviour in complex polymer blend systems than reliance on conventional thermal analysis alone.

1.10. Mechanical and Thermal Properties of Polymer Blends

The mechanical and thermal properties of polymer blends are strongly influenced by compatibility, intermolecular interactions, and phase morphology. Unlike homopolymers, polymer blends contain multiple structural regions, including continuous phases, dispersed phases, and interfacial domains, all of which contribute to the overall material behaviour. The effectiveness of stress transfer between these phases depends largely on the degree of interfacial adhesion and molecular interaction developed within the blend system. When interfacial interactions are weak, stress concentration and crack propagation tend to occur along phase boundaries, resulting in poor mechanical integrity and reduced performance [57, 112]. Consequently, compatibility plays a central role in determining the tensile strength, elasticity, toughness, thermal stability, and long-term durability of polymer blends.

Mechanical and thermal characterization are therefore essential not only for evaluating material performance but also for understanding structure-property relationships within blend systems. Variations in tensile strength, modulus, elongation at break, hardness, thermal degradation behaviour, and glass transition characteristics are often directly associated with changes in intermolecular interaction, phase homogeneity, and molecular mobility. For this reason, mechanical and thermal analyses are widely employed to assess the effectiveness of compatibilization and the overall quality of polymer blend systems [113-116].

Several studies have investigated the relationship between compatibility and the mechanical or thermal behaviour of PVC/polyurethane-based blends. Pielichowski and Hamerton [117] examined the miscibility and thermal behaviour of solution-cast PVC/chlorinated polyurethane (PVC/CPU) blends using DSC analysis. The investigated blends exhibited a single glass transition temperature within the range of 55–65 °C, indicating compatible phase behaviour over the studied composition range. The authors also reported improved thermal stability and attributed this behaviour to intermolecular dipole-dipole interactions between the polyurethane carbonyl groups and the chlorinated PVC structure, which may reduce diffusion of volatile degradation products through the polymer matrix.

Radhakrishnan and Gopinathan [118] investigated the thermal stability of PVC/NR-b-PU blends prepared by solution casting at compositions of 80/20, 60/40, 40/60, and 20/80 using thermogravimetric analysis (TGA). Their results demonstrated that thermal stability improved progressively with increasing polyurethane content, with the 20/80 PVC/NR-b-PU blend exhibiting the highest thermal resistance. The improved thermal behaviour was attributed to favourable polar interactions between PVC and the hard segments of the polyurethane block copolymer. Representative thermogravimetric curves of the investigated blends are shown in Figure 7.

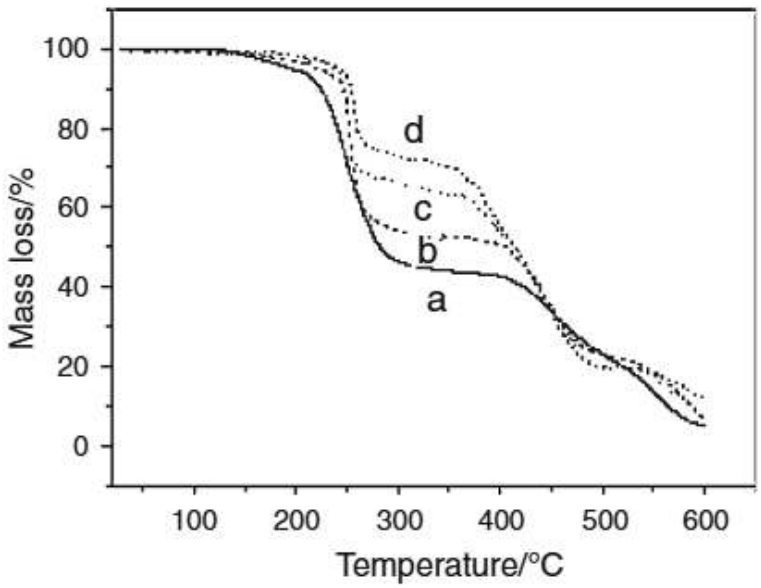

Figure 7. Thermogravimetric curves of PVC/NR-b-PU blends with different compositions [118].

Haponiuk and Balas [119] investigated the miscibility and tensile behaviour of PVC/polyurethane blends using DSC and tensile testing. Their results showed that blends containing up to 30 wt.% polyurethane exhibited single-phase transition behaviour, whereas additional low-temperature transitions appeared at polyurethane concentrations of 35 and 40 wt.%, indicating partial phase separation at higher TPU contents. Tensile testing further demonstrated that increasing polyurethane concentration and temperature reduced yield stress while increasing elongation at break. Based on these observations, the authors concluded that the polyurethane was partially dispersed within a continuous compatible phase structure.

Chang-Sik et al. [120] studied the fracture toughness and mechanical properties of plasticized PVC/TPU blends prepared by melt blending using two TPU grades with different hardness values. The investigated compositions ranged from 100/0 to 50/50 PVC/TPU ratios. Their results demonstrated that increasing TPU content progressively improved tensile strength, elongation at break, impact resistance, abrasion resistance, and thermal stability, while modulus and hardness decreased because of the increasing elastomeric character of the blends. The softer TPU system exhibited greater improvement in elongation at break due to the higher proportion of soft segments within the polyurethane structure. The authors concluded that TPU incorporation significantly improved the flexibility and toughness of plasticized PVC systems, although hardness decreased with increasing TPU concentration.

Similarly, Pita et al. [34] evaluated the mechanical behaviour of PVC/thermoplastic polyurethane and PVC/plasticizers, including DIDP and DOP. Their results showed that low-molecular-weight plasticizers progressively reduced modulus and yield stress because of disruption of intermolecular interactions within the PVC matrix. In contrast, PVC/TPU blends exhibited significantly higher energy absorption prior to yielding compared with conventionally plasticized PVC systems, indicating improved toughness and deformation resistance associated with the elastomeric nature of TPU. The study primarily focused on the influence of processing conditions and mechanical performance, while the compatibility behaviour and intermolecular interactions governing the observed property changes were not investigated.

Overall, the reported studies demonstrate that the mechanical and thermal behaviour of polymer blends is governed by intermolecular interaction. Improvements in flexibility, toughness, elongation behaviour, and thermal stability are frequently associated with enhanced interfacial interaction and more homogeneous phase structures.

1.11. Research Problem, Gaps, and Objectives

1.11.1. Problem Statement

Although PVC finds widespread industrial application because of its low cost, chemical resistance, mechanical strength, and processing versatility, its inherent rigidity, brittleness, and limited thermal stability restrict its use in applications requiring flexibility, elasticity, dynamic mechanical resistance, and elevated-temperature performance [12, 37, 38]. Thermoplastic polyurethane

(TPU), in contrast, exhibits excellent elasticity, toughness, abrasion resistance, and thermal performance that PVC lacks [48, 49, 52]. Nevertheless, TPU is substantially more expensive than PVC, often by approximately three times, limiting its use in high-volume and cost-sensitive applications [17, 18]. Consequently, blending PVC with TPU offers a practical approach for developing materials with balanced rigidity and flexibility while reducing reliance on higher-cost elastomeric materials.

In addition, the rigidity of PVC makes plasticization essential for both processing and application performance. Conventional plasticization of PVC relies predominantly on phthalate-based compounds, which are physically incorporated into the polymer matrix and therefore susceptible to migration, volatilization, and leaching during service conditions. These compounds have raised serious environmental and public health concerns because of their toxicity and endocrine-disrupting effects [15, 60-62]. Despite increasing regulatory restrictions and intensified efforts toward safer and more sustainable alternatives, phthalate-based plasticizers continue to dominate many industrial applications because of their low cost, high plasticization efficiency, and the limited availability of sustainable alternatives capable of providing comparable performance [121].

Among emerging sustainable alternatives, glycerol diacetate monolaurate represents a promising bio-plasticizer because it simultaneously addresses plasticizer sustainability and waste valorization within a circular-economy framework. The compound is derived from waste cooking oil (WCO), a largely underutilized waste stream that is generated globally in substantial quantities, a significant portion of which is improperly disposed of, contributing to environmental pollution and economic loss [73, 74].

Therefore, combining PVC, TPU, and a sustainable bio-plasticizer offers a potential route for developing materials with balanced mechanical and thermal properties while reducing dependence on conventional phthalate plasticizers and high-cost elastomeric systems. However, the final behaviour of such multicomponent polymer blends depends strongly on compatibility, intermolecular interactions, molecular mobility, and phase morphology developed during processing.

1.11.2. Research Gap

Some studies have investigated the compatibility and properties of PVC/polyurethane or PVC/plasticizer blends using conventional characterization techniques [117, 119, 122, 123]. However, a major research gap exists regarding the synergistic integration of thermoplastic polyurethane (TPU) and waste-derived bio-based plasticizers in PVC systems, as no study has comprehensively investigated their combined effects on compatibility, intermolecular interactions, phase morphology, and the resulting properties of sustainable PVC-based materials. Although compatibility plays a critical role in determining polymer blend performance, compatibility assessment in PVC/TPU systems has relied largely on conventional thermal characterization methods, while integrated approaches combining thermodynamic compatibility prediction with post-processing experimental validation remain limited. Furthermore, despite separate investigations of PVC/TPU blends and swelling behaviour [99], the use of swelling-based solubility parameter analysis as a predictive tool for thermodynamic compatibility, followed by multi-technique experimental validation, has not been comprehensively explored for the design of compatible and tunable ternary blend systems. Consequently, the relationships among thermodynamic compatibility, intermolecular interactions, molecular mobility, phase morphology, mechanical performance, and thermal stability have not been systematically established within a unified framework for PVC/TPU/bio-plasticizer blends. Moreover, the influence of TPU and the bio-plasticizer on the thermal stability behaviour of PVC systems, particularly resistance to dehydrochlorination, has not been investigated. In addition, thermally stimulated discharge (TSD) analysis remains underutilized for investigating intermolecular interactions, segmental mobility, and phase heterogeneity in polymer systems despite its high sensitivity toward localized molecular dynamics. Limited attention has also been given to glycerol diacetate monolaurate as a sustainable plasticizer derived from waste cooking oil, a highly abundant yet largely underutilized waste resource.

1.11.3. Objectives of the Research

General Objective

The general objective of this study is to develop and investigate PVC, TPU, bio-plasticizer blend systems through integrated thermodynamic, relaxation, spectroscopic, morphological, mechanical, and thermal analyses in order to establish structure–property relationships linking compatibility

behaviour to material performance from molecular to macroscopic scales. The study also aims to develop flexible and thermally balanced PVC-based materials by combining the complementary properties of PVC and TPU while reducing reliance on high-cost elastomeric systems and conventional phthalate plasticizers.

Specific Objectives

- To evaluate the thermodynamic compatibility of PVC with different TPU systems using swelling experiments and solubility parameter analysis prior to processing.
- To investigate the compatibility, intermolecular interactions, molecular mobility, and relaxation behaviour of PVC/TPU, PVC/bio-plasticizer, TPU/bio-plasticizer, and PVC/TPU/bio-plasticizer blends using DMA, TSD, and FTIR analyses.
- To examine the phase morphology and structural homogeneity of the developed blend systems using scanning electron microscopy (SEM).
- To evaluate the effects of TPU and glycerol diacetate monolaurate on the tensile strength, elasticity, elongation at break, and hardness of PVC-based blend systems.
- To investigate the thermal degradation and dehydrochlorination stability of the developed blend systems using conductivity-based thermal stability measurements and thermogravimetric analysis (TGA).
- To establish relationships among thermodynamic compatibility, intermolecular interactions, molecular mobility, phase morphology, and the resulting mechanical and thermal properties of PVC/TPU/bio-plasticizer blend systems.
- To evaluate the potential of waste cooking oil-derived glycerol diacetate monolaurate as a sustainable plasticizer for flexible PVC-based materials.

2. Materials and Methods

2.1. Materials

Suspension-grade poly(vinyl chloride) (PVC) with a K-value of 70 was supplied by BorsodChem Zrt. (Kazincbarcika, Hungary). Two thermoplastic polyurethanes (TPUs) differing in soft-segment chemistry, namely polyester-based and polyether-based TPU, were obtained from the same manufacturer and initially investigated for compatibility. Based on the preliminary thermodynamic evaluation and processing characteristics, the polyester-based TPU was selected for the subsequent experiments and detailed characterization studies.

The bio-based plasticizer glycerol diacetate monolaurate, derived from waste cooking oil, was purchased from Rikevita Fine Chemical & Food Industry Co., Ltd. (Shanghai, China). It has a reported molecular weight of 358.47 g/mol and a density of 0.99 g/cm³. Prior to processing, PVC formulations were stabilized using 1.2 phr of a CaZn stabilizer together with 0.3 phr of an external lubricant (E-wax). All materials were used as received.

For the swelling experiments and thermodynamic compatibility analysis, solvents with different polarity and solubility parameters were employed, including hexane (Hex), ethyl acetate (EA), methyl ethyl ketone (MEK), acetone (Ac), and isopropyl alcohol (IPA), together with their binary mixtures, were used to cover a broad range of Hildebrand solubility parameters.

Detailed information regarding the materials and solvents used in this study is summarized in Tables 1 and 2.

Table 1. Materials used in this research

Material	Type/Grade	Key Properties	Function	Source
Polyvinyl chloride (PVC)	Suspension, K= 70	High mechanical strength, rigidity, chemical resistance; fine powder; avg. particle size: 160 μm	Base polymer	BorsodChem Zrt, Hungary
Thermoplastic polyurethane (TPU)	Polyester -based and Polyether-based	High elasticity, abrasion resistance, toughness; transparent pellets (~3 mm diameter)	Base polymer	BorsodChem Zrt, Hungary

Glycerol diacetate monolaurate	Commercial grade	Molecular weight:358.47 g/mol; Density: 0.99 g/cm³	Bio-plasticizer	Rikevita Fine Chemical, China

Table 2. Base solvents used for swelling experiments and compatibility analysis

Solvents	Mw (g/mol)	Hildebrand Solubility Parameters($\boldsymbol{\delta}$) [$cal^{1/2}\ cm^{-3/2}$]
Hexane	86.18	7.24
Ethyl acetate	88.108	9.1
Methyl ethyl ketone	72.11	9.27
Acetone	58.08	9.77
Isopropyl alcohol	60.1	11.97

2.2. Blend Preparation

The polymer blends were prepared using suspension-polymerized PVC, TPU, and a bio-based plasticizer according to the formulations presented in Table 3. Prior to blending, PVC was dry-mixed with commercial additives, including a CaZn stabilizer and E-wax lubricant, to improve processing stability. The required quantities of PVC and TPU were subsequently introduced into a 10L laboratory mixer (MTI Mischtechnik, Detmold, Germany) and mixed at a rotational speed of 2500 rpm. Once the blend temperature reached approximately 80 °C, the bio-plasticizer was gradually incorporated in order to achieve effective dispersion throughout the polymer matrix. As the temperature increased to 125 °C during mixing, the rotor speed was reduced to 400 rpm and cooling water was circulated to maintain controlled processing conditions. After cooling to approximately 40 °C, the resulting dry blend, consisting of a slightly agglomerated powder, was collected for further melt processing.

The prepared mixtures were then processed using an electrically heated laboratory roll mill (Schwabenthan 150 U, Berlin, Germany) operated at 175 °C with a rotational speed of 21 rpm, and a roll speed ratio of 1:1. Under these conditions, the polymer matrix softened sufficiently to enable efficient distributive and dispersive mixing through continuous mechanical shearing. To improve blend homogeneity, the material was repeatedly cut, rotated, and manually repositioned

between the heated rolls during milling. The resulting sheets, with thicknesses ranging from approximately 0.4 to 0.6 mm, were subsequently compression molded at the same temperature under controlled pressure to obtain smooth and uniform specimens suitable for subsequent characterization. Following molding, the samples were cooled to room temperature under ambient conditions prior to testing.

Table 3. Compositions of the investigated PVC/TPU/bio-plasticizer blends expressed in parts per hundred resin (phr).

Identifier ➔	PVC	PVC/Bio (10/3)	PVC/Bio (10/5)	PVC/TPU (10/3)	PVC/TPU (10/5)	TPU	TPU/Bio (50/5)	TPU/Bio (50/10)	PVC/TPU/Bio (10/1/5)	PVC/TPU/Bio (10/2/5)
PVC	100	100	100	100	100	-	-	-	100	100
TPU	-	-	-	30	50	100	100	100	10	20
Bio-plasticizer	-	30	50	-	-	-	10	20	50	50
CaZn stab.	1.2	1.2	1.2	1.2	1.2				1.2	1.2
E-wax	0.3	0.3	0.3	0.3	0.3				0.3	0.3

Figure 8. Schwabenthan UL 150 electrically heated two-roll mill used for blend preparation.

2.3. Swelling Experiments and Solubility Parameter Analysis

2.3.1. Preparation of Solvent Mixtures

Solvent systems covering a broad range of solubility parameters were prepared using ethyl acetate (EA), hexane (Hex), acetone (Ac), methyl ethyl ketone (MEK), and isopropyl alcohol (IPA). The volume fractions of the individual solvents were adjusted according to the linear mixing rule in order to obtain mixtures with predetermined solubility parameter values and small incremental variations, as expressed by Equation 5 [124]:

$$\delta_{\text{mix}} = \sum_i \phi_i \, \delta_i \qquad (5)$$

where $\phi_i$and $\delta_i$represent the volume fraction and solubility parameter of each solvent component, respectively, while δ_{mix} denotes the solubility parameter of the resulting solvent mixture.

As an example, a solvent mixture with a solubility parameter of 11.2 $\text{cal}^{1/2} \cdot \text{cm}^{-3/2}$ was prepared by mixing 35 vol% acetone ($\delta = 9.77$) with 65 vol% isopropyl alcohol ($\delta = 11.97$), resulting in:

$$11.2 = (0.35 \times 9.77) + (0.65 \times 11.97)$$

In total, eighteen pure solvents and solvent mixtures with solubility parameters ranging from approximately 7.2 to 12.0 $\text{cal}^{1/2} \cdot \text{cm}^{-3/2}$ were prepared to enable a comprehensive thermodynamic assessment of polymer-solvent interactions. The compositions of the prepared solvent systems are summarized in Tables 4 - 6, where the numerical values preceding the solvent abbreviations indicate the volumetric percentage of each solvent component in the mixture.

Potential variations in the solubility parameter values caused by preferential solvent evaporation during mixture preparation were considered negligible, since the selected solvents have relatively similar evaporation characteristics under the applied experimental conditions.

Figure 9. Swelling of polymer samples in jars of different solvents and mixture solvents.

2.3.2 Swelling Measurements

Rectangular specimens of PVC, polyester-based TPU, and polyether-based TPU were prepared from compression moulded sheets for the swelling experiments. Each specimen, with an average mass of approximately 0.40 g, was dried to constant weight prior to immersion.

The samples were immersed in excess amounts of pure solvents and solvent mixtures with known solubility parameter values, as summarized in Tables 4-6, and maintained at room temperature (27 °C) throughout the measurements.

At selected time intervals, the specimens were removed from the solvent media, gently wiped with filter paper to remove residual surface solvent, and immediately weighed. The swelling behaviour was evaluated from the percentage increase in mass using Equation 6 [99]:

$$S(\%) = \frac{m_s - m_0}{m_0} \times 100 \qquad (6)$$

where m_0 represents the initial mass of the dry specimen and m_s denotes the mass of the swollen specimen.

The measurements were continued until equilibrium swelling was reached, which required approximately five days for all investigated polymers. The solvent or solvent mixture producing the highest degree of swelling was considered to possess a solubility parameter closest to that of the corresponding polymer. Accordingly, the solubility parameter associated with the maximum swelling value was taken as the effective solubility parameter of the investigated polymer [96, 97].

2.3.3 Determination of the Solubility Parameter of Glycerol Diacetate Monolaurate

The solubility parameter of glycerol diacetate monolaurate was estimated using the Small/Fedors molecular group contribution method based on the molecular structure, density, and molar attraction coefficient of the constituent functional groups [125].

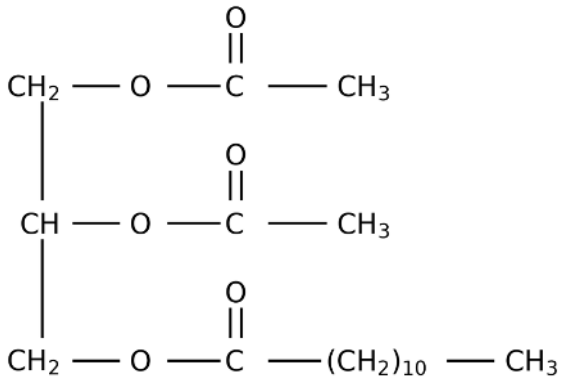

Figure 10. Molecular structure of glycerol diacetate monolaurate used for group contribution calculations.

The total molar attraction coefficient (ΣF) was determined from the cumulative contributions of the individual structural groups summarized in Table 4.

Table 4. Functional group contributions used for the estimation of the solubility parameter of glycerol diacetate monolaurate.

Group	Number (n)	F	n × F
CH_3	3	244	732
CH_2	12	133	1596
CH	1	28	28
Ester group (–O–C=O)	3	310	930
Total ΣF			3286

The solubility parameter was calculated according to Equation 7:

$$\delta = \frac{\Sigma F}{V} \qquad (7)$$

where $V$is the molar volume of the compound, calculated using: $V = \frac{M}{\rho}$, where M represents the molecular weight and ρ denotes the density of the material.

Using a molecular weight of approximately 358 g/mol and a density of 0.99 g/cm^3, the solubility parameter of glycerol diacetate monolaurate was estimated to be approximately:

$$\delta \approx 9.1\ \text{cal}^{1/2}\text{cm}^{-3/2}$$

2.4. Dynamic Mechanical Analysis (DMA)

Dynamic mechanical analysis (DMA) was performed using a Metravib DMA 25 instrument (ACOEM Group, Limonest, France) operated in tensile deformation mode. Rectangular specimens prepared from the roll-milled sheets, with dimensions of 30 mm × 15 mm × ~ 0.6 mm, were analysed over a temperature range from -120 °C to 120 °C. The measurements were conducted at a constant heating rate of 2 °C/min, while liquid nitrogen was used to achieve the required low-temperature conditions.

The viscoelastic response of the samples was evaluated at a fixed oscillation frequency of 10 Hz using a static displacement amplitude of 0.5 mm and a dynamic amplitude of 0.1 mm. During the measurements, the temperature dependence of the mechanical loss factor (tan δ) was continuously recorded. The glass transition temperature (T_g) of the investigated blends was determined from the maximum of the tan δ peak. Changes in the T_g values with blend composition were subsequently used to assess variations in segmental mobility and intermolecular interactions between PVC, TPU, and the bio-based plasticizer.

2.5. Thermally Stimulated Depolarization (TSD)

2.5.1. Sample Preparation for TSD

Disk-shaped specimens with a diameter of 26 mm and a thickness of approximately 0.5 mm were prepared from the compression-moulded sheets described previously in Section 2.2. Prior to TSD measurement, the specimen surfaces were coated with a thin conductive gold layer in order to ensure stable electrical contact with the electrodes and to reduce electrical noise associated with partial discharge during the measurements.

Gold sputtering was carried out using a sputter coater operated under a low-pressure argon atmosphere at 5–7 Pa and an applied voltage of 200 V. The deposited gold layer had a thickness of about 4 nm and a coated diameter of 18 mm.

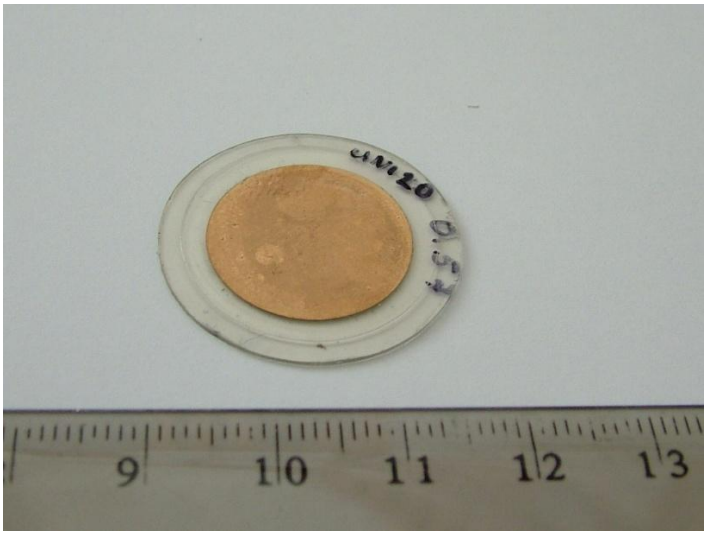

Figure 11. Sputter coating instrument.

Figure 12. Gold-coated polymer specimens.

2.5.2. TSD Measurement of Polymers and Blends

Thermally stimulated depolarization measurements were conducted using a TSCII instrument (SETARAM, Caluire, France). The prepared specimens were mounted inside the measurement chamber, which was first evacuated and subsequently filled with helium gas to improve heat transfer and minimize the presence of impurities that could interfere with the depolarization signal.

The samples were polarized at 120 °C and subsequently cooled to -120 °C at a controlled cooling rate of 5 °C/min using liquid nitrogen as the cooling medium. After polarization and cooling, the depolarization current was recorded continuously during reheating at the same heating rate.

Each experimental cycle required approximately two hours. Further details regarding the instrument configuration, measurement principle, and data evaluation procedure are available in the literature [106]. Schematic illustrations of the TSD setup and the measurement instrument are shown in Figures 13.

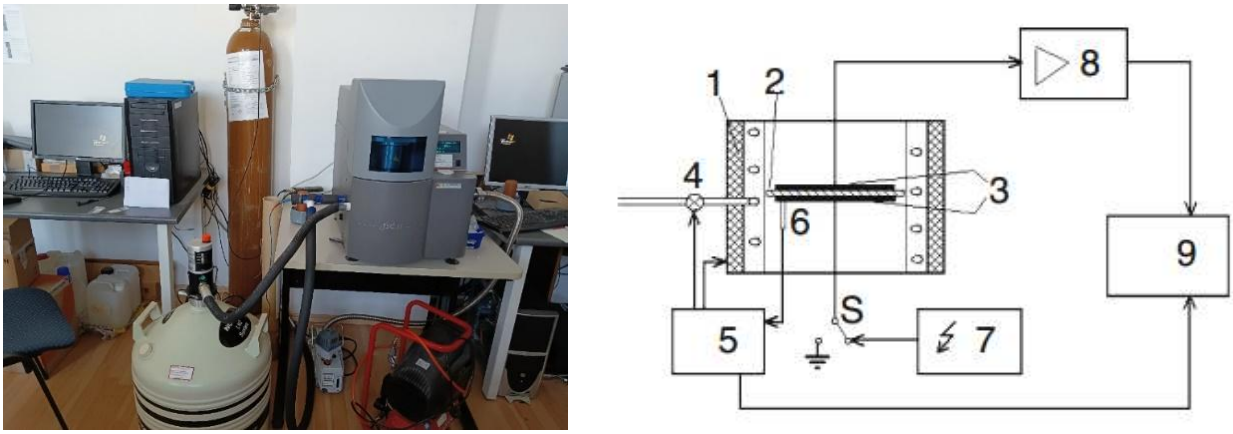

Figure 13. a) TSCII thermally stimulated depolarization instrument, b) Schematic illustration of the thermally stimulated depolarization (TSD) measurement setup [106].

1, heating–cooling chamber, 2 sample, 3 electrodes, 4 cooling control, 5 temperature programmer, 6 temperature sensor, 7 polarizing supply, 8 current amplifier, 9 data acquisition device, S earthing switch.

2.5.3. TSD Measurement of the Bio-Plasticizer

The TSD characterization of the liquid bio-plasticizer was performed using a procedure similar to that applied for the polymer specimens, except that conductive metal coating was not necessary and impossible because the liquid sample provided direct and continuous contact with the electrodes. Instead, a borosilicate glass fiber filter paper with a diameter of 7 mm, a thickness of approximately 0.2 mm, and a nominal pore size of 2.6 µm was used as a supporting carrier material.

Prior to testing, the glass fiber paper was thoroughly impregnated with the bio-plasticizer and placed in the specimen holder of the TSD instrument. Borosilicate glass was selected due to its high chemical resistance and low polarizability, thereby minimizing interference with the measured depolarization response. Additional details regarding TSD measurements of liquid materials are reported elsewhere [126, 127].

2.6. Fourier Transform Infrared Spectroscopy (FTIR) Spectroscopy

Intermolecular interactions within the PVC/TPU/bio-plasticizer systems were examined by Fourier transform infrared (FTIR) spectroscopy using a Bruker Tensor 27 spectrometer (Bruker

Optik GmbH, Ettlingen, Germany) equipped with a diamond attenuated total reflectance (ATR) unit.

The analyses were carried out over a wavenumber range of 400–4000 cm^{-1} using a spectral resolution of 4 cm^{-1}. For each specimen, 128 scans were collected to improve the signal-to-noise ratio. All measurements were performed under ambient laboratory conditions, while the ATR crystal was carefully cleaned before each analysis in order to avoid cross-contamination between samples.

Spectral acquisition and data processing were conducted using OPUS software (version 7.5, Bruker Optik GmbH). Particular attention was given to changes in characteristic absorption bands, including peak shifts, variations in band intensity, and peak broadening associated with the functional groups of PVC, TPU, and the bio-plasticizer. These spectral features were subsequently used to evaluate intermolecular interactions and compatibility within the investigated blend systems.

2.7. Scanning Electron Microscopy (SEM)

The morphology of the prepared polymer blends was examined using a Thermo Scientific Helios G4 PFIB SEM CXe system (Thermo Fisher Scientific, Waltham, MA, USA) equipped with a high-stability Schottky field-emission cathode.

To enhance the contrast between the blend phases, the specimens were immersed in methyl ethyl ketone (MEK) for 24 h in order to selectively remove the more soluble phase from the polymer system. Following solvent treatment, the samples were cross-sectioned and subsequently dried at 70 °C for 24 h to eliminate residual solvent and preserve the developed morphology before microscopic observation.

Prior to imaging, the specimens were mounted on conductive sample holders and coated with a thin gold layer to improve surface conductivity and minimize charging effects during SEM analysis. The observations were conducted under high-vacuum conditions using an accelerating voltage of 15 kV. Secondary electron (SE) imaging was performed in in-column (ICE) mode to obtain detailed information regarding phase morphology, phase dispersion, and the degree of phase separation within the investigated blends.

2.8. Tensile Testing

The tensile properties of the pure polymers and their blends were determined using a computer-controlled INSTRON universal testing machine (Instron, Norwood, MA, USA) equipped with a 1 kN load cell.

Test specimens were prepared from the compression-molded sheets using a precision die cutter (CTC-001162) to produce dumbbell-shaped samples conforming to ASTM D638 Type IV specifications. The specimens had a gauge length of 33 mm, a gauge width of 6 mm, and a thickness of approximately 0.6 mm. This specimen geometry was selected to ensure that deformation occurred predominantly within the gauge section while minimizing stress concentration and grip slippage during testing. Representative tensile test specimens are shown in Figure 14.

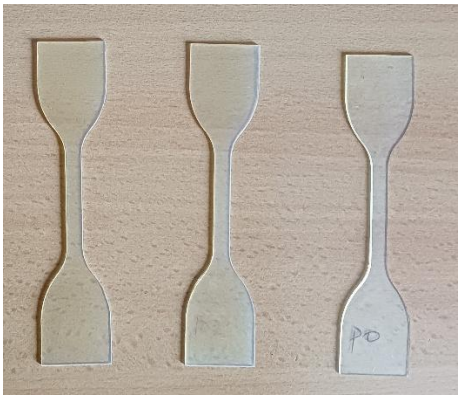

Figure 14. Dumbbell-shaped tensile test specimens.

The measurements were performed at ambient temperature using a crosshead speed of 10 mm/min. During testing, the samples were clamped between the stationary and movable grips of the testing machine, and tensile loading was applied along the longitudinal axis until specimen failure occurred. The applied force and corresponding elongation were continuously recorded throughout the test using the load cell and extensometer system. From the resulting stress–strain behavior, tensile strength, elongation at break, and Young's modulus were determined.

2.9. Hardness Measurement

The hardness of the pure polymers and their blends was determined by indentation testing based on the penetration depth of a standardized indenter under an applied load. Both Shore A and Shore

D hardness measurements were performed in order to enable consistent comparison across materials with different rigidity levels. While Shore A is generally more appropriate for softer materials and Shore D for harder materials, the combined use of both scales provided complementary information regarding the hardness behavior of the investigated formulations.

Shore A hardness was measured using a steel cone indenter under an applied force of 10 N, whereas Shore D hardness measurements were carried out using a pin-shaped cone indenter with a load of 50 N. During testing, the samples were positioned on a rigid, flat support surface while maintaining a slight clearance between the specimen and indenter prior to contact in order to prevent unintended surface loading.

The indentation force was applied perpendicular to the sample surface for a constant duration of 3 s. For each specimen, hardness values were recorded at five different locations and averaged to obtain representative and reliable results.

2.10. Thermogravimetric Analysis (TGA)

Thermogravimetric analysis (TGA) was performed using a Q600 simultaneous DSC–TGA analyzer (TA Instruments, New Castle, DE, USA) in order to evaluate the thermal stability and degradation behavior of PVC, TPU, and the bio-plasticized blends. For each measurement, approximately 10 mg of sample was placed in a platinum crucible and heated under an argon atmosphere with a flow rate of 100 mL/min to ensure inert testing conditions.

The measurements were performed over a temperature range of 30–550 °C at a constant heating rate of 10 °C/min. During the experiment, the change in sample mass was continuously monitored as a function of temperature. The obtained thermogravimetric (TG) and derivative thermogravimetric (DTG) curves were used to examine degradation stages, thermal decomposition behavior, and residual char formation. These results were further utilized to compare the influence of blend composition and bio-plasticizer incorporation on the thermal stability of the investigated materials.

2.11. Conductivity-Based Thermal Stability Testing

The thermal stability of the PVC-containing polymer blends was investigated using a Thermomat 895 instrument (Metrohm, Herisau, Switzerland). The method is based on monitoring the evolution

of hydrogen chloride (HCl) released during the thermal degradation of PVC through changes in the conductivity of an absorbent solution.

For each measurement, samples weighing between 0.5 and 0.85 g, corresponding to a PVC content of approximately 0.5g±2%, were introduced into the reaction chamber and maintained at a constant temperature of 180 °C. Nitrogen was employed as the carrier gas to transport the volatile degradation products into a conductivity cell containing deionized water as the absorption medium.

During thermal degradation, the released HCl dissolved in the water, resulting in an increase in conductivity (µS/cm), which was continuously recorded as a function of time. The characteristic thermal stability time was determined from the inflection point of the conductivity–time curve and used to compare the influence of TPU and bio-plasticizer incorporation on the thermal stability of the PVC-based blends.

3. Results and Discussion

3.1. Swelling Behavior and Thermodynamic Prediction of Compatibility

3.1.1. Swelling Behaviour and Polymer-Solvent Interactions

The swelling behavior of PVC, polyester-based TPU, and polyether-based TPU was investigated using eighteen solvents and solvent mixtures covering a broad range of solubility parameters. The corresponding percentage swelling ratios together with the solubility parameter values are summarized in Tables 5–7, while the swelling kinetics are presented in Figures 15–17. In the sample notation used, the numerical values preceding the solvent abbreviations indicate the volumetric percentage of each solvent component in the mixture.

Table 5. Percentage swelling ratios of PVC in various solvents and solvent mixtures as a function of immersion time.

Solvents/mixture of solvents	δ $(cal^{1/2}cm^{-3/2})$	10 min	20 min	40 min	1 hr	5 hr	1 day	3 days	5 days
100Hex	7.24	1.4	1.8	2.4	2.4	2.4	2.4	2.4	2.44
91.4Hex/EA 8.6	7.4	5.0	5.5	5.5	6.1	6.1	6.1	6.1	6.1
75Hex/25MEK	7.7	5.0	6.1	6.6	10.5	22.2	36.1	37.7	38.8
59.1Hex/40.9EA	8	7.5	13.3	18.6	22.0	33.3	36.6	37.3	40
46Hex/54MEK	8.3	14.6	22.5	35.4	48.3	54.8	67.6	73.5	76
27Hex/73EA	8.6	13.2	59.6	60.7	78.5	89.2	92.8	84.6	96.4
100EA	9.1	11.2	22.2	24.0	31.4	40.7	129.6	131.4	131.4
85EA/15Ac	9.2	27.6	35.3	40.0	55.3	140.0	146.2	149.6	150.7
100MEK	9.27	18.2	36.6	45.4	107.3	156.3	167.2	174.0	174.5
54MEK/46Ac	9.5	21.2	53.4	78.2	122.4	145.0	172.4	197.2	214
25EA/75Ac	9.6	30.0	43.3	53.3	83.3	116.6	133.3	136.6	136.6
100Ac	9.77	27.7	39.5	81.1	109.9	112.1	115.5	121	121
11IPA/89Ac	10	23.0	30.7	41.9	76.5	92.3	96.1	100	100
29IPA/71Ac	10.4	10.0	14.3	20.0	31.4	42.8	57.1	62.5	65.7
47IPA/53Ac	10.8	7.7	13.1	18.5	20.3	27.3	35.1	35.8	37
65IPA/35Ac	11.2	1.2	2.5	4.1	4.1	4.1	4.1	4.1	4.16

Solvents/mixture of solvents	δ ($cal^{1/2}cm^{-3/2}$)	10 min	20 min	40 min	1 hr	5 hr	1 day	3 days	5 days
83IPA/17Ac	11.6	1.1	1.6	1.6	2.0	2.5	2.5	2.5	2.5
100IPA	11.97	1.6	2.0	3.0	3.0	3.0	3.0	3.0	3

Table 6. Percentage swelling ratios of polyester-based TPU in various solvents and solvent mixtures as a function of immersion time.

Solvents/mixture of solvents	δ ($cal^{1/2}cm^{-3/2}$)	10 min	20 min	30 min	1 hr	5 hr	1 day	3 days	5 days
100Hex	7.24	0.27	0.27	0.27	0.54	0.81	1.62	1.62	1.89
91.4Hex/EA 8.6	7.4	3.1	5.3	9.6	10	11.3	11.7	11.8	11.8
75Hex/25MEK	7.7	14.7	18.8	22.5	27.3	28	29.8	29.0	29.16
59.1Hex/40.9EA	8	6.6	13.3	20	23.2	23.9	24.5	26.1	26.6
46Hex/54MEK	8.3	17.7	28.1	37.5	46.8	48	50	50	50
27Hex/73EA	8.6	15.6	25	34.3	43.7	45.3	46.8	47.5	47.8
100EA	9.1	20.58	38.5	55.67	69.6	81.2	81.4	81.7	81.79
85EA/15Ac	9.2	34.5	54.4	67.2	70.9	76.3	81	81.8	81.81
100MEK	9.27	33.5	60.4	79.9	96.7	107.4	110.7	112.0	113.1
54MEK/46Ac	9.5	43.6	77.6	89	102.2	111.7	115.5	117	117.4
25EA/75Ac	9.6	62.5	78.1	87.5	93.7	96.8	98.4	100	100
100Ac	9.77	34.5	58.3	74.0	83.9	87.0	91.9	92.2	92.28
11IPA/89Ac	10	57.6	65.3	69.2	76.9	80	82.6	84.5	84.6
29IPA/71Ac	10.4	38.1	57.1	60.6	70.0	76.1	76.1	76.2	76.2
47IPA/53Ac	10.8	26.0	34.7	47.8	50.0	51.1	51.7	52.1	52.1
65IPA/35Ac	11.2	19.0	23.8	28.5	33.3	40.4	42.4	42.8	42.8
83IPA/17Ac	11.6	1.1	1.6	2.7	3.3	3.3	3.3	3.3	3.3
100IPA	11.97	2.7	3.0	3.3	3.56	3.81	11.70	12.9	12.97

Table 7. Percentage swelling ratios of polyether-based TPU in various solvents and solvent mixtures as a function of immersion time.

Solvents/mixture of solvents	δ ($cal^{1/2}cm^{-3/2}$)	10 min	20 min	40 min	1 hr	5 hr	1 day	3 days	5 days
100Hex	7.24	0.58	0.78	0.97	1.36	1.95	4.88	4.88	4.88
91.4Hex/EA 8.6	7.4	1.66	4.16	6.2	6.6	10.3	11.4	12.2	12.5
75Hex/25MEK	7.7	12.1	16.8	20.5	21.4	26.1	28.5	29.1	30.0
59.1Hex/40.9EA	8	9.5	14.2	19.0	23.8	28.5	32.3	33.3	33.3
46Hex/54MEK	8.3	20.8	37.5	48.3	50.1	58.3	62.5	64.4	66.6
27Hex/73EA	8.6	12.0	20.1	28.0	36.0	48.0	51.3	52.0	52.0
100EA	9.1	11.6	22.4	30.4	44.6	62.9	66.5	66.5	66.5
85EA/15Ac	9.2	20.8	33.3	42.6	52.5	58.3	62.5	65.8	66.6
100MEK	9.27	25.9	39.81	56.0	76.8	90.9	95.8	96.7	97.2
54MEK/46Ac	9.5	28.0	48.0	64.3	76.0	82.4	83.6	84	84
25EA/75Ac	9.6	24.0	36.0	44.0	48.0	60.0	63.0	64.0	64.0
100Ac	9.77	18.6	29.5	38.6	49.5	56.0	56.1	56.2	56.52
11IPA/89Ac	10	20.0	28.0	44.0	49.6	52.0	54.4	55.6	56
29IPA/71Ac	10.4	25.0	33.3	45.8	52.5	54.1	62.5	65.1	66.6
47IPA/53Ac	10.8	15.5	19.2	28.4	34.6	45.4	49.4	50.0	50.0
65IPA/35Ac	11.2	9.0	11.8	16.3	18.8	27.3	31.9	34.1	36.36
83IPA/17Ac	11.6	3.9	4.3	13.0	17.3	19.5	20.8	21.6	21.7
100IPA	11.97	1.92	2.9	3	4.27	6.41	18.16	19.8	20.72

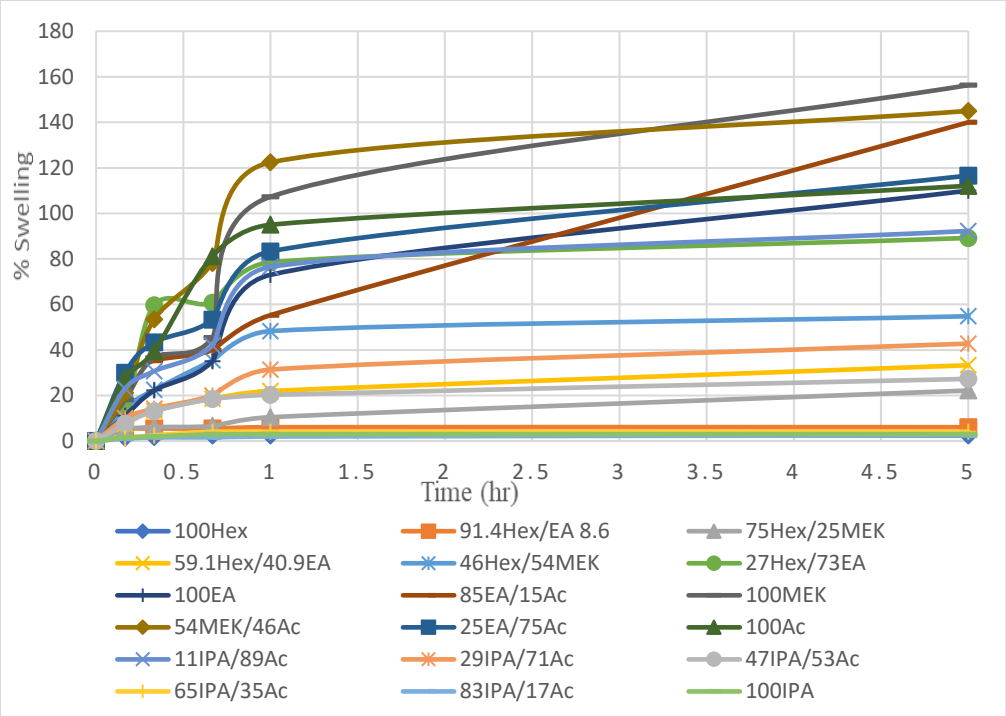

Figure 15. Swelling kinetics of PVC in solvents and solvent mixtures with different solubility parameters.

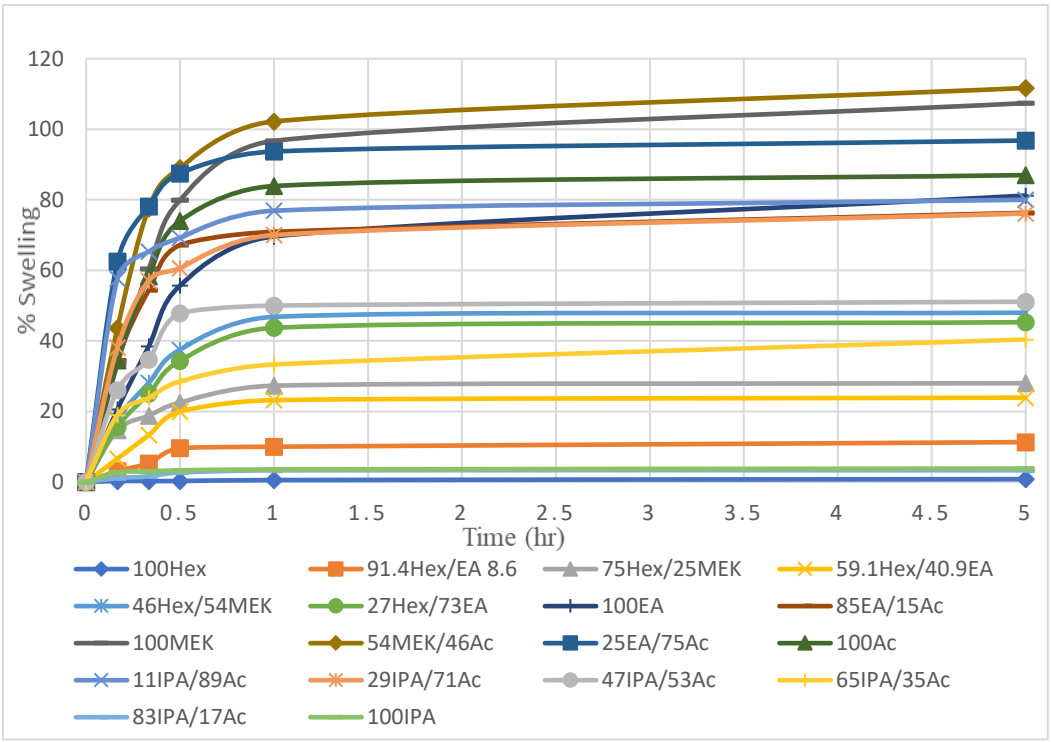

Figure 16. Swelling kinetics of polyester-based TPU in solvents and solvent mixtures with different solubility parameters.

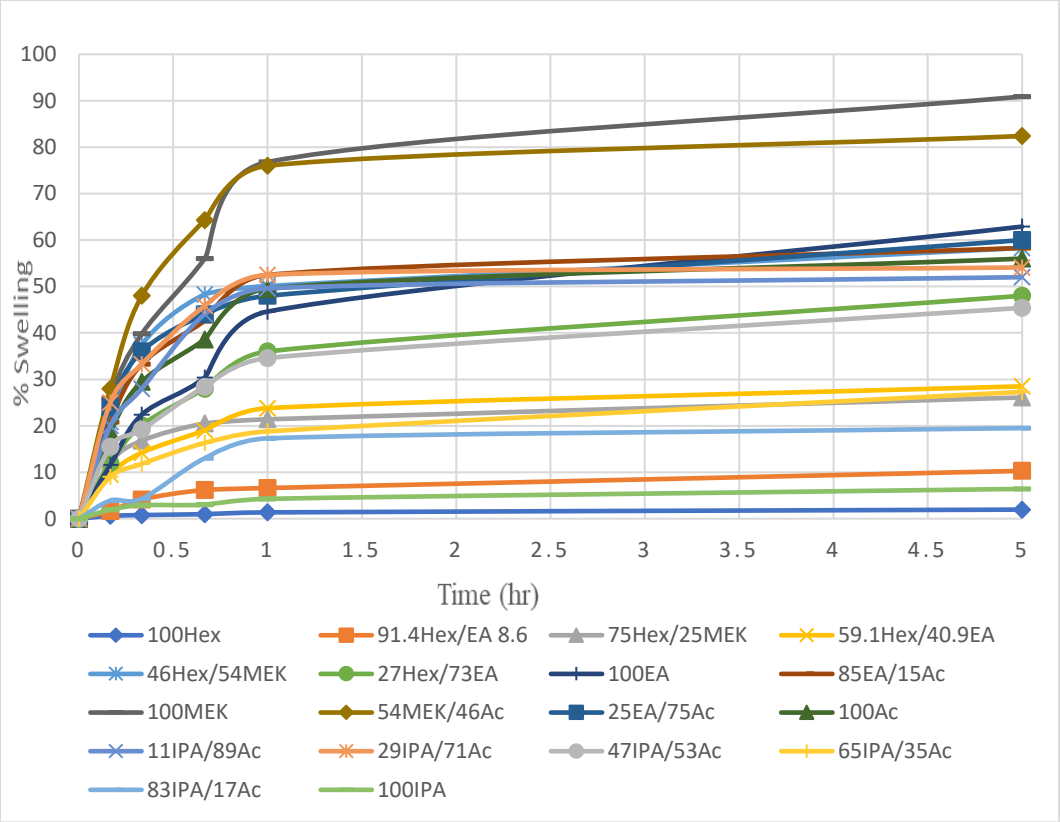

Figure 17. Swelling kinetics of polyether-based TPU in solvents and solvent mixtures with different solubility parameters.

The swelling curves obtained for all investigated polymers exhibited similar overall kinetic behavior. In each case, a rapid increase in solvent uptake was observed during the initial stage of immersion, particularly within the first hour, followed by a progressive decrease in swelling rate as equilibrium conditions were approached. Such behavior is characteristic of diffusion-controlled swelling processes in polymeric materials.

The pronounced solvent absorption observed during the early stages of immersion can be attributed to the high concentration gradient between the external solvent phase and the polymer surface, which promotes rapid diffusion of solvent molecules into the outer regions of the polymer matrix. As solvent penetration progresses, the intermolecular interactions between neighboring polymer chains gradually weaken, allowing increased chain mobility and expansion of the polymer network structure. With increasing solvent uptake, the concentration gradient progressively decreases, resulting in slower solvent diffusion and a corresponding reduction in the swelling rate.

Figures 15-17 show the swelling curves over the initial 5 hrs, during which the majority of solvent uptake occurs. At longer times (up to five days), only minor changes in swelling were observed, indicating that equilibrium conditions were gradually reached. The consistent kinetic trends observed for all samples support the reliability of the swelling measurements used for subsequent thermodynamic analysis.

3.1.2. Evaluation of Polymer Solubility Parameter and Compatibility

The equilibrium swelling behavior of PVC, polyester-based TPU, and polyether-based TPU was analyzed in solvents and solvent mixtures possessing a wide range of solubility parameters. The equilibrium swelling ratios obtained for each polymer were plotted as a function of solvent solubility parameter (δ), and the resulting swelling curves are presented in Figure 18.

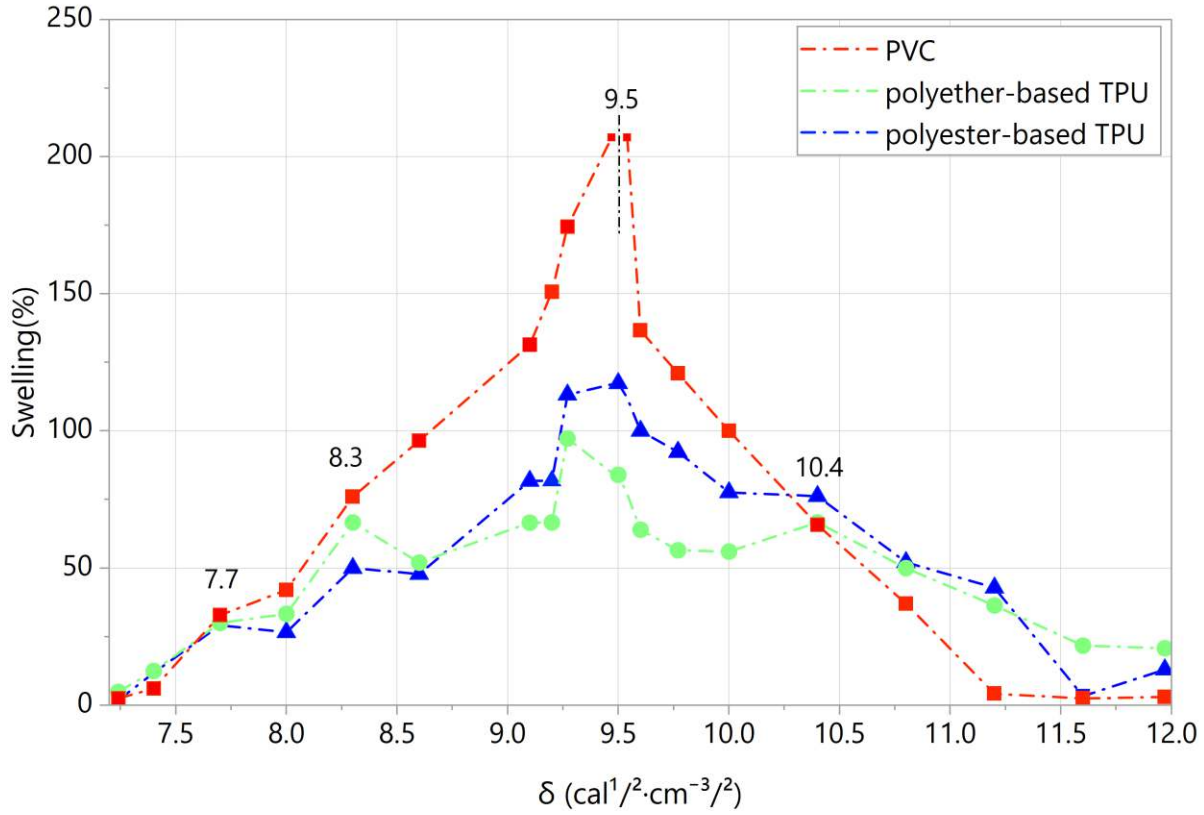

Figure 18. Equilibrium swelling curves of PVC, polyester-based TPU, and polyether-based TPU as a function of medium solubility parameter (δ).

PVC exhibited maximum swelling followed by complete dissolution at a solubility parameter of $9.5\ \mathrm{cal}^{1/2}\mathrm{cm}^{-3/2}$, resulting in an open swelling curve. Accordingly, this value was taken as the effective solubility parameter of PVC. In contrast, both TPUs did not undergo complete dissolution within the investigated solubility parameter range. This behavior is related to the segmented block copolymer structure of TPU, which contains chemically distinct hard and soft segments. If a solvent could dissolve one segment (either soft or hard), the other segment remains insoluble and restricts complete dissolution of the material.

The polyester-based TPU showed a maximum swelling at $\delta \approx 9.5\ \mathrm{cal}^{1/2}\mathrm{cm}^{-3/2}$coinciding with that of PVC. In comparison, the polyether-based TPU reached its maximum swelling at a slightly lower solubility parameter of $9.27\ \mathrm{cal}^{1/2}\mathrm{cm}^{-3/2}$and showed a comparatively lower swelling intensity. In addition, the TPU swelling curves displayed multiple maxima, reflecting the heterogeneity of segmented polyurethane systems. For instance, the swelling maximum observed near $8.3\ \mathrm{cal}^{1/2}\mathrm{cm}^{-3/2}$is mainly associated with the soft segments, whereas the peak around $10.4\ \mathrm{cal}^{1/2}\mathrm{cm}^{-3/2}$corresponds predominantly to the hard segments. These observations indicate that different structural domains within the TPU interact preferentially with solvents possessing different cohesive energy densities.

It was additionally observed that solvents having similar or small differences in overall solubility parameter values did not necessarily produce identical swelling behaviour. For instance, ethyl acetate and methyl ethyl ketone have solubility parameters of $9.1\ \mathrm{cal}^{1/2}\mathrm{cm}^{-3/2}$ and $9.27\ \mathrm{cal}^{1/2}\mathrm{cm}^{-3/2}$, respectively, with a small difference of $0.17\ \mathrm{cal}^{1/2}\mathrm{cm}^{-3/2}$, yet methyl ethyl ketone produced substantially greater swelling. This behavior can be explained by the fact that the total solubility parameter represents the combined contribution of dispersion, polar, and hydrogen-bonding interactions. Consequently, solvents with similar total solubility parameter values may still interact differently with a polymer if the relative contributions of these intermolecular forces differ.

The compatibility assessment was based on experimentally determined swelling behaviour, where the position of maximum swelling reflects the closest match in cohesive energy density between the polymer and the solvent [96, 97]. Accordingly, the proximity of these maxima among different materials provides a direct indication of their thermodynamic affinity. PVC exhibited dissolution

at $\delta \approx 9.5\ cal^{1/2}cm^{-3/2}$ while the polyester-based TPU exhibited maximum swelling at the same solubility parameter. This correspondence indicates a high degree of segmental thermodynamic compatibility between the two systems, as polymers with similar cohesive energy densities are expected to exhibit favourable interactions. In contrast, the polyether-based TPU exhibits a deviation in solubility parameter and a lower maximum swelling response, indicating weaker interactions with the PVC matrix.

This is further supported by its processing behaviour. As shown in Figure 19, the PVC/polyester-based TPU blends produced smooth and homogeneous compression-molded sheets, whereas the PVC/polyether-based TPU blends exhibited visible structural defects and poor uniformity.

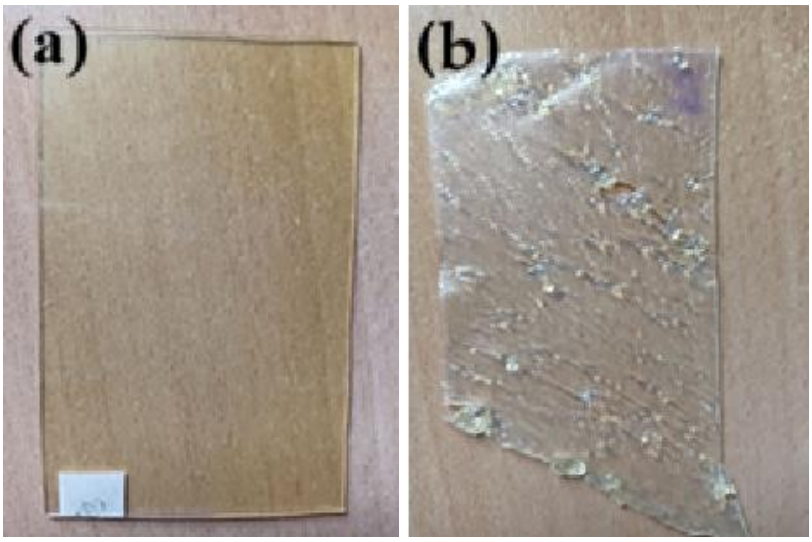

Figure 19. Compression-molded sheets of (a) PVC/polyester-based TPU blends, (b) PVC/polyether-based TPU blends.

These observations demonstrate that the thermodynamic prediction based on swelling behaviour is consistent with practical processability. Accordingly, the polyether-based TPU was excluded from further investigation, and subsequent analyses focused on the polyester-based TPU system.

The solubility parameter of the bio-based plasticizer was estimated using the molecular group contribution method as described in Section 2.3.3, was approximately 9.1 $cal^{1/2}cm^{-3/2}$, which is slightly lower than the values obtained for PVC and polyester-based TPU. Nevertheless, due to its relatively low molecular weight and higher molecular mobility, the bio-plasticizer exhibits a broader miscibility range and is therefore capable of interacting effectively with both components. Although plasticizers with higher solubility parameters may show stronger interactions with the

polymer matrix, they may also disrupt the hard-segment structure of TPU and negatively affect its elastic behavior. In contrast, the present bio-based plasticizer provides a suitable balance between compatibility and structural preservation, while additionally offering the environmental advantage of being derived from renewable waste cooking oil.

3.1.3. Conclusion

The swelling studies demonstrated diffusion-controlled solvent uptake behaviour for all investigated polymers, with rapid initial swelling followed by gradual equilibration. The multiple swelling maxima observed for the TPU systems reflected the heterogeneous nature of segmented polyurethanes arising from the presence of distinct soft and hard domains. It was also observed that solvents with similar or very close solubility parameter values did not produce similar swelling behavior due to differences in intermolecular interaction contributions.

PVC dissolved at 9.5 $cal^{1/2}cm^{-3/2}$, and polyester-based TPU exhibited maximum swelling at the same solubility parameter, indicating favourable thermodynamic compatibility between the two polymers. In contrast, polyether-based TPU showed lower swelling and maximum swelling at a different solubility parameter, suggesting weaker compatibility with the PVC matrix. These predictions were consistent with processing observations, where PVC/polyester-based TPU blends formed homogeneous sheets, whereas blends containing polyether-based TPU exhibited structural defects and poor uniformity. The bio-based plasticizer, despite having a slightly lower solubility parameter than PVC and polyester-based TPU, was predicted to be compatible with both polymers due to its relatively low molecular weight (high molecular mobility), which enables broader miscibility range. Moreover, its lower solubility parameter may additionally help preserve TPU elasticity.

Although thermodynamic compatibility is a precondition and provides an important basis for predicting blend behavior prior to processing, it does not guarantee compatibility in polymer systems because restricted chain diffusion and limited molecular-level mixing can hinder homogenization. Therefore, the compatibility predicted from swelling and solubility parameter analysis were further verified using complementary techniques capable of evaluating molecular mobility, relaxation behavior, and phase morphology, as discussed in the following sections.

3.2. Molecular Interactions and Compatibility

3.2.1. Dynamic Mechanical Analysis (DMA) of Polymer Blends

Dynamic mechanical analysis was employed to investigate the segmental mobility and phase interactions of PVC, TPU, and their binary and ternary blends. The temperature dependence of the mechanical loss factor (tan δ) is presented in Figure 20(a–d). The glass transition temperature (T_g) was determined from the maximum of the tan δ peak, while changes in peak position, shape, and intensity were used to evaluate variations in chain mobility and blend compatibility.

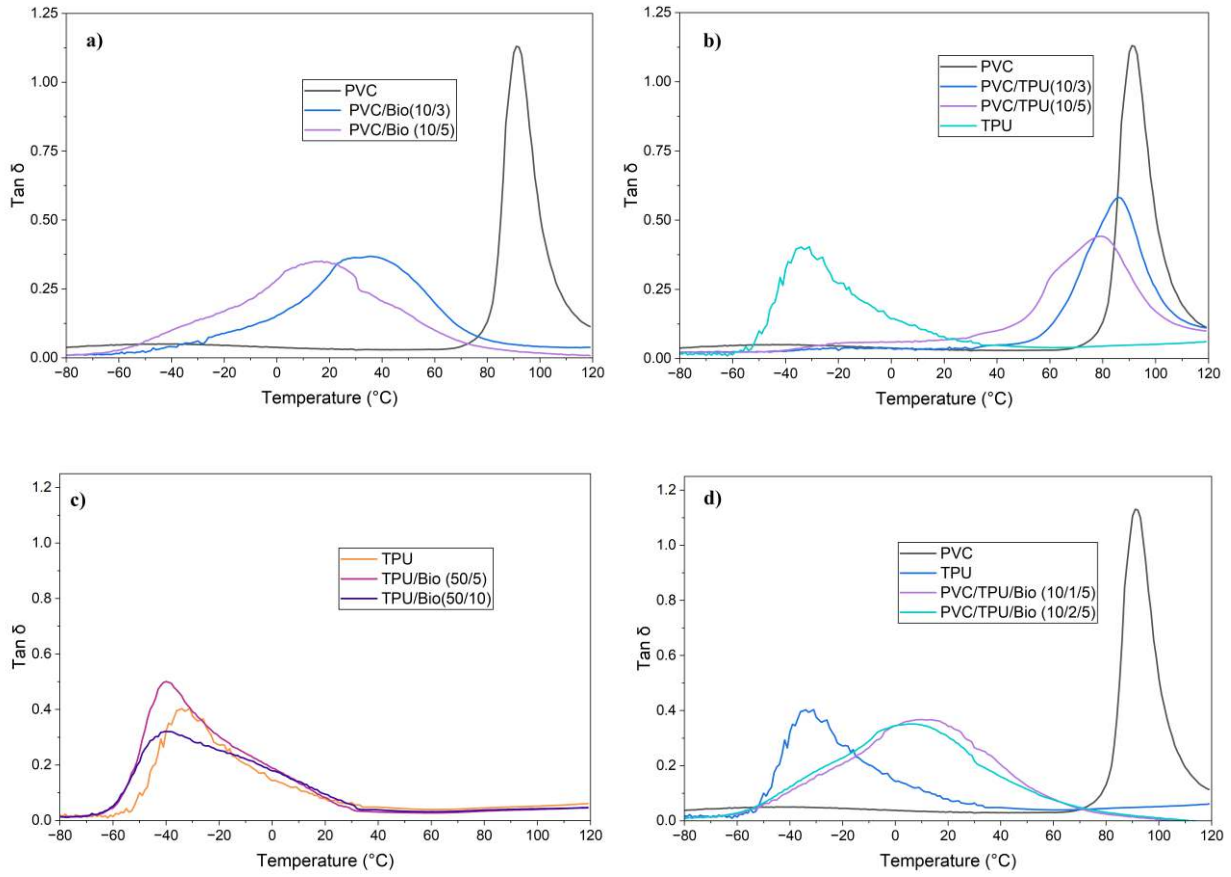

Figure 20. DMA tan δ curves of PVC, TPU, and their blends.

Neat PVC exhibited a sharp tan δ peak at approximately 92 °C, reflecting its rigid amorphous structure and restricted segmental mobility. Incorporation of the bio-plasticizer caused a pronounced shift of the relaxation peak toward lower temperatures together with noticeable peak broadening, indicating increased chain flexibility and a broader distribution of relaxation environments. The glass transition temperature decreased progressively with increasing plasticizer

content, reaching approximately 35 °C for PVC/Bio (10/3) and about 17 °C for PVC/Bio (10/5). This substantial reduction in T_g confirms the strong plasticization effect and favourable compatibility of the bio-based plasticizer with PVC through weakening of intermolecular PVC-PVC interactions and enhancement of cooperative chain motion.

Blending TPU with PVC (Figure 20b) also reduced the glass transition temperature, although the effect was less pronounced than that observed for the bio-plasticized systems. The main PVC-related relaxation shifted to approximately 86 °C for PVC/TPU (10/3) and 79 °C for PVC/TPU (10/5). The absence of a distinct secondary transition corresponding to neat PVC suggests significant intermolecular interaction and considerable phase mixing between PVC and TPU. However, at higher TPU content, especially in PVC/TPU (10/5), a weak low-temperature shoulder became visible, indicating localized phase heterogeneity associated with the TPU soft segments.

Neat TPU displayed a tan δ maximum near -32 °C, corresponding to the glass transition of the soft-segment domains (Figure 20c). The addition of the bio-plasticizer shifted this transition slightly toward lower temperatures (approximately -40 to -41 °C) and increased the damping intensity, reflecting enhanced flexibility within the soft-segment phase. Compared with PVC, the relatively small shift in T_g indicates that TPU already possesses considerable intrinsic chain mobility, while the plasticizer acts mainly as a secondary mobility enhancer.

The ternary PVC/TPU/bio-plasticizer blends (Figure 20d) exhibited distinctly different relaxation behaviour. Instead of separate PVC- and TPU-related transitions, a single broad tan δ peak appeared at substantially lower temperatures, approximately 12 °C for PVC/TPU/Bio (10/1/5) and about 5 °C for PVC/TPU/Bio (10/2/5). Simultaneously, the low-temperature TPU-related shoulder disappeared. This behaviour indicates improved compatibility between PVC and TPU in the presence of the bio-plasticizer, which promotes enhanced molecular interaction and reduces phase separation within the blend system.

3.2.2 TSD Results of Polymer Blends

To evaluate the compatibility and molecular interactions of the investigated systems, thermally stimulated depolarization (TSD) curves and peak maxima normalized to an electric field of 1 kV/mm and an electrode area of 30 cm² are presented in Figures 21–23.

3.2.2.1 TSD Curve Analysis of Polymer Blends

Figure 21 presents the TSD curves of neat PVC, neat TPU, and their blends with the bio-based plasticizer obtained at a heating rate of 5 °C/min. The depolarization current response (pA) is plotted as a function of temperature, revealing relaxation processes associated with molecular mobility and charge detrapping within the investigated systems.

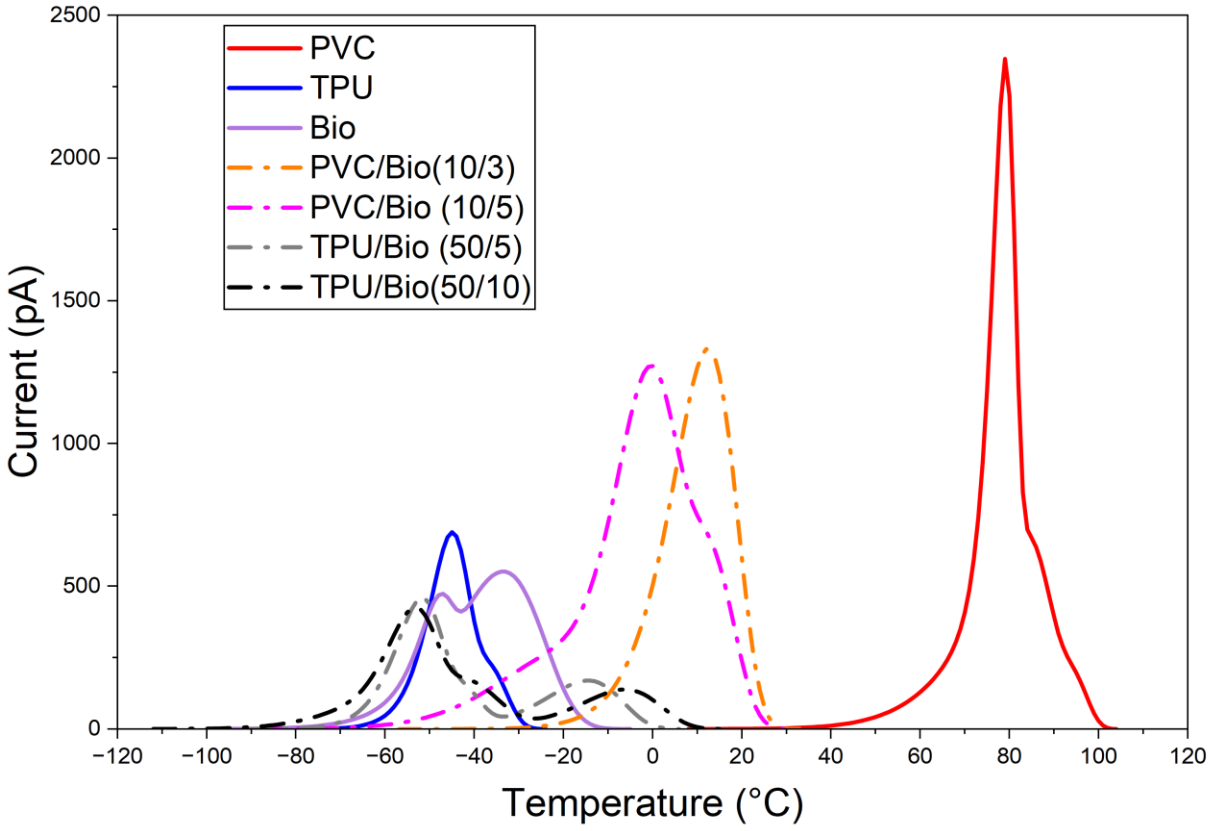

Figure 21. TSD curves of PVC/bio-plasticizer and TPU/bio-plasticizer blends.

Neat PVC exhibited a dominant relaxation peak at approximately 79 °C, which is attributed mainly to dipolar relaxation and charge detrapping processes within the rigid PVC matrix. The relatively high relaxation temperature reflects the restricted molecular mobility and strong intermolecular interactions characteristic of unplasticized PVC.

Upon incorporation of the bio-plasticizer, the PVC/bio-plasticizer systems retained a single dominant relaxation peak, while the relaxation temperature progressively shifted toward lower values with increasing plasticizer content. The intermediate position of the relaxation peaks

relative to the individual components indicates effective molecular interaction and successful plasticization of the PVC matrix. The shift toward lower temperatures suggests enhanced segmental mobility caused by weakening of intermolecular PVC-PVC interactions. Furthermore, the presence of a single dominant peak confirms good compatibility and indicates the formation of a homogeneous plasticized system without significant phase separation.

The TSD response of neat TPU exhibited two primary relaxation processes. The prominent peak located at -45.5 °C corresponds to the relaxation of the soft segments, whereas the second, less pronounced peak appearing near -35 °C is associated with the hard-segment domains. The relaxation associated with the hard segments was less detectable in the neat TPU curve, due to the restricted mobility of the hard segments and their relaxation at higher temperatures.

The addition of the bio-plasticizer influenced both relaxation processes of TPU. In the TPU/bio-plasticizer blends, the soft-segment relaxation shifted to lower temperatures, appearing at approximately -54 °C for TPU/Bio (50/10) and -52 °C for TPU/Bio (50/5), indicating enhanced flexibility and increased molecular mobility within the soft domains. Similarly, the hard-segment-related relaxations appeared at approximately -6.2 °C for TPU/Bio (50/10) and -14 °C for TPU/Bio (50/5). The reduction in relaxation temperature demonstrates that the bio-plasticizer also affects the hard segments by reducing segmental rigidity and facilitating molecular motion, making their relaxation more detectable within the tested temperature range. The TSD curves therefore confirm that the bio-plasticizer effectively increases the molecular mobility of both TPU segments, demonstrating good compatibility and efficient plasticization behavior.

The presence of two distinct relaxation peaks reflects the intrinsic segmented morphology of TPU rather than phase separation. This distinction is more clearly observed in TSD measurements because TSD probes localized dipolar molecular motions at a finer molecular scale compared with the cooperative viscoelastic relaxations detected by DMA.

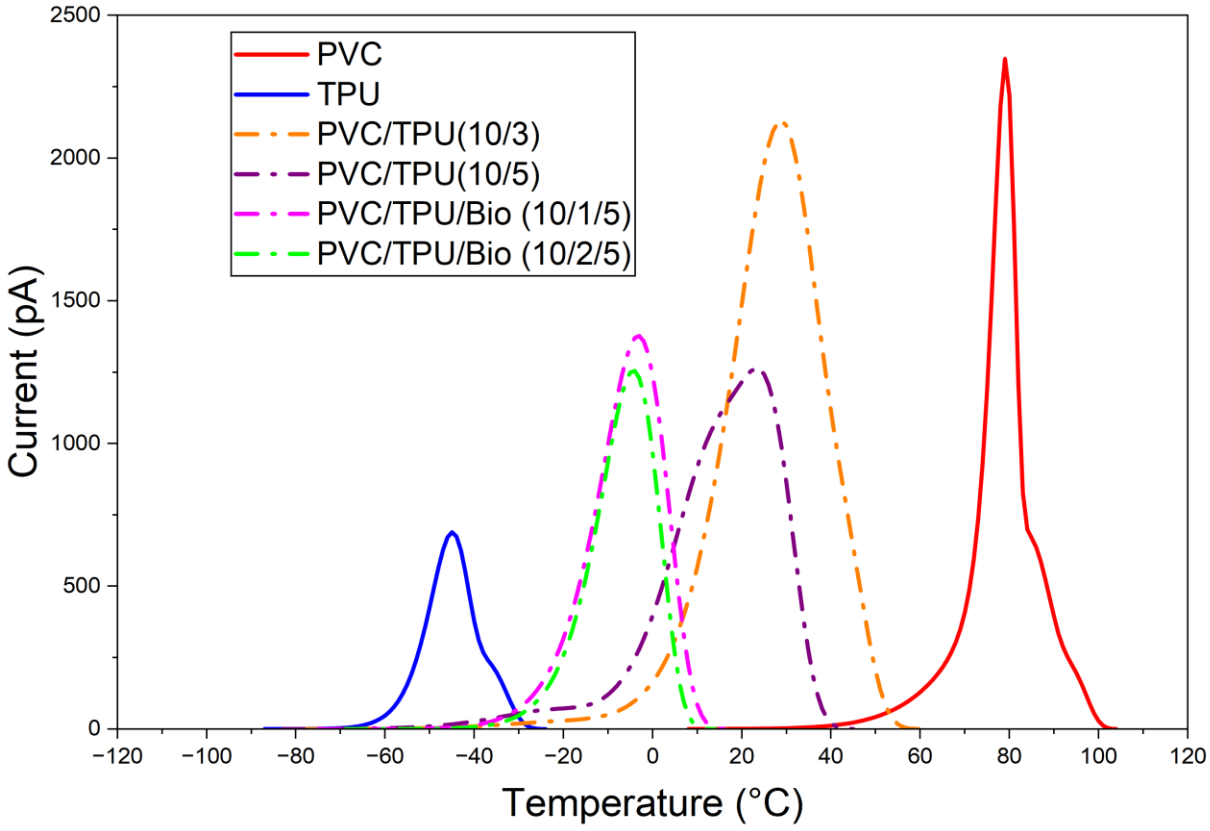

Figure 22. TSD curves of PVC/TPU and PVC/TPU/bio-plasticizer blends.

The PVC/TPU blends exhibited a single dominant relaxation peak positioned between those of neat PVC and neat TPU, representing the combined relaxation behaviour of the two polymers. The appearance of a single major relaxation peak rather than separate PVC and TPU transitions indicates significant intermolecular interaction and formation of a relatively well-mixed interphase with limited phase separation.

Consistent with the DMA results, the PVC/TPU (10/5) blend exhibited a weak low-temperature shoulder, suggesting localized phase heterogeneity at higher TPU contents. In contrast, the ternary PVC/TPU/bio-plasticizer blends displayed single broad relaxation peaks without evidence of phase segregation, indicating improved compatibility and enhanced intermolecular interaction in the presence of the bio-plasticizer. These observations are further supported by the SEM analysis discussed in the subsequent sections.

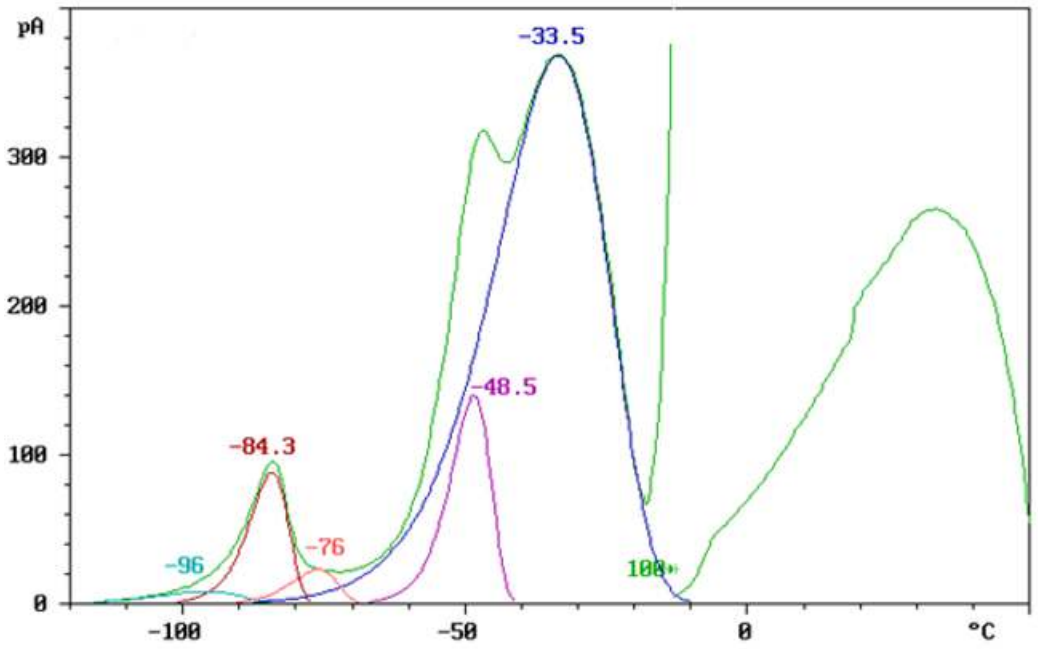

Figure 23. TSD result and resolved peaks of glycerol diacetate monolaurate.

The bio-plasticizer exhibited a glass transition near -35 °C, indicating its potential to improve flexibility within the polymer systems. In addition, multiple relaxation peaks were observed, suggesting that the material may contain minor secondary components or impurities originating from the synthesis process. The multiple relaxation peaks may also be associated with the motion of different molecular segments within the plasticizer structure, resulting in distinct dipolar relaxation processes [26].

3.2.2.2 TSD Peak Maxima Trends

The variation of TSD peak maxima, corresponding to the temperature of maximum depolarization during heating, is presented in Figures 24 and 25. These trends provide additional insight into the influence of TPU and the bio-plasticizer on the molecular mobility and relaxation behavior of the investigated blends.

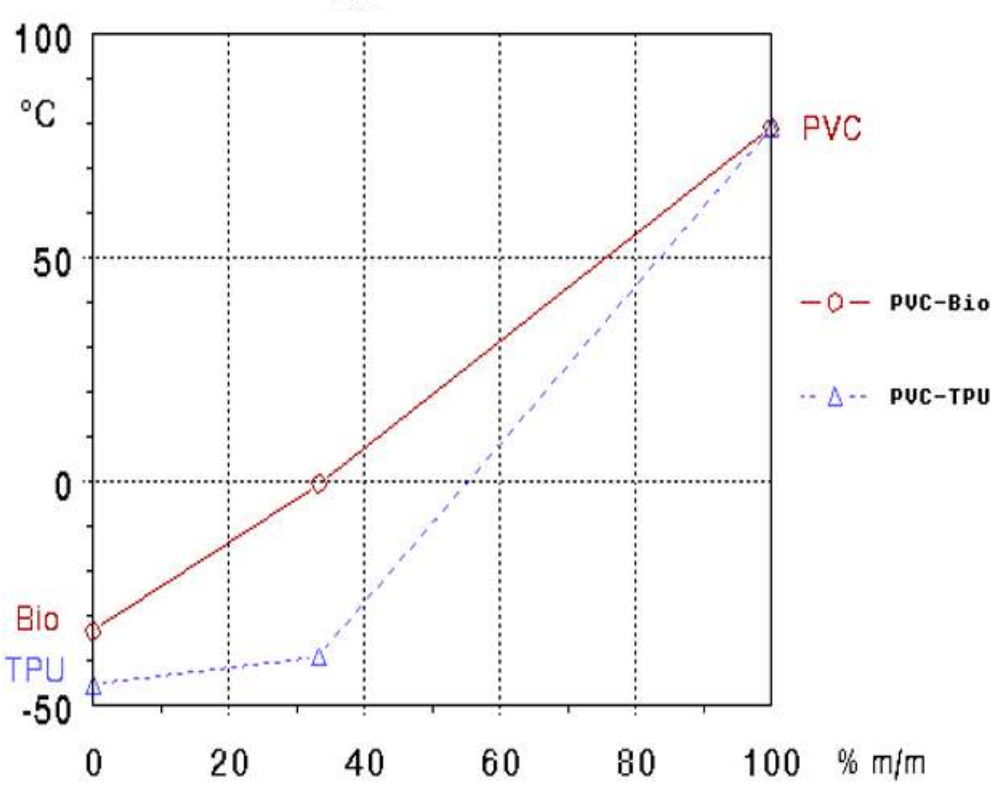

Figure 24. TSD peak maxima of PVC/bio-plasticizer and PVC/TPU blends.

For the PVC/bio-plasticizer system, the TSD peak maxima decreased progressively with increasing plasticizer content, exhibiting an approximately linear trend. This behaviour reflects the typical plasticization effect, where the bio-plasticizer weakens intermolecular interactions between PVC chains and enhances segmental mobility, resulting in reduced glass transition behaviour.

In contrast, the PVC/TPU blends exhibited a less linear dependence. Increasing TPU content caused a more pronounced reduction in the TSD peak maxima, particularly at higher TPU concentrations. This behaviour indicates that TPU effectively disrupts the rigid PVC matrix and strongly influences the dipolar relaxation behaviour of the blend. At 50 phr (33.3%) TPU, the reduction in relaxation temperature was greater than expected, suggesting that TPU acts as an efficient plasticizing component in terms of molecular mobility and T_g reduction.

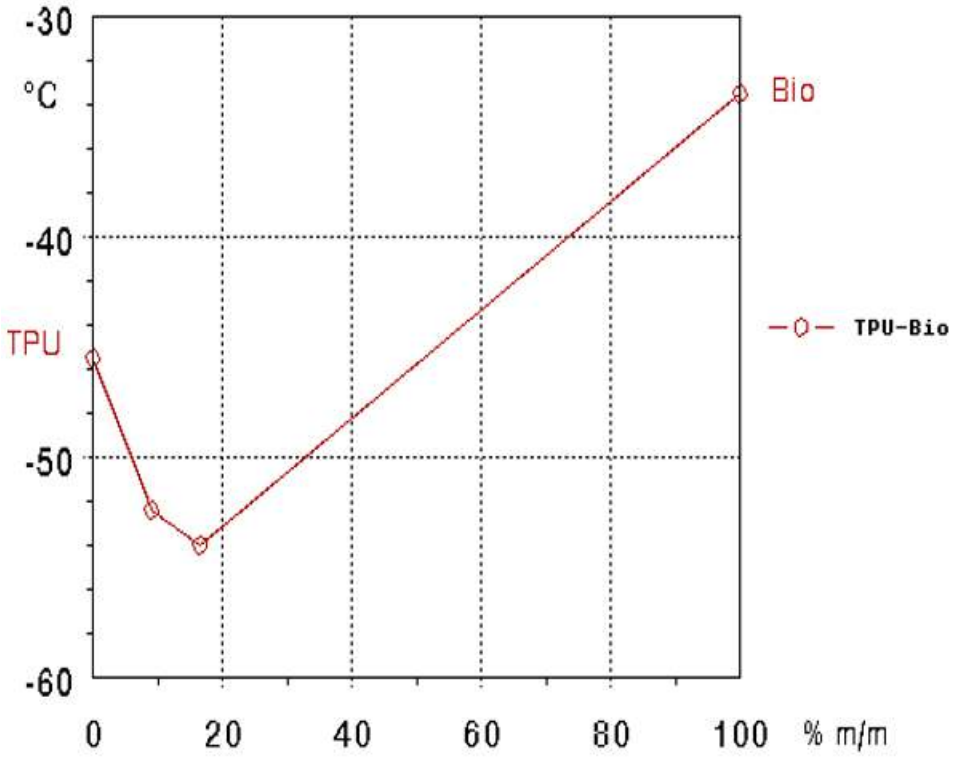

Figure 25. TSD peak maxima of TPU/bio-plasticizer blends.

The TSD peak maxima of the TPU/bio-plasticizer blends (Figure 25) exhibited an interesting trend characterized by a distinct minimum. This behavior arises because the T_g of the bio-plasticizer is higher than that of the apolar soft segments of TPU. At lower bio-plasticizer concentrations, the plasticizer enhances the mobility of the TPU soft segments, resulting in a decrease in the TSD peak maxima. However, with further increases in bio-plasticizer content, the plasticizer begins to dominate the matrix and progressively restricts segmental mobility, leading to a gradual increase in the TSD peak maxima. This trend demonstrates the dual role of the bio-plasticizer, which promotes flexibility at lower concentrations while progressively limiting molecular movement at higher concentrations.

3.2.2. Fourier Transform Infrared (FTIR) Analysis of Polymer Blends

The FTIR spectra of PVC, polyester-based TPU, the bio-plasticizer, and a representative PVC/TPU (10/3) blend are presented in Figure 26. The spectra of the individual components exhibited the characteristic absorption bands expected for their respective chemical structures,

including the C–Cl stretching vibration of PVC, the urethane-related N–H and C=O groups of TPU, and the ester carbonyl and C–O stretching vibrations of the bio-plasticizer.

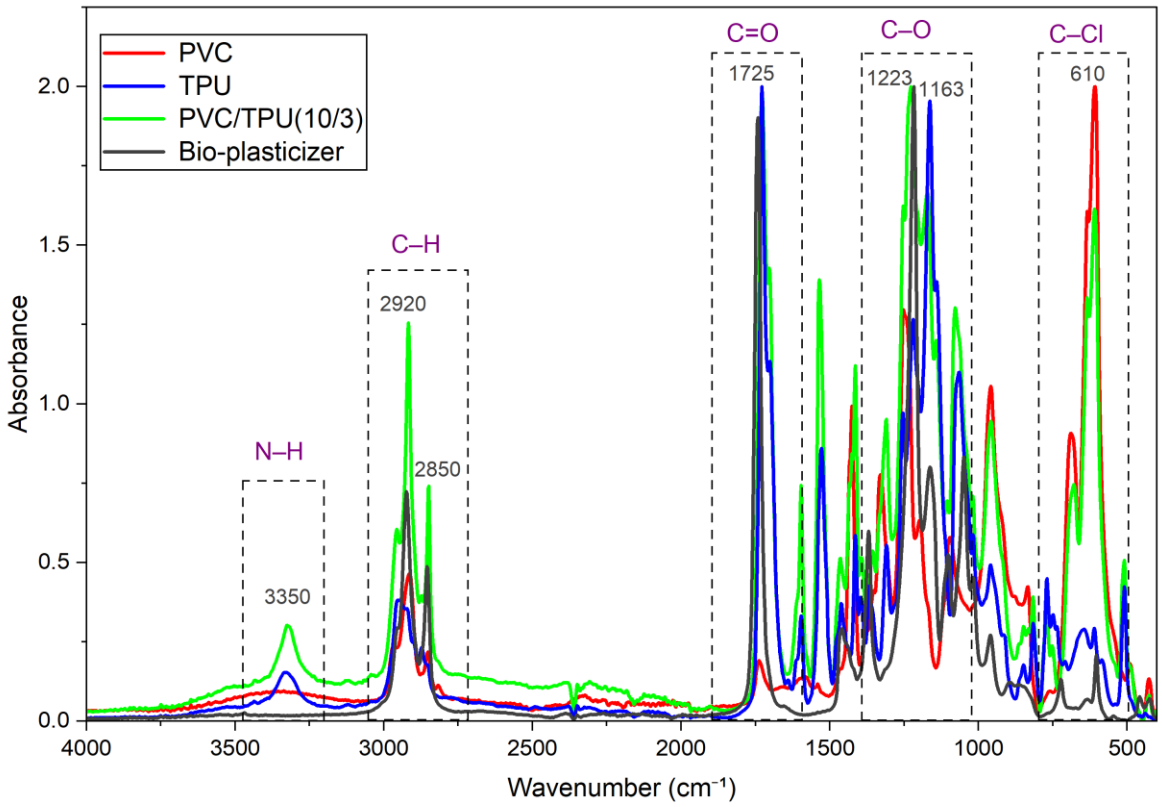

Figure 26. FTIR spectra of PVC, polyester-based TPU, the bio-plasticizer, and the representative PVC/TPU (10/3) blend.

In the PVC/TPU (10/3) blend, the main absorption bands of the individual components remained identifiable, indicating that blending occurred primarily through physical interaction without the formation of new covalent bonds. Nevertheless, slight spectral modifications were observed in regions associated with polar functional groups. Minor variations in the carbonyl region together with slight broadening of the C–O and N–H bands suggest the presence of intermolecular interactions between the blend components, most likely involving weak hydrogen bonding and dipolar interactions between the polar PVC chains and the urethane groups of TPU. Although no additional absorption bands appeared after blending, the observed spectral changes indicate alteration of the local chemical environment surrounding these functional groups.

The FTIR spectrum of the bio-plasticizer, glycerol diacetate monolaurate, confirmed its ester-functionalized structure through the presence of a strong ester carbonyl absorption together with characteristic C–O stretching bands. The absorption bands near 2920 and 2850 cm^{-1} corresponding to aliphatic ($–CH_2–$)stretching vibrations, further confirmed the presence of the laurate chain structure. In addition to the major absorption features, several weak secondary bands were detected, suggesting the possible presence of trace residual components or minor byproducts originating from the synthesis process. In particular, low-intensity bands near 600 cm^{-1} may indicate small amounts of residual fatty acid esters or unreacted lauric acid, implying incomplete esterification. These observations are consistent with the TSD results, which also suggested slight molecular heterogeneity within the bio-plasticizer system. However, the relatively low intensity of these additional features indicates that their concentration is minimal and that their impact on the overall material performance is negligible.

Overall, the FTIR analysis confirmed the presence of complementary polar functional groups and provided qualitative evidence of intermolecular interactions among PVC, TPU, and the bio-plasticizer. These observations further support the compatibility behaviour inferred from the swelling, DMA, and TSD analyses.

3.2.3. Scanning Electron Microscopy (SEM) Analysis of Polymer Blends

The SEM micrographs presented in Figure 27 illustrate the morphological characteristics of the PVC/TPU binary blends and the ternary PVC/TPU/bio-plasticizer system, revealing significant changes in phase structure with blend composition.

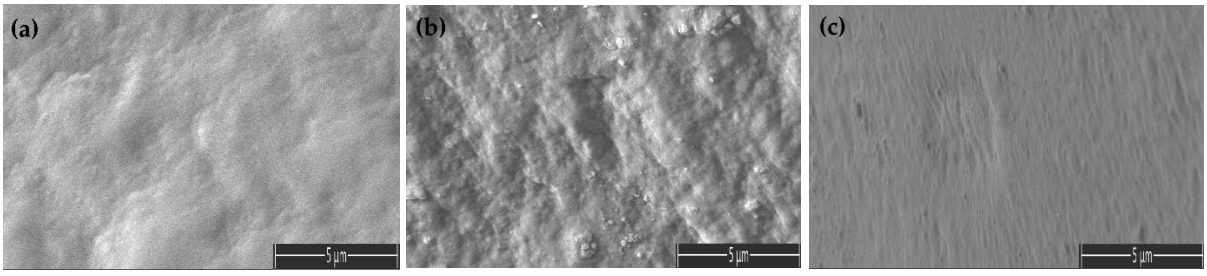

Figure 27. SEM micrographs of (a) PVC/TPU (10/3), (b) PVC/TPU (10/5), and (c) PVC/TPU/Bio-plasticizer (10/2/5).

The PVC/TPU (10/3) blend (Figure 27a) exhibited a relatively smooth and uniform surface with only minor irregularities, indicating favourable intermolecular interaction and reasonably good dispersion of TPU within the PVC matrix. However, increasing the TPU content to PVC/TPU (10/5) (Figure 27b) resulted in a noticeably rougher and more heterogeneous structure containing visible domains and localized discontinuities. The appearance of these TPU-rich regions suggests partial phase separation and reduced compatibility at higher TPU concentrations.

In contrast, the ternary PVC/TPU/Bio (10/2/5) blend displayed a considerably more homogeneous structure (Figure 27c). The surface appeared smoother and more continuous, with reduced phase contrast and without clearly separated domains, indicating improved phase dispersion and enhanced interfacial interaction between PVC and TPU in the presence of the bio-plasticizer. This improved morphology may be attributed to the ability of the plasticizer to increase chain mobility and reduce interfacial tension between the blend components.

These morphological observations are consistent with the DMA and TSD results, where the ternary blends exhibited reduced phase heterogeneity together with more unified relaxation behaviour. Overall, the SEM analysis provides direct visual evidence that incorporation of the bio-plasticizer improves compatibility and phase homogeneity within the PVC/TPU blend system.

3.2.4. Conclusion

The DMA, TSD, FTIR, and SEM analyses consistently demonstrated favourable compatibility and significant intermolecular interactions within the PVC/polyester-based TPU/bio-plasticizer systems. Both DMA and TSD analyses revealed progressive shifts of the relaxation peaks toward lower temperatures following TPU and bio-plasticizer incorporation, while the presence of single dominant transitions indicated good compatibility with the PVC matrix. In the ternary blends, the appearance of a broad single relaxation peak together with the disappearance of the low-temperature shoulder observed in the binary systems suggested improved compatibility and reduced phase separation. Due to its higher sensitivity toward dipolar relaxation processes and smaller probe scale compared with DMA, TSD additionally resolved the individual relaxation behaviour of the TPU soft and hard segments and confirmed that the bio-plasticizer enhanced the mobility of both domains. The TSD peak maxima trends further demonstrated that both TPU and the bio-plasticizer lowered the relaxation temperature of PVC blends, while the TPU/bio-

plasticizer system exhibited a characteristic minimum reflecting the dual influence of the plasticizer on segmental mobility at different concentrations. FTIR analysis revealed slight band broadening and spectral modifications in the C=O, N–H, and C–O regions, indicating intermolecular interactions primarily associated with dipolar interactions and weak hydrogen bonding.

These findings were further supported by SEM observations, which showed increased morphological heterogeneity at higher TPU contents, whereas the ternary blends exhibited smoother and more homogeneous morphologies with improved phase dispersion and reduced interfacial separation. Overall, the results are consistent with the thermodynamic compatibility predicted from the swelling and solubility parameter analyses discussed previously. The improved molecular-level compatibility and phase homogeneity observed in the ternary systems are also expected to significantly influence the mechanical performance and thermal stability of the blends, as discussed in the following sections.

3.3. Mechanical Performance and Structure–Property Relationships

The polymer blends prepared from PVC, TPU, and the bio-plasticizer exhibited a broad range of mechanical properties that could not be achieved by the individual components alone. The mechanical properties of the investigated formulations are summarized in Table 8, while the corresponding stress-strain curves are presented in Figure 28.

Table 8. Tensile properties of the investigated polymer blends.

Properties	PVC	PVC/Bio (10/3)	PVC/Bio (10/5)	PVC/TPU (10/3)	PVC/TPU (10/5)	TPU	TPU/Bio (50/5)	TPU/Bio (50/10)	PVC/TPU /bio (10/1/5)	PVC/TPU/bio (10/2/5)
Tensile strength (MPa)	52.2	44.3	20.8	43.3	27.8	52.9	49.9	34.2	32.3	27
Young's modulus (MPa)	2768	94	5.9	987.2	457.5	8.2	6.9	3.5	27.7	4.9
Elongation at break (%)	86	151	310	225	194	610	615	620	250	360

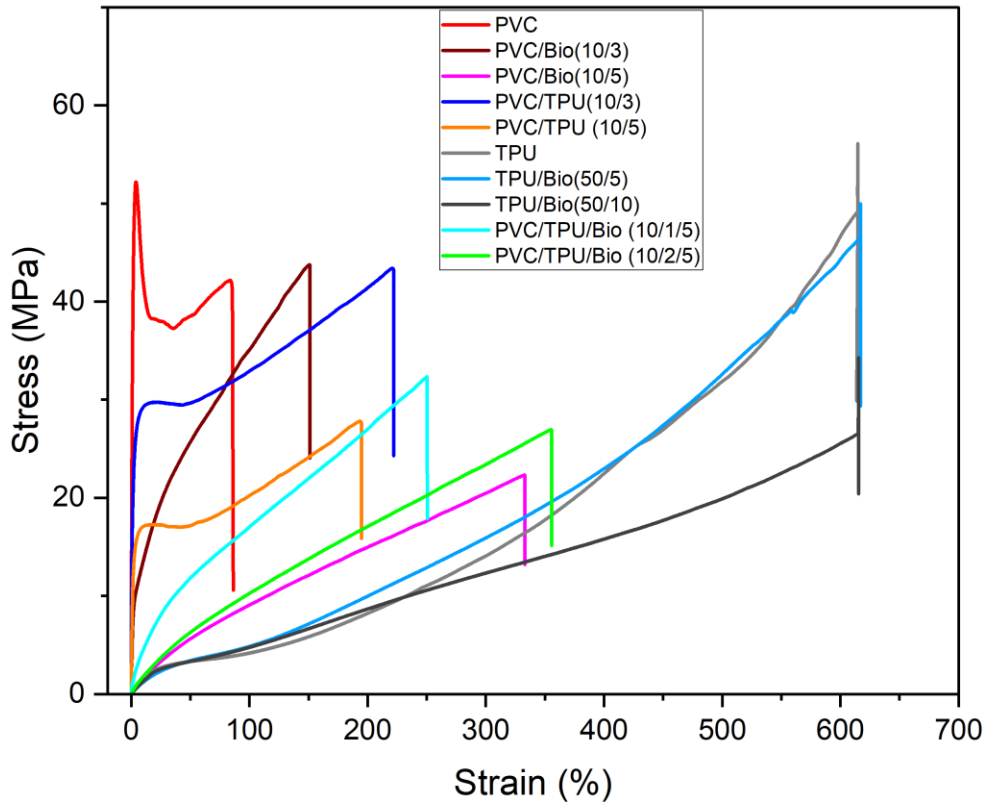

Figure 28. Stress-strain curves of the investigated polymer blends.

3.3.1. Tensile Strength

Tensile strength represents the maximum stress a material can withstand before fracture under tensile loading and is strongly influenced by intermolecular interactions, molecular mobility, and phase morphology [128]. The tensile strength values of the investigated blends are presented in Figure 29. Pure PVC exhibited a tensile strength of 52.2 MPa, reflecting the rigid nature of the PVC matrix and the strong intermolecular interactions between polymer chains. This behaviour is consistent with the relatively high glass transition temperature observed in the DMA analysis, where restricted segmental mobility contributes to increased structural rigidity.

Incorporation of the bio-plasticizer significantly reduced the tensile strength of PVC. The PVC/Bio (10/5) blend exhibited a tensile strength of 20.8 MPa due to enhanced chain mobility and reduced intermolecular cohesion within the PVC matrix. This behaviour correlates with the substantial

reduction in T_g observed in the DMA measurements. The resulting high flexibility makes this formulation suitable for applications such as flexible tubing, cable insulation, and soft packaging materials. Reducing the bio-plasticizer content to 30 phr resulted in a higher tensile strength of 44.3 MPa, indicating a more balanced combination of flexibility and mechanical integrity. This formulation may therefore be suitable for applications requiring moderate flexibility together with adequate mechanical strength, such as flexible flooring and medical-grade hoses.

Blending TPU with PVC also modified the mechanical response of the system. The PVC/TPU (10/3) blend exhibited a tensile strength of 43.3 MPa, suggesting that TPU contributes flexibility and toughness while PVC maintains structural stability. The DMA, TSD, and SEM analyses of this blend indicated significant intermolecular interaction with only minor phase heterogeneity. The balanced strength and toughness of this blend may be advantageous for applications such as protective films and automotive interior components. However, increasing the TPU content to PVC/TPU (10/5) reduced the tensile strength to 27.8 MPa. This reduction is associated with increased phase separation, as evidenced by the more pronounced low-temperature shoulder observed in the DMA and TSD analyses together with the heterogeneous morphology revealed by SEM. The resulting decrease in interfacial adhesion limits efficient stress transfer between the phases.

Pure TPU exhibited a tensile strength of 52.9 MPa, arising from its segmented structure in which the hard segments provide strength while the soft segments contribute elasticity. Incorporation of the bio-plasticizer progressively reduced the tensile strength of TPU, with TPU/Bio (50/5) and TPU/Bio (50/10) exhibiting strengths of 49.9 MPa and 34.2 MPa, respectively. This decrease reflects the increased molecular flexibility induced by the plasticizer.

The ternary PVC/TPU/bio-plasticizer blends exhibited a balanced combination of strength, flexibility, and elasticity. In these systems, PVC contributed rigidity, TPU imparted toughness and elastic behaviour, while the bio-plasticizer enhanced chain mobility and simultaneously improved compatibility between PVC and TPU, as confirmed by the DMA, TSD, FTIR, and SEM analyses. The improved phase homogeneity enabled the ternary blends to achieve enhanced flexibility while retaining moderate tensile strength, thereby overcoming the significant loss of mechanical performance typically associated with highly plasticized PVC systems. As a result, these ternary

blends hold strong potential for applications requiring a combination of flexibility, elasticity, and mechanical durability.

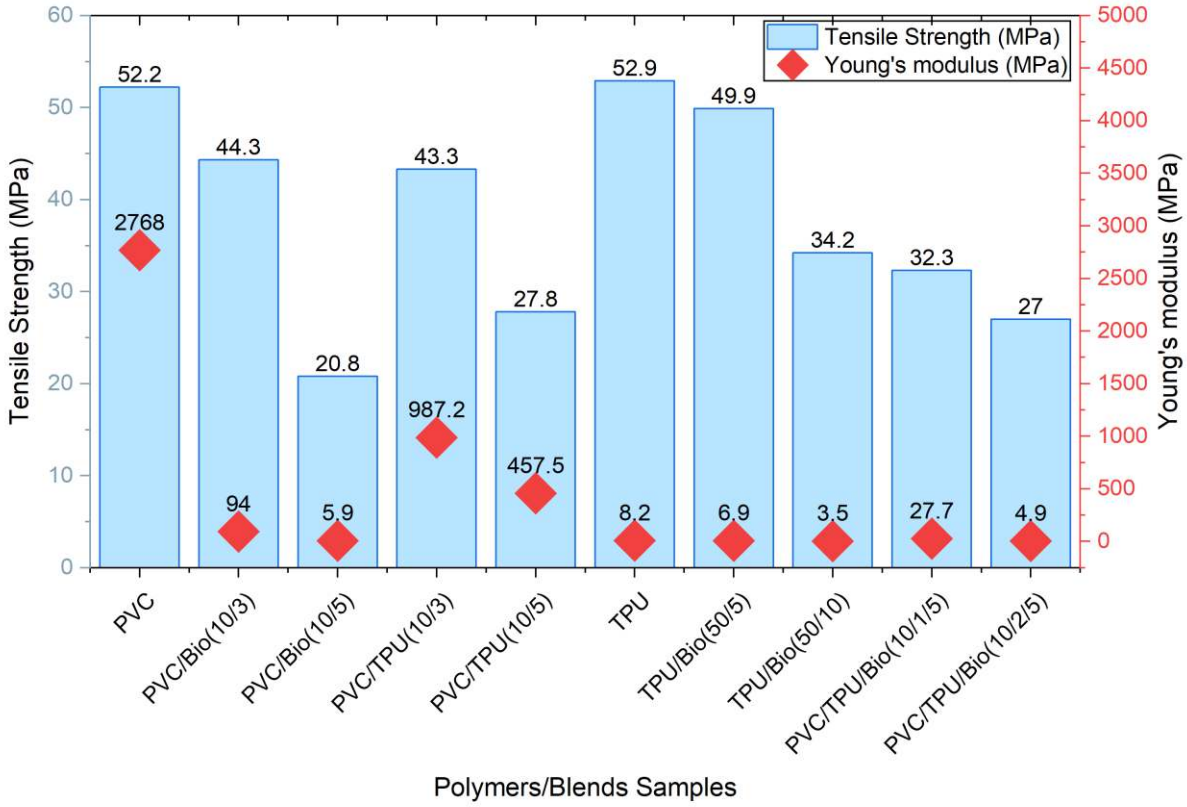

Figure 29. Tensile strength and Young's modulus of polymer blends with varying compositions.

3.3.2. Elasticity

Young's modulus describes the stiffness of a material and its resistance to elastic deformation under tensile loading. Higher modulus values correspond to greater rigidity, whereas lower values indicate increased elasticity and flexibility [129]. The variations in Young's modulus for the investigated blends are presented in Figure 29.

As observed from the stress-strain curves (Figure 28), pure PVC exhibited a steep initial slope corresponding to a high Young's modulus of 2768 MPa, reflecting its rigid structure and strong intermolecular interactions arising from the polar C–Cl groups along the polymer backbone. The high modulus is consistent with the DMA and TSD results, where PVC exhibited relaxation peaks

at relatively high temperatures, indicating restricted molecular mobility and a stiff polymer network. Such rigidity makes pure PVC suitable for structural and load-bearing applications.

Incorporation of the bio-plasticizer significantly reduced the stiffness of PVC. The Young's modulus decreased to 5.9 MPa for PVC/Bio (10/5), indicating substantial softening caused by increased free volume and reduced intermolecular cohesion within the PVC matrix. Reducing the bio-plasticizer content to 30 phr partially restored the modulus to 94 MPa, suggesting a more balanced combination of flexibility and structural integrity. This behavior is also reflected in the stress-strain curves, where PVC/Bio (10/3) exhibited an intermediate slope between rigid PVC and highly plasticized PVC.

The incorporation of TPU also reduced the modulus due to the elastomeric nature of TPU. Pure TPU exhibited a low modulus of 8.2 MPa, confirming its high elasticity and flexibility. In the PVC/TPU blends, the modulus progressively decreased with increasing TPU content. The PVC/TPU (10/3) blend retained a modulus of 987.2 MPa, indicating that PVC still preserved considerable structural rigidity while TPU introduced flexibility and toughness. Increasing the TPU content to PVC/TPU (10/5) further reduced the modulus to 457.5 MPa as the elastomeric characteristics of TPU became increasingly dominant.

Blending TPU with the bio-plasticizer produced an additional reduction in stiffness. TPU/Bio (50/5) exhibited a modulus of 6.9 MPa, while TPU/Bio (50/10) showed a further decrease to 3.5 MPa. This reduction is associated with enhanced chain mobility and reduced rigidity within the TPU hard-segment domains caused by plasticizer incorporation. The corresponding stress-strain curves displayed very low initial slopes, confirming the highly elastic nature of these formulations.

The ternary PVC/TPU/bio-plasticizer blends exhibited Young's modulus values of 27.7 MPa for PVC/TPU/Bio (10/1/5) and 4.9 MPa for PVC/TPU/Bio (10/2/5), demonstrating a synergistic combination of TPU elasticity and bio-plasticizer-induced molecular mobility. The improved compatibility and phase homogeneity previously confirmed by DMA, TSD, and SEM analyses contributed to the balanced mechanical response of these systems. While TPU and plasticized TPU inherently exhibit high elasticity, the ternary blends achieved substantial flexibility while utilizing the more rigid and economically favorable PVC matrix. Moreover, the ternary systems provided significant improvement in elasticity without severe loss of tensile strength compared with the binary PVC/bio-plasticizer and PVC/TPU blends. Such balanced mechanical behavior makes

these blends attractive for flexible engineering and soft polymer applications requiring repeated deformation and bending.

3.3.3. Elongation at Break

Elongation at break represents the ability of a material to deform under tensile loading before fracture and is commonly used as an indicator of flexibility and ductility [128]. The elongation at break values of the investigated blends are presented in Figure 30.

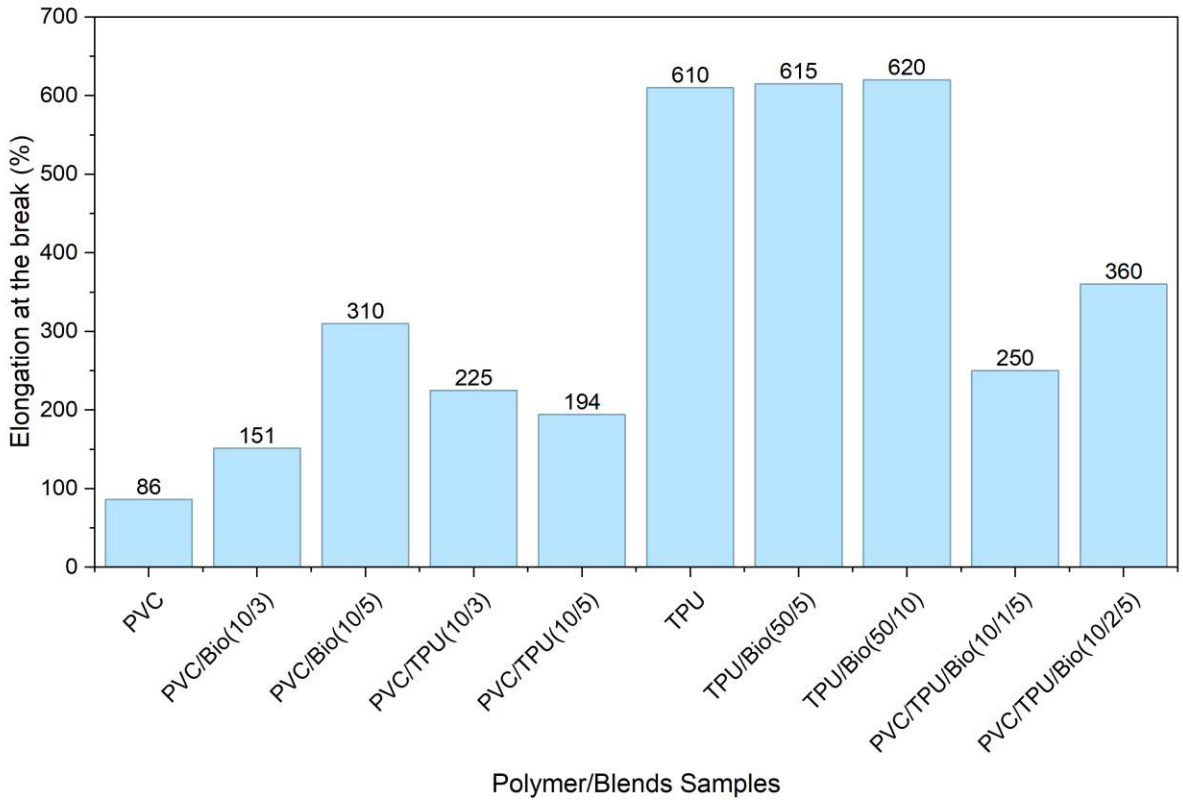

Figure 30. Elongation at break of polymer blends with varying compositions.

Pure PVC exhibited an elongation at break of 86%, reflecting its relatively rigid structure and restricted chain mobility. During tensile deformation, pronounced neck formation was observed (Figure 31a), indicating localized yielding prior to fracture, which is characteristic of rigid thermoplastic materials. The addition of the bio-plasticizer significantly increased the elongation at break of PVC. The PVC/Bio (10/5) blend exhibited an elongation of 310%, demonstrating the strong plasticization effect of the bio-plasticizer through enhanced chain mobility and reduced

intermolecular forces within the PVC matrix. In contrast to rigid PVC, the plasticized systems exhibited more uniform deformation without visible necking (Figure 31b), indicating improved stress distribution and enhanced flexibility. Reducing the bio-plasticizer content to 30 phr still maintained a relatively high elongation of 151%, confirming that even moderate plasticization substantially improves the ductility of PVC.

The PVC/TPU blends also exhibited significantly improved elongation compared with pure PVC. PVC/TPU (10/3) showed an elongation at break of 225%, indicating the effective contribution of TPU elasticity to the blend system. However, increasing the TPU content to PVC/TPU (10/5) slightly reduced the elongation to 194%. This reduction is associated with increased phase heterogeneity at higher TPU concentrations, as previously indicated by the DMA, TSD, and SEM analyses, which may limit efficient stress transfer and homogeneous deformation within the blend.

Pure TPU exhibited a very high elongation at break of 610%, reflecting the highly elastic nature of its segmented structure, where the soft segments allow extensive deformation while the hard segments preserve structural integrity. Incorporation of the bio-plasticizer further enhanced TPU flexibility, with TPU/Bio (50/5) and TPU/Bio (50/10) exhibiting elongations of 615% and 620%, respectively. These results indicate that the bio-plasticizer effectively enhances chain mobility within the TPU matrix without substantially compromising elastic recovery.

The ternary PVC/TPU/bio-plasticizer blends demonstrated a balanced combination of flexibility, elasticity, and structural integrity. PVC/TPU/Bio (10/2/5) exhibited an elongation at break of 360%, while PVC/TPU/Bio (10/1/5) showed a lower elongation of 250% due to the reduced TPU contribution. These results indicate that the simultaneous incorporation of TPU and the bio-plasticizer effectively improves the elasticity and elongation at break of PVC while maintaining moderate mechanical strength. The improved compatibility and phase homogeneity previously confirmed by DMA, TSD, and SEM analyses contributed significantly to the enhanced deformation behaviour of the ternary systems.

Another notable observation during tensile testing was the transition of the samples from transparent to a whitish appearance during deformation (Figure 31). This stress-induced whitening is attributed to crazing and microvoid formation within the polymer matrix, which scatter incident light [129]. In rigid PVC, whitening was highly localized within the necked region, whereas the plasticized and TPU-containing blends exhibited more uniform whitening patterns, reflecting their

more homogeneous deformation behaviour and improved stress distribution. Although this phenomenon does not directly influence the measured mechanical properties, it may serve as a useful qualitative indicator of strain distribution and deformation mechanisms within the blends.

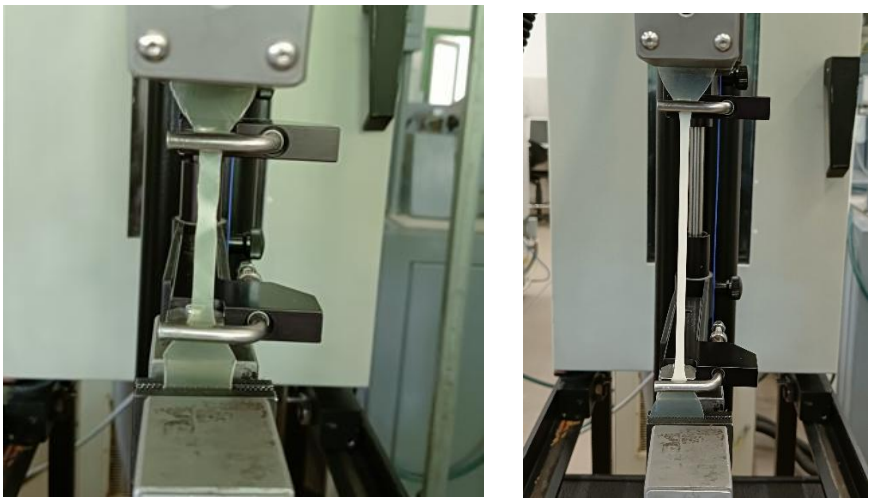

(a) (b)

Figure 31. (a) Stress localization and neck formation in rigid PVC; (b) Uniform deformation behaviour in plasticized PVC during tensile loading.

3.3.4. Hardness

Hardness describes the resistance of a material to surface deformation or indentation under an applied load [129]. In this research, both Shore A and Shore D hardness scales were used to evaluate the mechanical response of the blends over a broad hardness range. Shore A measurements were particularly suitable for softer and highly flexible formulations, whereas Shore D was more appropriate for rigid materials such as unplasticized PVC. The measured hardness values are summarized in Table 9 and illustrated in Figure 32.

Table 9. Shore A and Shore D hardness values of the investigated blend compositions.

Properties	PVC	PVC/Bio (10/3)	PVC/Bio (10/5)	PVC/TPU (10/3)	PVC/TPU (10/5)	TPU	TPU/Bio (50/5)	TPU/Bio (50/10)	PVC/TPU/ bio(10/1/5)	PVC/TPU/bio (10/2/5)
Hardness (Shore A)	97.78	84.2	87.2	98.6	98.4	85.6	79	77.4	80	81
Hardness (Shore D)	83	9.1	11.7	26.4	24.9	12.9	10.8	8.3	10.1	9.9

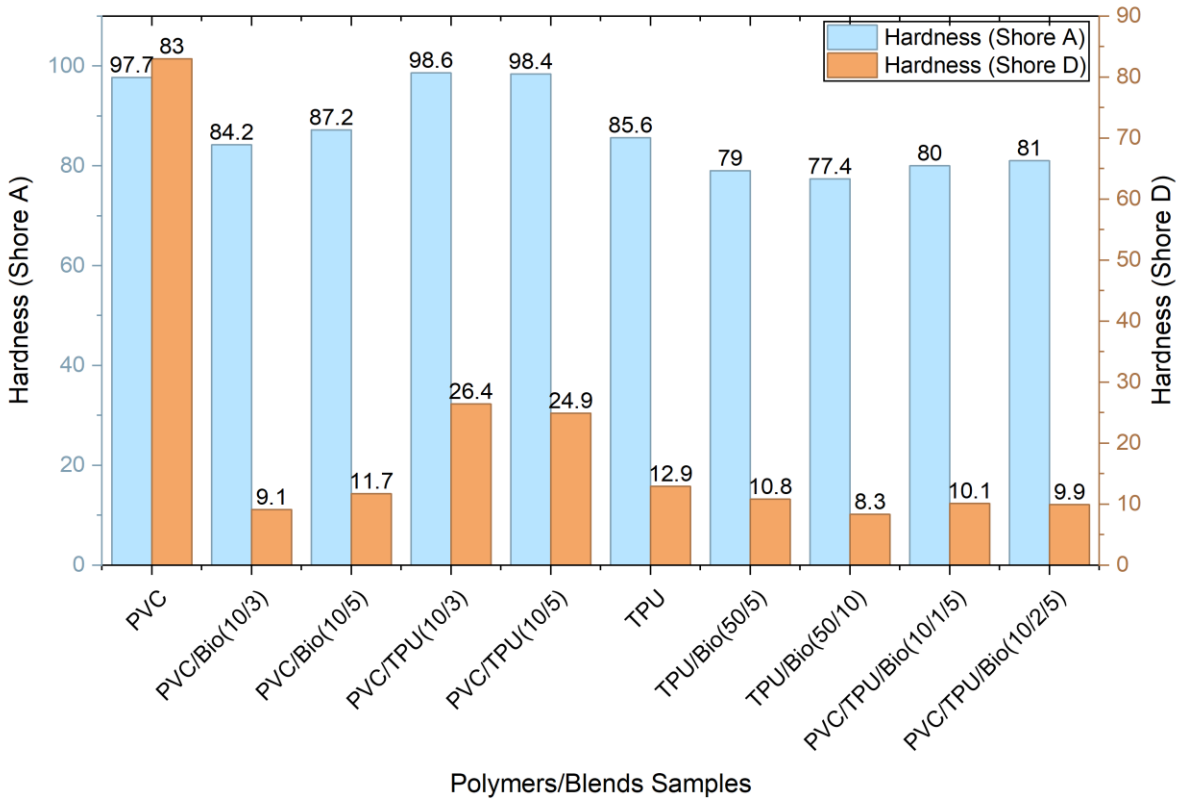

Figure 32. Shore A and Shore D hardness values of polymer blends with varying compositions.

Pure PVC exhibited the highest hardness among the investigated materials, reflecting its rigid molecular structure and strong intermolecular interactions that restrict surface deformation. This behaviour is consistent with the DMA and TSD analyses, where PVC exhibited relatively high glass transition temperatures together with limited molecular mobility. Incorporation of the bio-plasticizer caused a substantial reduction in hardness due to increased free volume and enhanced chain mobility within the PVC matrix. The resulting softening behaviour is therefore directly associated with the reduction in intermolecular cohesion and increased flexibility observed in the thermal relaxation analyses.

The incorporation of TPU into PVC also reduced the hardness of the blends while simultaneously introducing greater elasticity and resilience. Owing to its segmented structure consisting of flexible soft segments and reinforcing hard segments, TPU balanced the rigidity of PVC with elastomeric flexibility, resulting in blends with intermediate hardness values.

Blends containing both TPU and the bio-plasticizer exhibited a progressive decrease in hardness with increasing plasticizer content. The combined effect of TPU elasticity and bio-plasticizer-induced softening produced a broad range of tunable hardness values, demonstrating the ability to tailor the mechanical response of the blends through composition adjustment.

3.3.5. Conclusion

The mechanical properties of the investigated blends demonstrated that the combined incorporation of TPU and the bio-plasticizer enables effective tuning of tensile strength, elasticity, elongation at break, and hardness over a broad range that could not be achieved by the individual components alone. Incorporation of the bio-plasticizer significantly increased chain mobility and flexibility, leading to reduced tensile strength, Young's modulus, and hardness, while substantially improving elongation at break. TPU incorporation also enhanced elasticity and elongation at break through its elastomeric segmented structure; however, excessive TPU content resulted in partial phase heterogeneity, which limited stress transfer efficiency and reduced mechanical performance in some binary blends.

The ternary PVC/TPU/bio-plasticizer systems exhibited the most balanced mechanical behaviour, combining the rigidity of PVC, the elasticity of TPU, and the flexibility induced by the bio-plasticizer. These blends achieved substantial improvements in elasticity and elongation without severe loss of tensile strength, while also providing tunable hardness characteristics. Importantly, the ternary systems achieved mechanical flexibility and elasticity comparable to TPU-rich materials while utilizing the more cost-effective PVC matrix, thereby reducing reliance on higher-cost elastomeric components. The enhanced mechanical performance of the ternary blends is consistent with the improved compatibility and phase homogeneity previously confirmed by DMA, TSD, FTIR, and SEM analyses. Overall, the results demonstrate that the bio-plasticizer not only improves flexibility and molecular mobility but also promotes more effective interaction between PVC and TPU, enabling the development of flexible PVC-based systems with balanced mechanical properties and tunable performance characteristics.

3.4. Thermal Behavior and Stability

3.4.1. Dehydrochlorination Resistance of PVC-Containing Blends

The thermal stability of the PVC-containing blends was evaluated by monitoring the conductivity-time behavior associated with hydrogen chloride (HCl) evolution during thermal degradation. The conductivity curves of neat PVC and PVC-based binary and ternary blends are presented in Figure 33. The thermal stability time was determined from the inflection point of each conductivity curve, corresponding to the transition into the rapid autocatalytic stage of PVC dehydrochlorination. Minor conductivity increases observed at earlier times may result from trace HCl release from thermally labile sites; however, these do not represent the rapid degradation stage. Therefore, the stability time reflects the point at which HCl evolution accelerates and was used as a comparative measure of resistance to dehydrochlorination [130].

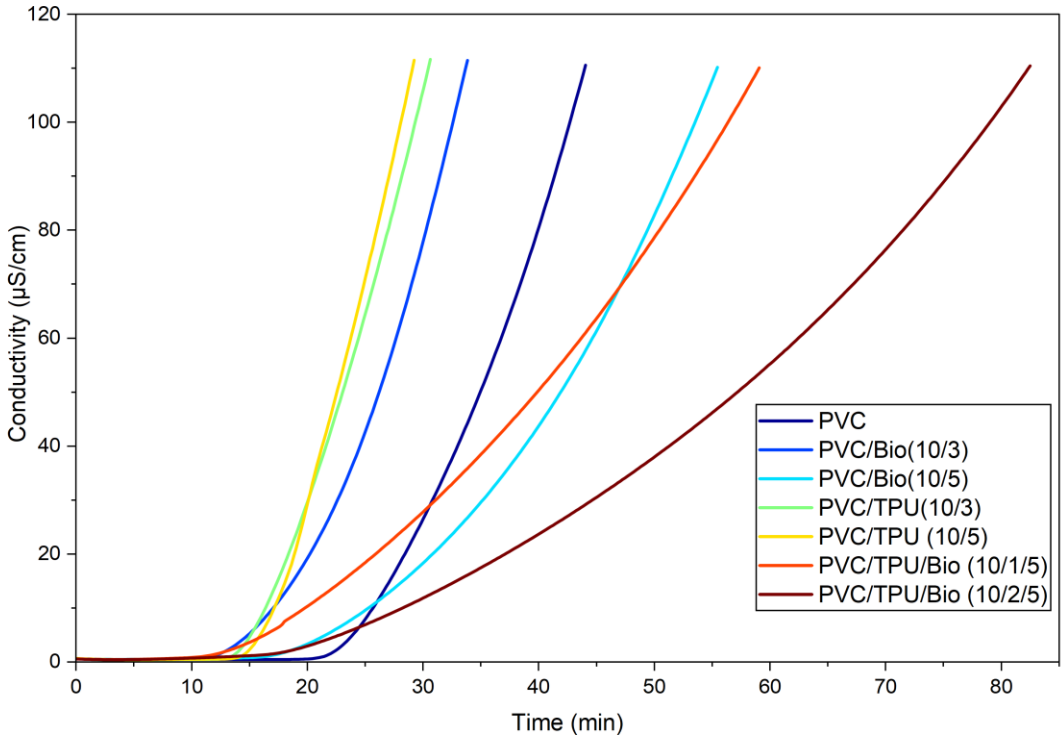

Figure 33. Conductivity–time curves of PVC and PVC-containing blends.

Neat PVC exhibited a thermal stability time of 35.2 min, corresponding to the onset of rapid autocatalytic dehydrochlorination. Incorporation of the bio-plasticizer at lower concentration, PVC/Bio (10/3), reduced the stability time to 26.4 min, indicating earlier initiation of degradation

due to increased segmental mobility and facilitated C–Cl bond cleavage. However, increasing the plasticizer content to 50 phr, PVC/Bio (10/5), increased the stability time to 42.2 min, suggesting that modifications in the local molecular environment at higher plasticizer concentrations partially counteract the mobility effect and delay dehydrochlorination.

The incorporation of TPU alone resulted in a considerable reduction in thermal stability. Both PVC/TPU (10/3) and PVC/TPU (10/5) exhibited stability times of approximately 23 min, significantly lower than that of neat PVC. This reduction is consistent with the partial phase heterogeneity observed by SEM and the relaxation behaviour detected by DMA and TSD analyses, which may facilitate localized degradation and accelerate dehydrochlorination.

In contrast, the ternary PVC/TPU/bio-plasticizer blends exhibited substantially improved thermal stability. The stability times increased to 40.2 min for PVC/TPU/Bio (10/1/5) and 57.7 min for PVC/TPU/Bio (10/2/5), indicating a pronounced delay in HCl evolution. This improvement is consistent with the enhanced compatibility and phase homogeneity previously confirmed by DMA, TSD, FTIR, and SEM analyses. The more uniform molecular environment and improved interphase interactions within the ternary systems appear to reduce the susceptibility of PVC chains to rapid autocatalytic degradation.

Overall, the results demonstrate that the thermal stability of PVC-based blends is governed not only by molecular mobility but also by the overall phase structure and intermolecular interactions within the system. While TPU or plasticization alone may accelerate degradation, their combined incorporation in the ternary blends effectively improved resistance to dehydrochlorination and delayed the onset of rapid thermal degradation.

3.4.2. Thermogravimetric Analysis (TGA and DTG)

Thermogravimetric analysis was employed to investigate the thermal decomposition behaviour of PVC, TPU, and representative binary and ternary blend systems. Selected compositions were analysed to identify the dominant degradation characteristics and to complement the thermal stability trends obtained from the conductivity-based dehydrochlorination measurements.

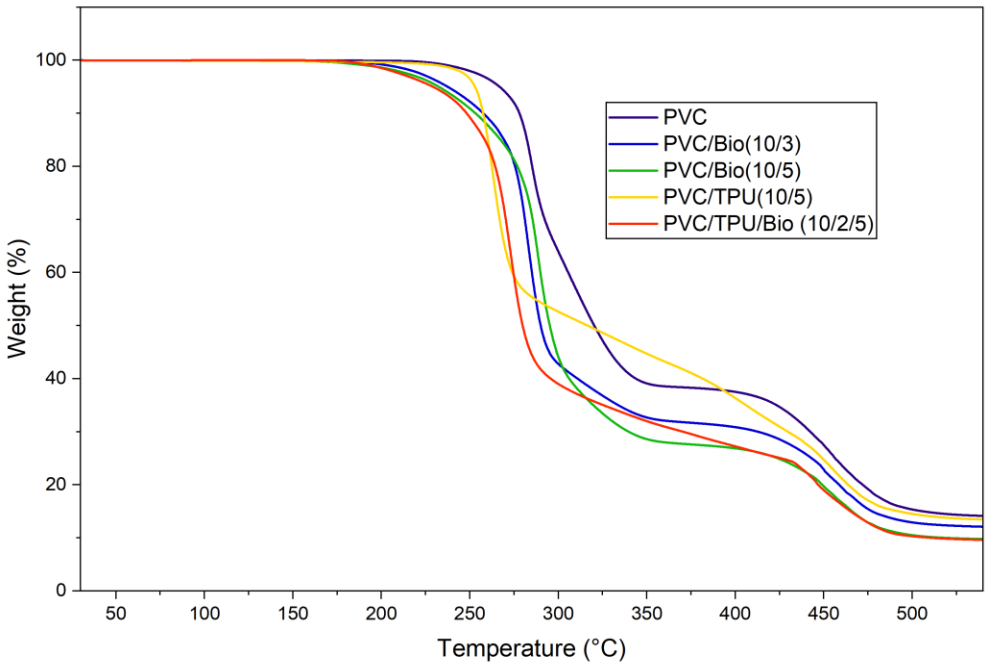

Figure 34. Thermogravimetric (TG) curves of PVC and selected PVC-containing blends.

The TG curves shown in Figure 34 reveal the characteristic multi-step degradation behaviour of PVC and PVC-containing blends. Neat PVC exhibited an initial major mass-loss stage beginning near 270 °C, corresponding to dehydrochlorination and formation of conjugated polyene sequences, followed by a second degradation stage associated with backbone decomposition and char formation. The relatively high residual mass is attributed to the formation of carbonaceous char promoted by chlorine-containing structures.

Incorporation of the bio-plasticizer modified the degradation profile of PVC in a composition-dependent manner. At lower plasticizer content, PVC/Bio (10/3) exhibited a slight shift of the degradation onset toward lower temperatures, consistent with increased chain mobility and facilitated degradation initiation. In contrast, PVC/Bio (10/5) displayed a more continuous mass-loss transition across the primary degradation region, suggesting redistribution of degradation processes rather than simple acceleration of degradation. This behaviour is consistent with the delayed HCl evolution observed in the conductivity-based thermal stability measurements.

The PVC/TPU (10/5) blend exhibited a broadened degradation region due to overlapping decomposition contributions from PVC and TPU. Although TPU did not suppress the initial

degradation stage of PVC, its incorporation moderated the sharp mass-loss behaviour characteristic of neat PVC, resulting in a more gradual decomposition profile. A further modification was observed in the ternary PVC/TPU/Bio (10/2/5) blend. Although the initial degradation onset occurs within a temperature range similar to that of the binary systems, the mass-loss behavior exhibits a smoother and more continuous transition throughout the main degradation region, suggesting a redistribution of degradation processes rather than a direct shift in onset temperature. This behavior indicates modified degradation kinetics resulting from changes in the molecular environment of the ternary blend.

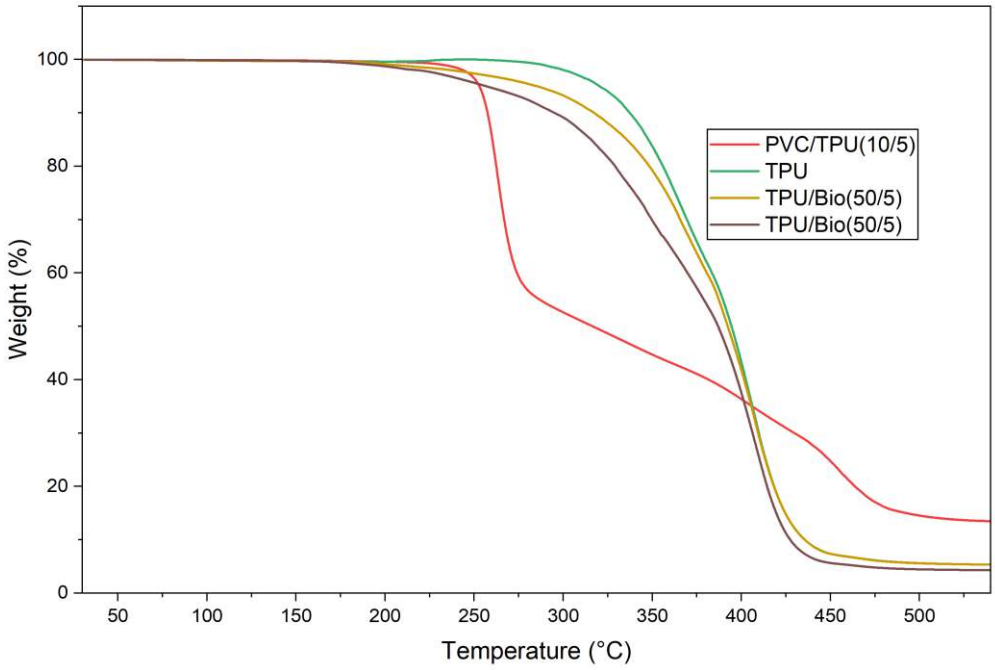

Figure 35. Thermogravimetric (TG) curves of TPU-based systems and PVC/TPU blends.

The TG curves of the TPU-based systems are presented in Figure 35. Neat TPU exhibited a dominant single-step degradation process at higher temperatures than PVC, corresponding mainly to degradation of urethane linkages followed by decomposition of the segmented TPU structure. Incorporation of the bio-plasticizer caused a modest shift of the degradation process toward lower temperatures, reflecting increased molecular mobility together with the lower thermal resistance of the plasticizer. The PVC/TPU blend exhibited a combined degradation profile containing

contributions from both PVC and TPU, with the initial degradation dominated by PVC and the broader high-temperature degradation region associated with TPU decomposition.

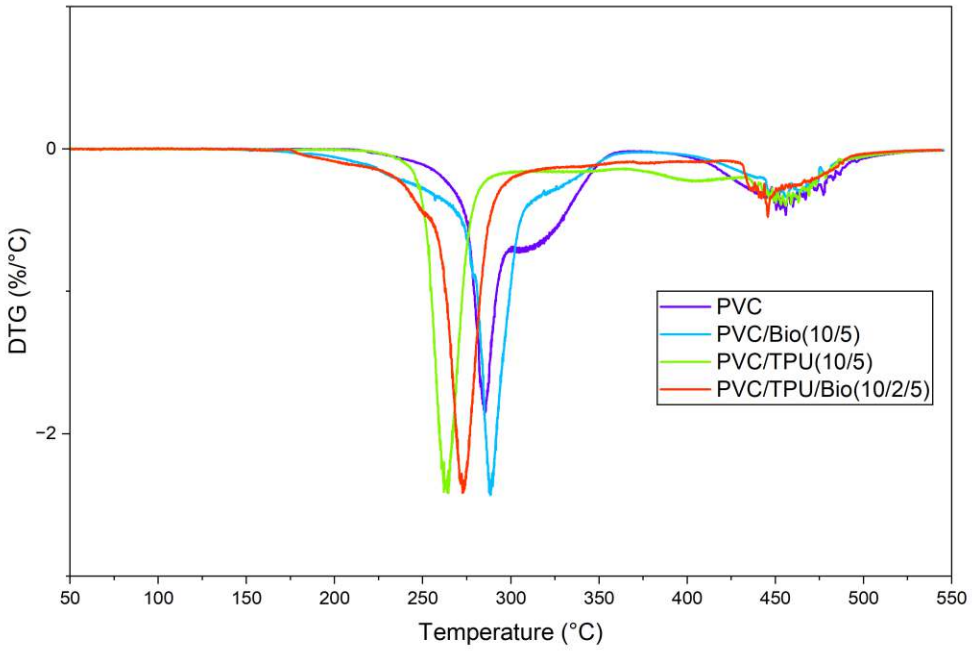

Figure 36. Derivative thermogravimetric (DTG) curves of selected PVC-based systems.

The DTG curves shown in Figure 36 provide additional insight into the degradation kinetics of the investigated systems. Neat PVC exhibited a sharp primary DTG peak corresponding to dehydrochlorination, followed by a broader secondary degradation peak associated with decomposition of the conjugated backbone [131]. In the PVC/Bio (10/5) blend, the primary degradation peak became broader, indicating redistribution of degradation processes caused by modified intermolecular interactions. The PVC/TPU (10/5) blend exhibited partial asymmetry of the primary degradation peak due to overlapping degradation events originating from PVC and TPU. Notably, the ternary PVC/TPU/Bio (10/2/5) blend exhibited further broadening and attenuation of the primary DTG peak and smoother transitions between degradation stages, consistent with suppression of rapid autocatalytic dehydrochlorination observed in the conductivity-based thermal stability measurements.

Overall, the TG and DTG analyses demonstrated that the thermal degradation characteristics of the blends are governed not only by the intrinsic thermal stability of the individual components

but also by intermolecular interactions and phase morphology within the system. The bio-plasticizer plays an important role in modifying the molecular environment and degradation kinetics, thereby contributing to the improved thermal stability behaviour observed in the ternary blends.

3.4.3. Conclusion

The conductivity-based thermal stability and TG/DTG analyses demonstrated that the thermal degradation behaviour of the investigated blends is strongly influenced by blend composition, intermolecular interactions, and phase morphology. Incorporation of the bio-plasticizer or TPU individually altered the thermal stability of PVC by modifying molecular mobility and the local degradation environment. While lower bio-plasticizer contents and TPU incorporation accelerated the initiation of degradation and reduced dehydrochlorination resistance, higher bio-plasticizer content resulted in delayed HCl evolution and more gradual degradation behaviour. The TG and DTG analyses further showed that these modifications were associated with redistribution and broadening of the degradation processes rather than simple shifts in degradation onset temperatures.

The ternary PVC/TPU/bio-plasticizer systems exhibited the most favourable thermal stability behaviour, showing delayed dehydrochlorination, smoother mass-loss transitions, and attenuation of the sharp DTG degradation peaks characteristic of neat PVC. These improvements are consistent with the enhanced compatibility and phase homogeneity previously confirmed by DMA, TSD, FTIR, and SEM analyses. Overall, the thermal analyses confirmed that the combined incorporation of TPU and the bio-plasticizer improves not only the flexibility and mechanical performance of PVC-based systems but also modifies the degradation behaviour in a manner that suppresses rapid autocatalytic degradation, thereby enhancing the overall thermal stability of the ternary blends.

4. General Conclusions

This dissertation investigated the development of sustainable PVC/TPU/bio-plasticizer blend systems using glycerol diacetate monolaurate derived from waste cooking oil as an alternative to conventional phthalate-based plasticizers. The study was motivated by the need to overcome the inherent rigidity, brittleness, and limited thermal stability of PVC while simultaneously reducing dependence on potentially toxic petroleum-based plasticizers and high-cost elastomeric materials.

The research combined thermodynamic compatibility prediction with comprehensive experimental validation in order to establish relationships among intermolecular interactions, molecular mobility, phase morphology, and the resulting mechanical and thermal behaviour of the developed blend systems. Thermodynamic compatibility between PVC and TPU systems was first evaluated using swelling experiments and solubility parameter analysis. Since thermodynamic prediction alone cannot fully guarantee compatibility in polymer systems, complementary post-processing analyses were subsequently employed to investigate the developed blends.

Dynamic mechanical analysis (DMA), thermally stimulated discharge (TSD) analysis, Fourier transform infrared spectroscopy (FTIR), and scanning electron microscopy (SEM) were used to evaluate compatibility behaviour, intermolecular interactions, relaxation characteristics, and phase morphology. Particular emphasis was placed on the application of TSD analysis because of its high sensitivity toward localized molecular mobility and intermolecular interactions in polymer systems. Mechanical characterization was performed to investigate tensile strength, elasticity, elongation at break, and hardness, while thermal stability and degradation behaviour were examined using conductivity-based thermal stability measurements and thermogravimetric analysis.

The results demonstrated that blending PVC with TPU and glycerol diacetate monolaurate significantly modified the mechanical and thermal behaviour of the systems. The developed blends exhibited improved flexibility, elasticity, elongation at break, and toughness compared with unmodified PVC systems, while maintaining useful structural and thermal characteristics. The study further showed that compatibility behaviour strongly influenced the final performance of the blends through its effect on intermolecular interaction, molecular mobility, and phase morphology.

The dissertation also demonstrated the importance of integrating thermodynamic compatibility prediction with complementary experimental techniques for reliable evaluation of polymer blend systems. The combined use of swelling-based solubility parameter analysis together with relaxation, spectroscopic, morphological, mechanical, and thermal analyses provided a more comprehensive understanding of compatibility behaviour from molecular to macroscopic scales.

Overall, this research contributes to the development of flexible, thermally balanced, and more sustainable PVC-based materials while advancing understanding of compatibility behaviour in multicomponent polymer systems. In addition, the use of glycerol diacetate monolaurate derived from waste cooking oil provides both environmental and sustainability benefits by reducing reliance on conventional phthalate plasticizers and promoting the valorization of underutilized waste resources.

4.1. Future Perspectives and Industrial Relevance

This research contributes toward the development of flexible and thermally balanced PVC-based materials by combining the complementary properties of PVC and TPU while reducing reliance on high-cost elastomeric systems and conventional phthalate plasticizers. The results demonstrated that PVC, TPU, and bio-plasticizer blends are both thermodynamically and technologically compatible, and that the developed systems exhibit combinations of properties that could not be achieved by the individual components alone.

Rather than targeting a single end-use product, the study establishes fundamental compatibility-property relationships and sustainable formulation strategies for PVC/TPU/bio-plasticizer blends. The tunable mechanical and thermal characteristics demonstrated in this work provide a framework for designing materials with balanced rigidity, elasticity, toughness, and thermal stability for a broad range of potential industrial applications.

For example, the PVC/TPU/Bio (10/2/5) blend formulation showed significant improvement in elasticity and elongation at break without substantial reduction in tensile strength, suggesting potential suitability for applications requiring repeated deformation and bending, such as flexible cables subjected to repeated bending and deformation. Similarly, by adjusting blend composition, other formulations can be optimized for different applications depending on the required combination of mechanical, thermal, electrical, and chemical resistance properties.

The verified thermodynamic and technological compatibility established in this research provides a strong foundation for further formulation optimization and application-oriented material design in PVC/TPU/bio-plasticizer systems. Future work may therefore focus on comprehensive property mapping across broader blend compositions in order to identify optimized formulations for specific applications. In this regard, the collaboration established during this research with BorsodChem may provide opportunities for future industrial-scale implementation of the developed formulations and processing strategies.

5. New Scientific Results (Claims)

Based on the results and analyses presented in this dissertation, several major scientific findings and original contributions are established. The following claims are derived from the integrated investigation of compatibility, intermolecular interactions, molecular mobility, phase morphology, and the resulting mechanical and thermal behaviour of the developed blend systems.

Claim 1

A thermodynamic compatibility evaluation methodology based on swelling experiments and solubility parameter analysis was established and successfully applied to predict the compatibility of PVC with different TPU systems prior to processing. The results demonstrated that PVC exhibits strong compatibility with polyester-based TPU and comparatively weaker compatibility with polyether-based TPU. The predicted compatibility behaviour was validated through processing behaviour, where PVC/polyester-based TPU blends formed homogeneous sheets while PVC/polyether-based TPU blends produced defective and non-uniform structures, and was further confirmed through the unified relaxation behaviour observed in DMA and TSD analyses.

Claim 2

The bio-based plasticizer, glycerol diacetate monolaurate derived from waste cooking oil, enhances compatibility between PVC and polyester-based TPU through modification of intermolecular interactions and phase morphology. DMA and TSD analyses revealed disappearance of the partial phase-separated relaxation shoulder observed in binary blends, FTIR analysis indicated intermolecular interactions involving polar functional groups, and SEM observations confirmed improved phase homogeneity in the ternary systems. These findings demonstrated that the bio-plasticizer acts not only as a plasticizing agent but also as a compatibilizing component within the ternary blend system.

Claim 3

The ternary PVC/TPU/bio-plasticizer systems achieved balanced mechanical performance through substantial improvements in elasticity, flexibility, and elongation at break while maintaining moderate tensile strength and tunable hardness within a PVC-rich matrix. The results further demonstrated that improved compatibility and phase homogeneity directly govern the mechanical behaviour and deformation characteristics of the blends, enabling elastomer-like elasticity while

retaining the more cost-effective PVC matrix rather than relying solely on higher elastomer content.

Claim 4

The combined incorporation of polyester-based TPU and the bio-based plasticizer improved the thermal stability behaviour of PVC-based systems through modification of the molecular environment and suppression of rapid autocatalytic degradation. Conductivity-based thermal stability measurements revealed delayed dehydrochlorination and extended thermal stability times in the ternary blends, while TG and DTG analyses showed smoother degradation behaviour, redistribution of degradation processes, and attenuation of the sharp degradation behaviour associated with neat PVC. These improvements were consistent with the enhanced intermolecular interactions and improved phase homogeneity established through the relaxation, spectroscopic, and morphological analyses.

Claim 5

The bio-based plasticizer exhibited a concentration-dependent dual effect on the segmental mobility of TPU systems, enhancing molecular mobility at lower concentrations while progressively restricting segmental motion at higher concentrations due to the increasing influence of the higher-T_g bio-plasticizer on TPU segmental dynamics. This behavior reveals the complex role of the bio-plasticizer in governing TPU molecular dynamics and indicates that its influence extends beyond conventional plasticization behaviour.

List of Publications

1) **Yitbarek Firew Minale**, Ivan Gajdoš, Pavol Štefčák, Ľudmila Dulebová, Tomasz Jachowicz, Tamás Szabó, Annamaria Polyákné Kovács, Andrea Ádámné Major, Kálmán Marossy, ″Thermodynamic and Technological Compatibility of Polyvinyl Chloride, Thermoplastic Polyurethane, and Bio-Plasticizer Blends″, *Polymers*, 2025, 17, doi: https://doi.org/10.3390/polym17091149 **(Q1)**

2) **Yitbarek Firew Minale**, Ivan Gajdoš, Pavol Štefčák, Tamás Szabó, Annamaria Polyákné Kovács, Andrea Ádámné Major, Kálmán Marossy, ″Mechanical Properties of PVC/TPU Blends Enhanced with a Sustainable Bio-Plasticizer″, *Sustainability*, 2025, 17, doi: https://doi.org/10.3390/su17052033 **(Q2)**

3) **Yitbarek Firew Minale**, Ivan Gajdoš, Tamás Szabó, Annamaria Polyákné Kovács, Andrea Ádámné Major, Kálmán Marossy, Grzegorz Janowski, ″Thermal Behavior and Stability of PVC/TPU Blends Plasticized with a Bio-Based Plasticizer″, *Thermo,* 2026, 6, doi: https://doi.org/10.3390/thermo6020026 s **(Q2)**

4) **Yitbarek Firew Minale**, Ivan Gajdoš, Tamas Szabo, Annamaria Polyákné Kovács, Kálmán Marossy, Andrea Ádámné Major, ″Segmental Dynamics and Thermo-Mechanical Response of PVC/TPU Blends Plasticized with a Bio-Based Plasticizer″, NOVUS SCIENTIA Conference Proceedings, 2026.

5) **Yitbarek Firew Minale**, Kálmán Marossy, Andrea Ádámné Major, Annamária Polyákné Kovács, ″Miscibility of PVC/PU Based Blends: a mini- review″, *Doktorandusz Almanach*, 2023, 2, pp. 21-27.

6) **Yitbarek Firew Minale**, Anmaw Getahun Alelgn, Annamária Polyákné Kovács, Ivan Gajdoš, Kálmán Marossy, Andrea Major, ″Optimizing Processing Temperatures of PET in Injection Moulding: A Time-Temperature History Approach for Waste Reduction″, *Doktorandusz Almanach*, 2023, 2, pp. 45-52.

Conference presentations

1) **Yitbarek Firew Minale**, Marossy Kálmán, *Oral presentation*, Enhancing the Mechanical Properties of PVC/TPU Blends Using a Sustainable Bio-Plasticizer, MultiScience - XXXVIII. microCAD International Multidisciplinary Scientific Conference, Miskolc, Hungary, May 29th, 2025.

2) **Yitbarek Firew Minale**, Kálmán Marossy, Andrea Ádámné Major, Annamaria Polyákné Kovács, *Oral presentation*, Determining Miscibility of Polyblends through Swelling Measurements, 4th International Conference on Engineering and Applied Natural Sciences (ICEANS 2024), Konya, Turkey, August 25th, 2024.

3) **Yitbarek Firew Minale**, Kálmán Marossy, *Oral presentation*, Predicting the Thermodynamic Compatibility of PVC based Ternary Blends, microCAD International Multidisciplinary Scientific Conference, Miskolc, Hungary, May 30th, 2024.

4) **Yitbarek Firew Minale**, Kálmán Marossy, Andrea Ádámné Major, Annamaria Polyákné Kovács, *Oral presentation*, Compatibility and Mechanical Properties of PVC Based Ternary Blends, Hungarian Science Day, University of Miskolc, Miskolc, Hungary, November 14th, 2023.

5) **Yitbarek Firew Minale**, Kálmán Marossy, Andrea Ádámné Major, Annamaria Polyákné Kovács, *Oral presentation*, Investigigating the Compatibility of PVC Based Ternary Blends, XXIII. PhD Student Materials Science Day (Anyagtudományi Nap), Veszprém, Hungary, November 20th, 2023.

6) **Yitbarek Firew Minale**, Kálmán Marossy, Andrea Ádámné Major, Annamaria Polyákné Kovács, *Oral presentation*, Investigigating the Mechanical Properties of PVC Based Ternary Blends, 9th International Scientific Conference on Advances in Mechanical Engineering (ISCAME), Debrecen, Hungary, November 10th, 2023.

Reference

[1] L. Robeson, Historical perspective of advances in the science and technology of polymer blends. Polymers, 6 (2014) 1251-1265. https://doi.org/10.3390/polym6051251

[2] Z. Chen, T. Li, Y. Yang, X. Liu, and R. Lv, Mechanical and tribological properties of PA/PPS blends. Wear, 257 (2004) 696-707. https://doi.org/10.1016/j.wear.2004.03.013

[3] H. A. Mannan, H. Mukhtar, T. Murugesan, R. Nasir, D. F. Mohshim, and A. Mushtaq, Recent applications of polymer blends in gas separation membranes. Chemical Engineering & Technology, 36 (2013) 1838-1846. https://doi.org/10.1002/ceat.201300342

[4] L. Utracki, Economics of polymer blends. Polymer Engineering & Science, 22 (1982) 1166-1175. https://doi.org/10.1002/pen.760221717

[5] J. Ramiro, J. Eguiazabal, and J. Nazabal, Synergistic mechanical behaviour and improved processability of poly (ether imide) by blending with poly (trimethylene terephthalate). Polymers for Advanced Technologies, 14 (2003) 129-136. https://doi.org/10.1002/pat.340

[6] V. Siracusa, S. Karpova, A. Olkhov, A. Zhulkina, R. Kosenko, and A. Iordanskii, Gas transport phenomena and polymer dynamics in PHB/PLA blend films as potential packaging materials. Polymers, 12 (2020) 647. https://doi.org/10.3390/polym12030647

[7] J. Muller, C. González-Martínez, and A. Chiralt, Combination of poly (lactic) acid and starch for biodegradable food packaging. Materials, 10 (2017) 952. https://doi.org/10.3390/ma10080952

[8] S. S. Murthe, S. Sreekantan, and R. B. S. Mydin, Study on the physical, thermal and mechanical properties of SEBS/PP (styrene-ethylene-butylene-styrene/polypropylene) blend as a medical fluid bag. Polymers, 14 (2022) 3267. https://doi.org/10.3390/polym14163267

[9] K. F. Hasan *et al.*, Advanced Bioinspired Personal Thermoregulation Textiles for Outdoor Radiative Cooling. ACS Applied Materials & Interfaces, (2025). https://doi.org/10.1021/acsami.4c18812

[10] K. Lewandowski and K. Skórczewska, A brief review of poly (vinyl chloride)(PVC) recycling. Polymers, 14 (2022) 3035. https://doi.org/10.3390/polym14153035

[11] G. I. Edo *et al.*, Poly (vinyl chloride)(PVC): an updated review of its properties, polymerization, modification, recycling, and applications. Journal of Materials Science, 59 (2024) 21605-21648. https://doi.org/10.1007/s10853-024-10471-4

[12] N. Kumari, C. Mohan, and A. Negi, An investigative study on the structural, thermal and mechanical properties of clay-based PVC polymer composite films. Polymers, 15 (2023) 1922. https://doi.org/10.3390/polym15081922

[13] B. S. Rajput, T. A. P. Hai, and M. D. Burkart, High bio-content thermoplastic polyurethanes from azelaic acid. Molecules, 27 (2022) 4885. https://doi.org/10.3390/molecules27154885

[14] F. Chiellini, M. Ferri, A. Morelli, L. Dipaola, and G. Latini, Perspectives on alternatives to phthalate plasticized poly (vinyl chloride) in medical devices applications. Progress in polymer science, 38 (2013) 1067-1088. https://doi.org/10.1016/j.progpolymsci.2013.03.001

[15] K. Khosravi and G. W. Price, Determination of phthalates in soils and biosolids using accelerated solvent extraction coupled with SPE cleanup and GC–MS quantification. Microchemical Journal, 121 (2015) 205-212. https://doi.org/10.1016/j.microc.2015.03.013

[16] P. Jia, M. Zhang, L. Hu, and Y. Zhou, Green plasticizers derived from soybean oil for poly (vinyl chloride) as a renewable resource material. Korean journal of chemical engineering, 33 (2016) 1080-1087. https://doi.org/10.1007/s11814-015-0213-9

[17] P. Somdee, T. Lassu-Kuknyo, C. Konya, T. Szabo, and K. Marossy, Thermal analysis of polyurethane elastomers matrix with different chain extender contents for thermal conductive application. Journal of Thermal Analysis and Calorimetry, 138 (2019) 1003-1011. https://doi.org/10.1007/s10973-019-08183-y

[18] E. H. Backes *et al.*, Thermoplastic polyurethanes: synthesis, fabrication techniques, blends, composites, and applications. Journal of Materials Science, 59 (2024) 1123-1152. https://doi.org/10.1007/s10853-023-09077-z

[19] J. Oh *et al.*, Synthesis of thermoplastic polyurethanes containing bio-based polyester polyol and their fiber property. Polymers, 14 (2022) 2033. https://doi.org/10.3390/polym14102033

[20] M. F. Sonnenschein, *Polyurethanes: science, technology, markets, and trends*. John Wiley & Sons, 2021.

[21] S. D. Satavalekar, P. B. Savvashe, and S. T. Mhaske, Triester–amide based on thiophene and ricinoleic acid as an innovative primary plasticizer for poly (vinyl chloride). RSC advances, 6 (2016) 115101-115112. https://doi.org/10.1039/C6RA20098B

[22] C. A. da Silva *et al.*, Biodiesel and bioplastic production from waste-cooking-oil transesterification: An environmentally friendly approach. Energies, 15 (2022) 1073. https://doi.org/10.3390/en15031073

[23] K. Román and G. Zsoldos, PVC/LDPE Blends: Relationship Between Thermal/Mechanical Properties, Structure and Blend Behaviour. International Journal of Engineering and Management Sciences, 4 (2019) 162-165. https://doi.org/10.21791/IJEMS.2019.1.20.

[24] D. Paul, Strategies for Compatibilization of Polymer Blends. Advances in Polymer Blends and Alloys Technology, 4 (1993) 80-80. https://doi.org/10.1016/S0079-6700(97)00054-3

[25] B. A. Miller-Chou and J. L. Koenig, A review of polymer dissolution. Progress in polymer science, 28 (2003) 1223-1270. https://doi.org/10.1016/S0079-6700(03)00045-5

[26] K. Marossy, Thermally stimulated discharge (TSD) study of low-temperature transitions in chlorine-containing polymers. Journal of Thermal Analysis and Calorimetry, 148 (2023) 1899-1903. https://doi.org/10.1007/s10973-022-11803-9

[27] K. Marossy, Thermally stimulated depolarization (TSD) current study of plasticized PVC. Polymer Bulletin, 41 (1998) 729-736. https://doi.org/10.1007/s002890050425

[28] S. Su, Prediction of the Miscibility of PBAT/PLA Blends. Polymers, 13 (2021) 2339. https://doi.org/10.3390/polym13142339

[29] A. Graziano, S. Jaffer, and M. Sain, Review on modification strategies of polyethylene/polypropylene immiscible thermoplastic polymer blends for enhancing their mechanical behavior. Journal of elastomers & plastics, 51 (2019) 291-336. https://doi.org/10.1177/0095244318783806

[30] F. P. La Mantia, M. Morreale, L. Botta, M. C. Mistretta, M. Ceraulo, and R. Scaffaro, Degradation of polymer blends: A brief review. Polymer Degradation and Stability, 145 (2017) 79-92. https://doi.org/10.1016/j.polymdegradstab.2017.07.011

[31] M. Palabiyik and S. Bahadur, Mechanical and tribological properties of polyamide 6 and high density polyethylene polyblends with and without compatibilizer. Wear, 246 (2000) 149-158. https://doi.org/10.1016/S0043-1648(00)00501-9

[32] M. Walters and D. Keyte, Heterogeneous structure in blends of rubber polymers. Rubber Chemistry and Technology, 38 (1965) 62-75. https://doi.org/10.5254/1.3535639
[33] Y. H. Kim and R. P. Wool, A theory of healing at a polymer-polymer interface. Macromolecules, 16 (1983) 1115-1120. https://doi.org/10.1021/ma00241a013
[34] V. J. Pita, E. Sampaio, and E. E. Monteiro, Mechanical properties evaluation of PVC/plasticizers and PVC/thermoplastic polyurethane blends from extrusion processing. Polymer Testing, 21 (2002) 545-550. https://doi.org/10.1016/S0142-9418(01)00122-2
[35] K. R. Sharma, *Polymer thermodynamics: blends, copolymers and reversible polymerization*. CRC Press, 2011.
[36] Y. Tian *et al.*, PVC Dechlorination for Facilitating Plastic Chemical Recycling: A Systematic Literature Review of Technical Advances, Modeling and Assessment. Sustainability, 16 (2024) 8331. https://doi.org/10.3390/su16198331
[37] K. Kobetičová and R. Černý, Ecotoxicity assessment of short-and medium-chain chlorinated paraffins used in polyvinyl-chloride products for construction industry. Science of the Total Environment, 640 (2018) 523-528. https://doi.org/10.1016/j.scitotenv.2018.05.300
[38] Y. Ma, S. Liao, Q. Li, Q. Guan, P. Jia, and Y. Zhou, Physical and chemical modifications of poly (vinyl chloride) materials to prevent plasticizer migration-Still on the run. Reactive and Functional Polymers, 147 (2020) 104458. https://doi.org/10.1016/j.reactfunctpolym.2019.104458
[39] V. Lipik, V. Martsul, and M. Abadie, Dehydrochlorination of PVC compositions during thermal degradation. Eurasian Chemico-Technological Journal, 4 (2002) 25-29. https://doi.org/10.18321/ectj514
[40] B. Bouchoul, M. T. Benaniba, and V. Massardier, Thermal and mechanical properties of bio-based plasticizers mixtures on poly (vinyl chloride). Polímeros, 27 (2017) 237-246. https://doi.org/10.1590/0104-1428.14216
[41] W. H. Starnes and X. Ge, Mechanism of autocatalysis in the thermal dehydrochlorination of poly (vinyl chloride). Macromolecules, 37 (2004) 352-359. https://doi.org/10.1021/ma0352835
[42] B. Baum and L. Wartman, Structure and mechanism of dehydrochlorination of polyvinyl chloride. Journal of Polymer Science, 28 (1958) 537-546. https://doi.org/10.1002/pol.1958.1202811805
[43] L. J. González-Ortiz, M. Arellano, C. F. Jasso, E. Mendizábal, and M. J. Sánchez-Peña, Thermal stability of plasticized poly (vinyl chloride) compounds stabilized with pre-heated mixtures of calcium and/or zinc stearates. Polymer degradation and stability, 90 (2005) 154-161. https://doi.org/10.1016/j.polymdegradstab.2005.04.013
[44] V. Yanborisov and S. Borisevich, Quantum-chemical modeling of the mechanism of autocatalytic dehydrochlorination of PVC. Theoretical and Experimental Chemistry, 41 (2005) 352-358. https://doi.org/10.1007/s11237-006-0002-y
[45] T. Mekonnen, P. Mussone, H. Khalil, and D. Bressler, Progress in bio-based plastics and plasticizing modifications. Journal of Materials Chemistry A, 1 (2013) 13379-13398. https://doi.org/10.1039/C3TA12555F
[46] J. Czogała, E. Pankalla, and R. Turczyn, Recent attempts in the design of efficient PVC plasticizers with reduced migration. Materials, 14 (2021) 844. https://doi.org/10.3390/ma14040844

[47] M. Kollár and G. Zsoldos, Investigating poly-(vinyl-chloride)-polyethylene blends by thermal methods. Journal of thermal analysis and calorimetry, 107 (2012) 645-650. https://doi.org/10.1007/s10973-011-1939-1
[48] R. Kaur, P. Singh, S. Tanwar, G. Varshney, and S. Yadav, Assessment of bio-based polyurethanes: Perspective on applications and bio-degradation. Macromol, 2 (2022) 284-314. https://doi.org/10.3390/macromol2030019
[49] L. Wan *et al.*, Flame-retarded thermoplastic polyurethane elastomer: From organic materials to nanocomposites and new prospects. Chemical Engineering Journal, 417 (2021) 129314. https://doi.org/10.1016/j.cej.2021.129314
[50] P. Somdee, M. A. Ansari, and K. Marossy, Thermo-mechanical properties of flexible and rigid polyurethane (PU)/Cu composites. Polymer Composites, 44 (2023) 401-412. https://doi.org/10.1002/pc.27105
[51] S. Wu, S. Ma, Q. Zhang, and C. Yang, A comprehensive review of polyurethane: Properties, applications and future perspectives. Polymer, 327 (2025) 128361. https://doi.org/10.1016/j.polymer.2025.128361
[52] P. Somdee, T. Lassú-Kuknyó, C. Kónya, T. Szabó, and K. Marossy, Thermal analysis of polyurethane elastomers matrix with different chain extender contents for thermal conductive application. Journal of Thermal Analysis and Calorimetry, 138 (2019) 1003-1010. http://dx.doi.org/10.1007/s10973-019-08183-y
[53] P. Jia, H. Xia, K. Tang, and Y. Zhou, Plasticizers derived from biomass resources: A short review. Polymers, 10 (2018) 1303. https://doi.org/10.3390/polym10121303
[54] M. G. A. Vieira, M. A. Da Silva, L. O. Dos Santos, and M. M. Beppu, Natural-based plasticizers and biopolymer films: A review. European polymer journal, 47 (2011) 254-263. https://doi.org/10.1016/j.eurpolymj.2010.12.011
[55] G. A. Schwartz, M. Paluch, Á. Alegría, and J. Colmenero, High pressure dynamics of polymer/plasticizer mixtures. The Journal of chemical physics, 131 (2009). https://doi.org/10.1063/1.3187938
[56] C. White, B. Pejcic, M. Myers, and X. Qi, Development of a plasticizer-poly (methyl methacrylate) membrane for sensing petroleum hydrocarbons in water. Sensors and Actuators B: Chemical, 193 (2014) 70-77. https://doi.org/10.1016/j.snb.2013.11.095
[57] S. H. Clasen, C. M. Müller, and A. T. Pires, Maleic anhydride as a compatibilizer and plasticizer in TPS/PLA blends. Journal of the Brazilian Chemical Society, 26 (2015) 1583-1590. http://dx.doi.org/10.5935/0103-5053.20150126
[58] H. Hlisníková, I. Petrovičová, B. Kolena, M. Šidlovská, and A. Sirotkin, Effects and mechanisms of phthalates' action on reproductive processes and reproductive health: a literature review. International journal of environmental research and public health, 17 (2020) 6811. https://doi.org/10.3390/ijerph17186811
[59] L. Cobellis *et al.*, High plasma concentrations of di-(2-ethylhexyl)-phthalate in women with endometriosis. Human Reproduction, 18 (2003) 1512-1515. https://doi.org/10.1093/humrep/deg254
[60] Z.-M. Zhang, H.-H. Zhang, Y.-W. Zou, and G.-P. Yang, Distribution and ecotoxicological state of phthalate esters in the sea-surface microlayer, seawater and sediment of the Bohai Sea and the Yellow Sea. Environmental Pollution, 240 (2018) 235-247. https://doi.org/10.1016/j.envpol.2018.04.056

[61] X.-L. Cao, Determination of phthalates and adipate in bottled water by headspace solid-phase microextraction and gas chromatography/mass spectrometry. Journal of Chromatography A, 1178 (2008) 231-238. https://doi.org/10.1016/j.chroma.2007.11.095

[62] E. Fasano, T. Cirillo, F. Esposito, and S. Lacorte, Migration of monomers and plasticizers from packed foods and heated microwave foods using QuEChERS sample preparation and gas chromatography/mass spectrometry. LWT-Food Science and Technology, 64 (2015) 1015-1021. https://doi.org/10.1016/j.lwt.2015.06.066

[63] A. Giuliani, M. Zuccarini, A. Cichelli, H. Khan, and M. Reale, Critical review on the presence of phthalates in food and evidence of their biological impact. International journal of environmental research and public health, 17 (2020) 5655. https://doi.org/10.3390/ijerph17165655

[64] H. C. Erythropel, M. Maric, J. A. Nicell, R. L. Leask, and V. Yargeau, Leaching of the plasticizer di (2-ethylhexyl) phthalate (DEHP) from plastic containers and the question of human exposure. Applied microbiology and biotechnology, 98 (2014) 9967-9981. https://doi.org/10.1007/s00253-014-6183-8

[65] Y.-M. Lee *et al.*, Distribution of phthalate esters in air, water, sediments, and fish in the Asan Lake of Korea. Environment International, 126 (2019) 635-643. https://doi.org/10.1016/j.envint.2019.02.059

[66] Q. Zhang *et al.*, Concentrations and distribution of phthalate esters in the seamount area of the Tropical Western Pacific Ocean. Marine pollution bulletin, 140 (2019) 107-115. https://doi.org/10.1016/j.marpolbul.2019.01.015

[67] L. Caporossi *et al.*, Female reproductive health and exposure to phthalates and bisphenol A: A cross sectional study. Toxics, 9 (2021) 299. https://doi.org/10.3390/toxics9110299

[68] (2025). *Phthalates Risk Evaluation under TSCA*. [Online] Available: https://www.epa.gov/assessing-and-managing-chemicals-under-tsca/phthalates?

[69] (2018). *Commission Regulation (EU) 2018/2005 of 17 December 2018 amending Annex XVII to Regulation (EC) No 1907/2006 concerning phthalates*. [Online] Available: https://eur-lex.europa.eu/eli/reg/2018/2005/oj/eng?

[70] T. Zheng *et al.*, Structural modification of waste cooking oil methyl esters as cleaner plasticizer to substitute toxic dioctyl phthalate. Journal of Cleaner Production, 186 (2018) 1021-1030. https://doi.org/10.1016/j.jclepro.2018.03.175

[71] A. Alhanish and M. Abu Ghalia, Developments of biobased plasticizers for compostable polymers in the green packaging applications: A review. Biotechnology Progress, 37 (2021) e3210. https://doi.org/10.1002/btpr.3210

[72] L. Lenzi *et al.*, Further step in the transition from conventional plasticizers to versatile bioplasticizers obtained by the valorization of levulinic acid and glycerol. ACS Sustainable Chemistry & Engineering, 11 (2023) 9455-9469. https://doi.org/10.1021/acssuschemeng.3c01536

[73] G. De Feo, C. Ferrara, L. Giordano, and L. S. Ossèo, Assessment of Three Recycling Pathways for Waste Cooking Oil as Feedstock in the Production of Biodiesel, Biolubricant, and Biosurfactant: A Multi-Criteria Decision Analysis Approach. Recycling, 8 (2023) 64. https://doi.org/10.3390/recycling8040064

[74] Y. Zhao, C. Wang, L. Zhang, Y. Chang, and Y. Hao, Converting waste cooking oil to biodiesel in China: environmental impacts and economic feasibility. Renewable and Sustainable Energy Reviews, 140 (2021) 110661. https://doi.org/10.1016/j.rser.2020.110661

[75] W. H. Foo *et al.*, Recent advances in the conversion of waste cooking oil into value-added products: A review. Fuel, 324 (2022) 124539. https://doi.org/10.1016/j.fuel.2022.124539
[76] Y. F. Minale *et al.*, Mechanical Properties of PVC/TPU Blends Enhanced with a Sustainable Bio-Plasticizer. Sustainability (2071-1050), 17 (2025). https://doi.org/10.3390/su17052033
[77] A. Qadeer, K. L. Kirsten, Z. Ajmal, X. Jiang, and X. Zhao, Alternative plasticizers as emerging global environmental and health threat: another regrettable substitution? Environmental science & technology, 56 (2022) 1482-1488. https://doi.org/10.1021/acs.est.1c08365
[78] Z. Zhang *et al.*, Research progress of novel bio-based plasticizers and their applications in poly (vinyl chloride). Journal of Materials Science, 56 (2021) 10155-10182. https://doi.org/10.1007/s10853-021-05934-x
[79] H. Zhu, J. Yang, M. Wu, Q. Wu, J. Liu, and J. Zhang, "Biobased plasticizers from tartaric acid: synthesis and effect of alkyl chain length on the properties of poly (vinyl chloride). ACS Omega 6: 13161–13169," ed, 2021.
[80] Z. He *et al.*, Designing anti-migration furan-based plasticizers and their plasticization properties in poly (vinyl chloride) blends. Polymer Testing, 91 (2020) 106793. https://doi.org/10.1016/j.polymertesting.2020.106793
[81] J. I. Mnyango and S. P. Hlangothi, Polyvinyl chloride applications along with methods for managing its end-of-life items: A review. Progress in Rubber, Plastics and Recycling Technology, 42 (2026) 3-61. https://doi.org/10.1177/14777606241308652
[82] D. Braun, Poly (vinyl chloride) on the way from the 19th century to the 21st century. Journal of Polymer Science Part A: Polymer Chemistry, 42 (2004) 578-586. https://doi.org/10.1002/pola.10906
[83] I. Salahshoori, M. N. Jorabchi, K. Valizadeh, A. Yazdanbakhsh, A. Bateni, and S. Wohlrab, A deep insight of solubility behavior, mechanical quantum, thermodynamic, and mechanical properties of Pebax-1657 polymer blends with various types of vinyl polymers: A mechanical quantum and molecular dynamics simulation study. Journal of Molecular Liquids, 363 (2022) 119793. https://doi.org/10.1016/j.molliq.2022.119793
[84] D. M. Leisz, L. W. Kleiner, and P. G. Gertenbach, Prediction of the glass transition temperature for compatible polymer blends of varying compositions. Thermochimica Acta, 35 (1980) 51-58. https://doi.org/10.1016/0040-6031(80)85020-9
[85] V. Arrighi, J. M. Cowie, S. Fuhrmann, and A. Youssef, Miscibility criterion in polymer blends and its determination. Encyclopedia of polymer blends, (2010) 153-198. https://doi.org/10.1002/9783527805204.ch5
[86] K. Marossy and J. Tóth, Anomalous behaviour of PVC–CPVC–CPE blends. Plastics, rubber and composites, 34 (2005) 438-442. https://doi.org/10.1179/174328905X66162
[87] S. Mazinani, S. Darvishmanesh, R. Ramazani, and B. Van der Bruggen, Miscibility of polyimide blends: Physicochemical characterization of two high performance polyimide polymers. Reactive and Functional Polymers, 111 (2017) 88-101. https://doi.org/10.1016/j.reactfunctpolym.2016.12.010
[88] M. N. Subramanian, *Polymer blends and composites: chemistry and technology*. John Wiley & Sons, 2017.
[89] M. M. Coleman and P. C. Painter, Hydrogen bonded polymer blends. Progress in polymer science, 20 (1995) 1-59. https://doi.org/10.1016/0079-6700(94)00038-4

[90] J. S. Higgins, J. E. Lipson, and R. P. White, A simple approach to polymer mixture miscibility. Philosophical Transactions of the Royal Society A: Mathematical, Physical and Engineering Sciences, 368 (2010) 1009-1025. https://doi.org/10.1098/rsta.2009.0215
[91] S. Jeong, Investigation of intrinsic characteristics of polymer blends via molecular simulation: a review. Korea-Australia Rheology Journal, 35 (2023) 249-266. https://doi.org/10.1007/s13367-023-00076-9
[92] M. Sangkhawasi, T. Remsungnen, A. S. Vangnai, P. Maitarad, and T. Rungrotmongkol, Prediction of the glass transition temperature in polyethylene terephthalate/polyethylene vanillate (PET/PEV) blends: a molecular dynamics study. Polymers, 14 (2022) 2858. https://doi.org/10.3390/polym14142858
[93] H. M. Jeong, J. H. Song, S. Y. Lee, and B. K. Kim, Miscibility and shape memory property of poly (vinyl chloride)/thermoplastic polyurethane blends. Journal of materials science, 36 (2001) 5457-5463. https://doi.org/10.1023/A:1012481631570
[94] H. A. Schneider, Conformational entropy contributions to the glass temperature of blends of miscible polymers. Journal of research of the National Institute of Standards and Technology, 102 (1997) 229. https://doi.org/10.6028/jres.102.018
[95] E. Fekete and B. Pukánszky, Effect of molecular interactions on the miscibility and structure of polymer blends. European Polymer Journal, 41 (2005) 727-736. https://doi.org/10.1016/j.eurpolymj.2004.10.038
[96] D. David and T. Sincock, Estimation of miscibility of polymer blends using the solubility parameter concept. Polymer, 33 (1992) 4505-4514. https://doi.org/10.1016/0032-3861(92)90406-M
[97] J. Zhu, R. Balieu, and H. Wang, The use of solubility parameters and free energy theory for phase behaviour of polymer-modified bitumen: a review. Road Materials and Pavement Design, 22 (2021) 757-778. https://doi.org/10.1080/14680629.2019.1645725
[98] R. F. Fedors, A method for estimating both the solubility parameters and molar volumes of liquids. Polymer Engineering & Science, 14 (1974) 147-154. https://doi.org/10.1002/pen.760140211
[99] M. Abu-Abdeen and I. Elamer, Mechanical and swelling properties of thermoplastic elastomer blends. Materials & Design, 31 (2010) 808-815. https://doi.org/10.1016/j.matdes.2009.07.059
[100] E. Manias and L. A. Utracki, Thermodynamics of polymer blends. Polymer blends handbook, 282 (2014) 171-289.
[101] M. Radhakrishnan Nair and M. Gopinathan Nair, Compatibility studies and characterisation of a PVC/NR blend system using NR/PU block copolymer. Polymer Bulletin, 56 (2006) 619-631. https://doi.org/10.1007/s00289-006-0524-4
[102] S. Aid, A. Eddhahak, Z. Ortega, D. Froelich, and A. Tcharkhtchi, Experimental study of the miscibility of ABS/PC polymer blends and investigation of the processing effect. Journal of Applied Polymer Science, 134 (2017). https://dx.doi.org/10.1002/app.44975
[103] C. Radhakrishnan, P. Kumari, A. Sujith, and G. Unnikrishnan, Dynamic mechanical properties of styrene butadiene rubber and poly (ethylene-co-vinyl acetate) blends. Journal of Polymer Research, 15 (2008) 161-171. https://doi.org/10.1007/s10965-007-9155-1
[104] K. Marossy, "Theory and Practical Application of Polymer Blends and Alloys," L. P. Slides, Ed., ed. Miskolc, Hungary, 2006.
[105] J. Fried, "Applications of thermal analysis to the study of polymer blends," in *Developments in Polymer Characterisation—4*: Springer, 1983, pp. 39-90.

[106] K. Marossy, Practical approach to thermally stimulated discharge (TSD) method on polymers. Journal of Thermal Analysis and Calorimetry, 129 (2017) 161-170. https://doi.org/10.1007/s10973-017-6098-6
[107] D. Wang, Y. Li, X.-M. Xie, and B.-H. Guo, Compatibilization and morphology development of immiscible ternary polymer blends. Polymer, 52 (2011) 191-200. https://doi.org/10.1016/j.polymer.2010.11.019
[108] W. Wu, X.-l. Luo, and D.-z. Ma, Miscibility of the segmented polyurethane blends with chlorinated poly (vinyl chloride). European polymer journal, 35 (1999) 985-990. https://doi.org/10.1016/S0014-3057(98)00195-5
[109] N. Tourta, A. Meghezzi, and H. Boussehel, Morphological and thermal properties of polystyrene/poly (vinyl chloride) blends. Revue des Composites et des Materiaux Avances, 32 (2022) 211.
[110] A. Saffar, E. Jalali Dil, P. J. Carreau, A. Ajji, and M. R. Kamal, Phase behavior of binary blends of PP/PP-g-AA: limitations of the conventional characterization techniques. Polymer International, 65 (2016) 508-515. https://doi.org/10.1002/pi.5082
[111] Y. F. Minale *et al.*, Thermodynamic and Technological Compatibility of Polyvinyl Chloride, Thermoplastic Polyurethane, and Bio-Plasticizer Blends. Polymers, 17 (2025) 1149. https://doi.org/10.3390/polym17091149
[112] P. Srihanam, Y. Srisuwan, T. Phromsopha, A. Manphae, and Y. Baimark, Improvement in phase compatibility and mechanical properties of poly (L-lactide)-b-poly (ethylene glycol)-b-poly (L-lactide)/thermoplastic starch blends with citric acid. Polymers, 15 (2023) 3966. https://doi.org/10.3390/polym15193966
[113] O. M. Folarin and E. Sadiku, Thermal stabilizers for poly (vinyl chloride): A review. Int. J. Phys. Sci, 6 (2011) 4323-4330. DOI: 10.5897/IJPS11.654
[114] Y.-z. Bao, H. Zhi-Ming, L. Shen-Xing, and W. Zhi-Xue, Thermal stability, smoke emission and mechanical properties of poly (vinyl chloride)/hydrotalcite nanocomposites. Polymer degradation and Stability, 93 (2008) 448-455. https://doi.org/10.1016/j.polymdegradstab.2007.11.014
[115] J. Liu, G. Chen, and J. Yang, Preparation and characterization of poly (vinyl chloride)/layered double hydroxide nanocomposites with enhanced thermal stability. Polymer, 49 (2008) 3923-3927. https://doi.org/10.1016/j.polymer.2008.07.014
[116] V. Krasinskyi, V. Kochubei, Y. Klym, and O. Suberlyak, Thermogravimetric research into composites based on the mixtures of polypropylene and modified polyamide. Eastern-European Journal of Enterprise Technologies, (2017) 44-50. https://doi.org/10.15587/1729-4061.2017.108465
[117] K. Pielichowski and I. Hamerton, Compatible poly (vinyl chloride)/chlorinated polyurethane blends: thermal characteristics. European Polymer Journal, 36 (2000) 171-181. https://doi.org/10.1016/S0014-3057(99)00054-3
[118] M. Radhakrishnan Nair and M. Gopinathan Nair, Thermogravimetric analysis of PVC/NR-b-PU blends. Journal of thermal analysis and calorimetry, 103 (2011) 863-872. https://doi.org/10.1007/s10973-010-1113-1
[119] J. Haponiuk and A. Balas, Thermal properties of poly (vinyl chloride)/polyurethane blends. Journal of thermal analysis, 43 (1995) 215-218. https://doi.org/10.1007/BF02635987
[120] C.-S. Ha, Y. Kim, W.-K. Lee, W.-J. Cho, and Y. Kim, Fracture toughness and properties of plasticized PVC and thermoplastic polyurethane blends. Polymer, 39 (1998) 4765-4772. https://doi.org/10.1016/S0032-3861(97)10326-3

[121] Y. Xiao *et al.*, Simultaneous Determination of Nine Phthalates in Vegetable Oil by Atmospheric Pressure Gas Chromatography with Tandem Mass Spectrometry (APGC-MS/MS). Toxics, 11 (2023) 200. https://doi.org/10.3390/toxics11030200
[122] P. H. Daniels, A brief overview of theories of PVC plasticization and methods used to evaluate PVC-plasticizer interaction. Journal of vinyl and additive technology, 15 (2009) 219-223. https://doi.org/10.1002/vnl.20211
[123] P. Dziendzioł, S. Waśkiewicz, and K. Jaszcz, New Biobased Plasticizers for PVC Derived from Saturated Dimerized Fatty Acids. Materials, 18 (2025) 2155. https://doi.org/10.3390/ma18092155
[124] V. G. Bhamare, R. R. Joshi, M. S. Gangurde, and V. V. Pawar, Theoretical consideration of solubility by Hildebrand solubility approach. interactions, 26 (2021) 28. https://doi.org/10.30574/wjarr.2021.12.3.0680
[125] A. Gyul'maliev, L. Zekel', K. M. Kadiev, and F. Zhagfarov, Determination of the Hansen Solubility Parameter from the Structural Composition Data of Solvent Molecules. Chemistry and Technology of Fuels and Oils, 59 (2023) 748-755. https://doi.org/10.1007/s10553-023-01580-y
[126] C. L. Ihemaguba and K. Marossy, Combined thermal analysis of fluid plasticizers. Journal of Thermal Analysis and Calorimetry, (2020) 1-7. https://doi.org/10.1007/s10973-020-10315-8
[127] K. Tamási and K. Marossy, Combined thermal analysis of plant oils. Journal of Thermal Analysis and Calorimetry, (2021) 1-8. https://doi.org/10.1007/s10973-020-10470-y
[128] R. F. Landel and L. E. Nielsen, *Mechanical properties of polymers and composites*. CRC press, 1993.
[129] R. O. Ebewele, *Polymer science and technology*. CRC press, 2000.
[130] A. I. Al-Mosawi, A novel evaluation method for dehydrochlorination of plasticized Poly (vinyl chloride) containing heavy metal-free thermal stabilizing synergistic agent. Polymers for Advanced Technologies, 32 (2021) 3278-3286. https://doi.org/10.1002/pat.5339
[131] W. Starnes Jr, Structural and mechanistic aspects of the thermal degradation of poly (vinyl chloride). Progress in polymer science, 27 (2002) 2133-2170. https://doi.org/10.1016/S0079-6700(02)00063-1

Appendix

■ **TSD raw curves and detail evaluations**

- **PVC** 5K/min ↓ 5K/min ↑

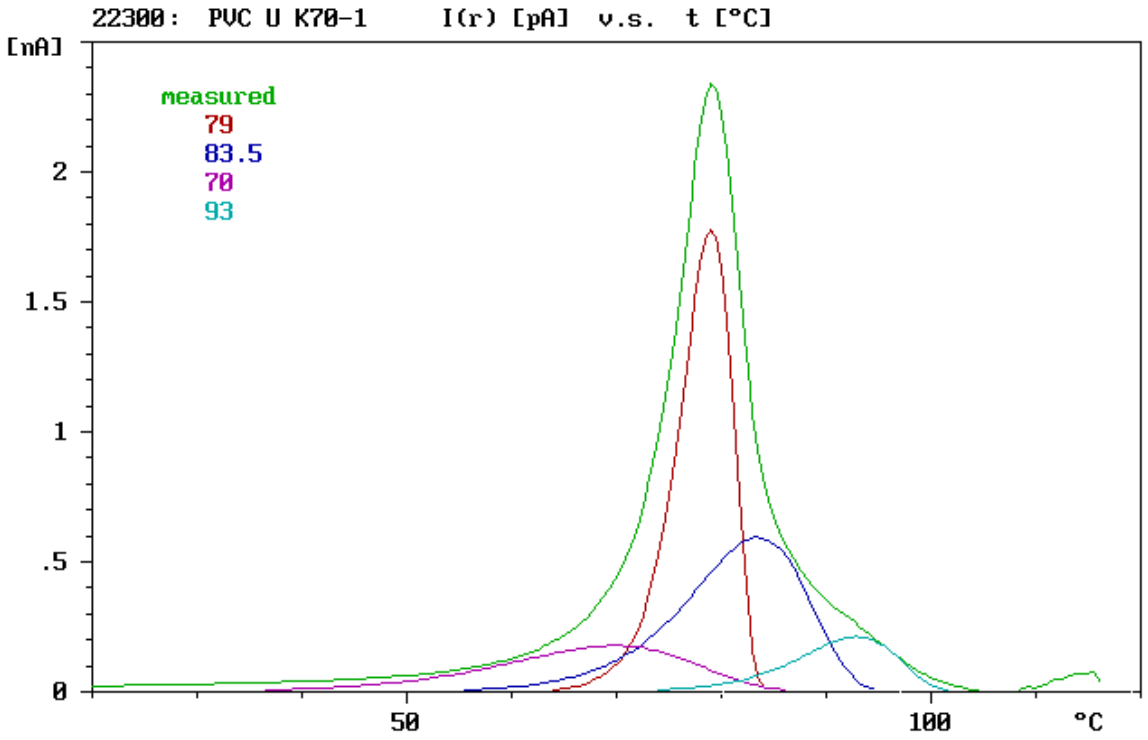

const=	23.576	
A=	52.21666	
B=	-17.12681	A_e= 142 kJ/mol

ϑ_{max}	79	°C		τ_0	1.048e-61	s	B	
I_{max}	1780	pA		Q_0	140276	pAs	C	
A_e	421	kJ/mol		$\Delta\varepsilon$	5.3	-	n/col	2/**4**
ϑ_{max}	83.5	°C		τ_0	1.972e-26	s	B	
I_{max}	595	pA		Q_0	105940	pAs	C	
A_e	188	kJ/mol		$\Delta\varepsilon$	4.0	-	n/col	3/**1**
ϑ_{max}	70	°C		τ_0	2.756e-15	s	B	
I_{max}	178	pA		Q_0	49675	pAs	C	
A_e	109	kJ/mol		$\Delta\varepsilon$	1.9	-	n/col	4/**5**
ϑ_{max}	93	°C		τ_0	2.308e-33	s	B	
I_{max}	213	pA		Q_0	31362	pAs	C	
A_e	241	kJ/mol		$\Delta\varepsilon$	1.2	-	n/col	5/**3**

ϑ_{max}		°C		τ_0		s	B	
I_{max}		pA		Q_0		pAs	C	
A_e		kJ/mol		$\Delta\varepsilon$		-	n/col	6/C
ϑ_{max}		°C		τ_0		s	B	
I_{max}		pA		Q_0		pAs	C	
A_e		kJ/mol		$\Delta\varepsilon$		-	n/col	7/ D

∫- -+ = pAs; (Δε=)

■ **PVC/Bio(10/3)** 5K/min ↓ 5K/min ↑

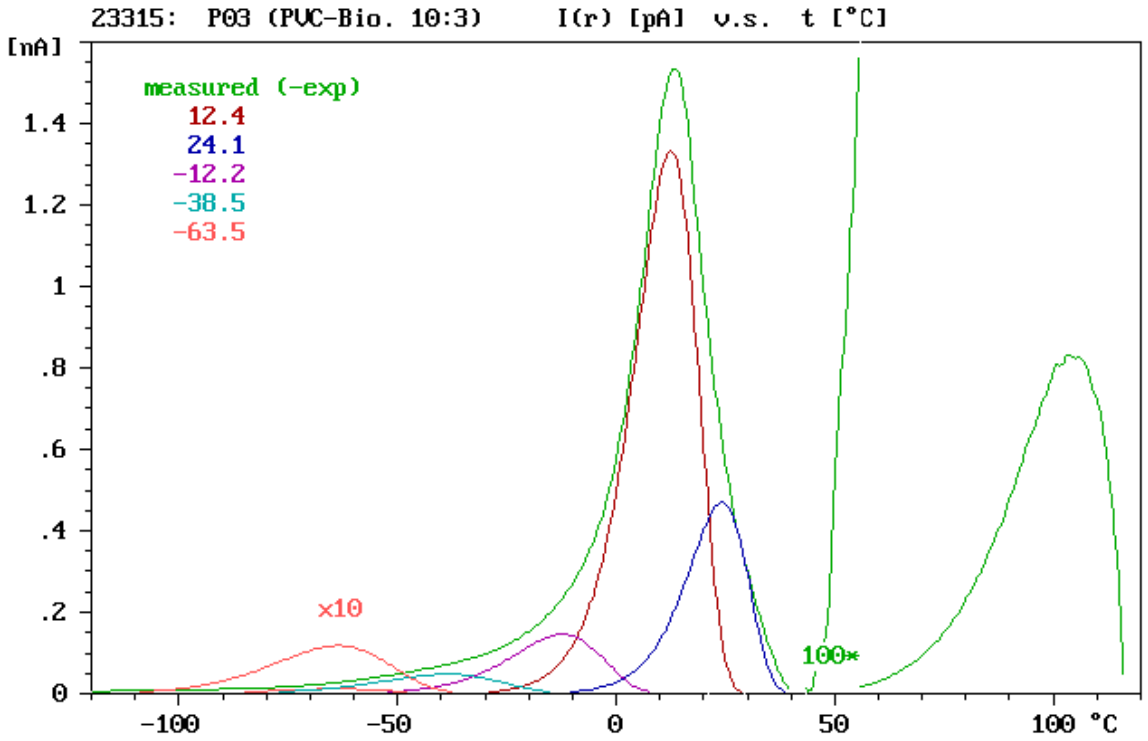

const=	23.576		
A=	40.37308		
B=	-10.3121	A_e= 85.7	kJ/mol

ϑ_{max}	12,4	°C		τ_0	8.506e-16	s	B	
I_{max}	1333	pA		Q_0	302262	pAs	C	
A_e	93	kJ/mol		$\Delta\varepsilon$	11.4	-	n/col	2/4
ϑ_{max}	24.1	°C		τ_0	2.970e-17	s	B	
I_{max}	470	pA		Q_0	102644	pAs	C	
A_e	105	kJ/mol		$\Delta\varepsilon$	3.86	-	n/col	3/1

ϑ_{max}	-12.2	°C		τ_0	3.154e-9	s	B	
I_{max}	146	pA		Q_0	47275	pAs	C	
A_e	53	kJ/mol		$\Delta\varepsilon$	1.8	-	n/col	4/**5**
ϑ_{max}	-38.5	°C		τ_0	1.292e-5	s	B	
I_{max}	48	pA		Q_0	20170	pAs	C	
A_e	32	kJ/mol		$\Delta\varepsilon$	0.76	-	n/col	5/**3**
ϑ_{max}	-63.5	°C		τ_0	5.613e-5	s	B	
I_{max}	11.8	pA		Q_0	4818	pAs	C	
A_e	26	kJ/mol		$\Delta\varepsilon$	0.18	-	n/col	6/**C**
ϑ_{max}		°C		τ_0		s	B	
I_{max}		pA		Q_0		pAs	C	
A_e		kJ/mol		$\Delta\varepsilon$		-	n/col	7/**D**

$\int$-120- -65 = 3744 pAs; ($\Delta\varepsilon$ = 0.14)

■ **PVC/Bio (10/5)** 5K/min ↓ 5K/min ↑

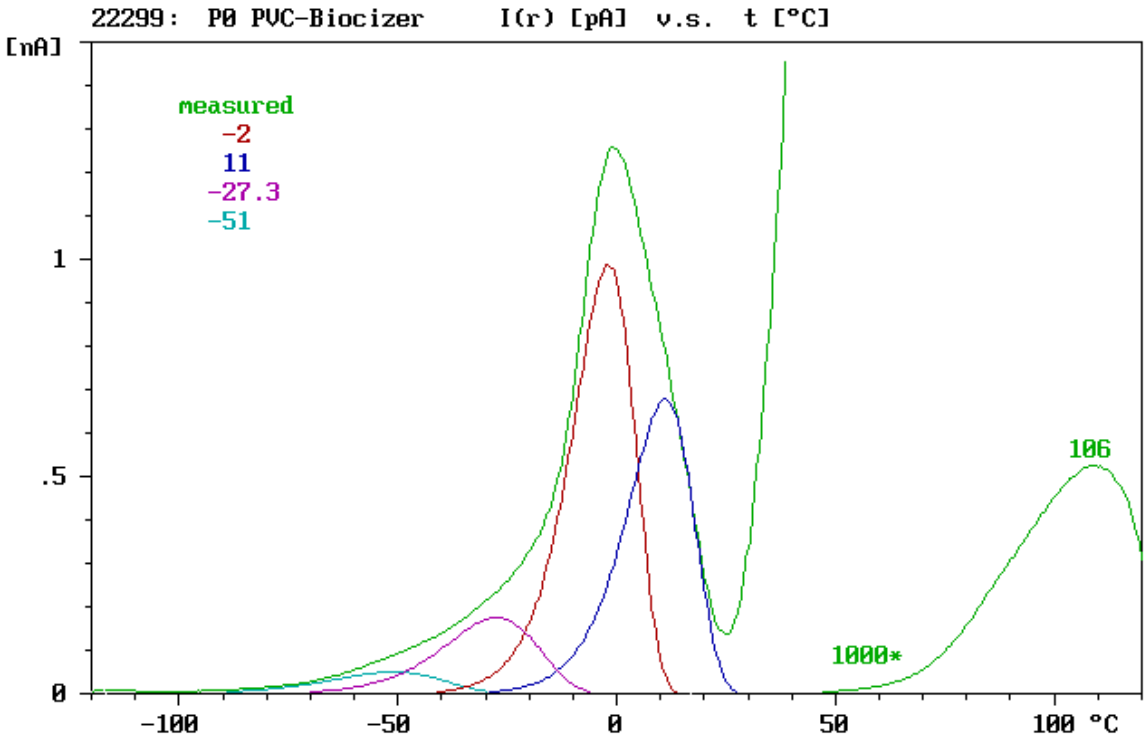

const=	23.576		
A=	35.45122		
B=	-8.253238	A_e= 68.6	kJ/mol

ϑ_{max}	-2	°C		τ_0	3.644e-15	s	B	
I_{max}	988	pA		Q_0	220639	pAs	C	

A_e	85	kJ/mol		$\Delta\varepsilon$	8.3	-	n/col	2/**4**
ϑ_{max}	11	°C		τ_0	9.410e-15	s	B	
I_{max}	678	pA		Q_0	162276	pAs	C	
A_e	87	kJ/mol		$\Delta\varepsilon$	6.1	-	n/col	3/**1**
ϑ_{max}	-27.3	°C		τ_0	3.683e-8	s	B	
I_{max}	175	pA		Q_0	58813	pAs	C	
A_e	45	kJ/mol		$\Delta\varepsilon$	2.2	-	n/col	4/**5**
ϑ_{max}	-51	°C		τ_0	1.450e-7	s	B	
I_{max}	50	pA		Q_0	20965	pAs	C	
A_e	30	kJ/mol		$\Delta\varepsilon$	0.755	-	n/col	5/**3**
ϑ_{max}	106	°C		τ_0	1.227e-9	s	B	not reli-
I_{max}	435000	pA		Q_0	1.8e8	pAs	C	able!
A_e	81	kJ/mol		$\Delta\varepsilon$	6768	-	n/col	~~6/C~~
ϑ_{max}		°C		τ_0		s	B	
I_{max}		pA		Q_0		pAs	C	
A_e		kJ/mol		$\Delta\varepsilon$		-	n/col	7/ **D**

$\int$- -+ = pAs; ($\Delta\varepsilon$=)

■ **PVC/TPU (10/3)** 5K/min ↓ 5K/min ↑

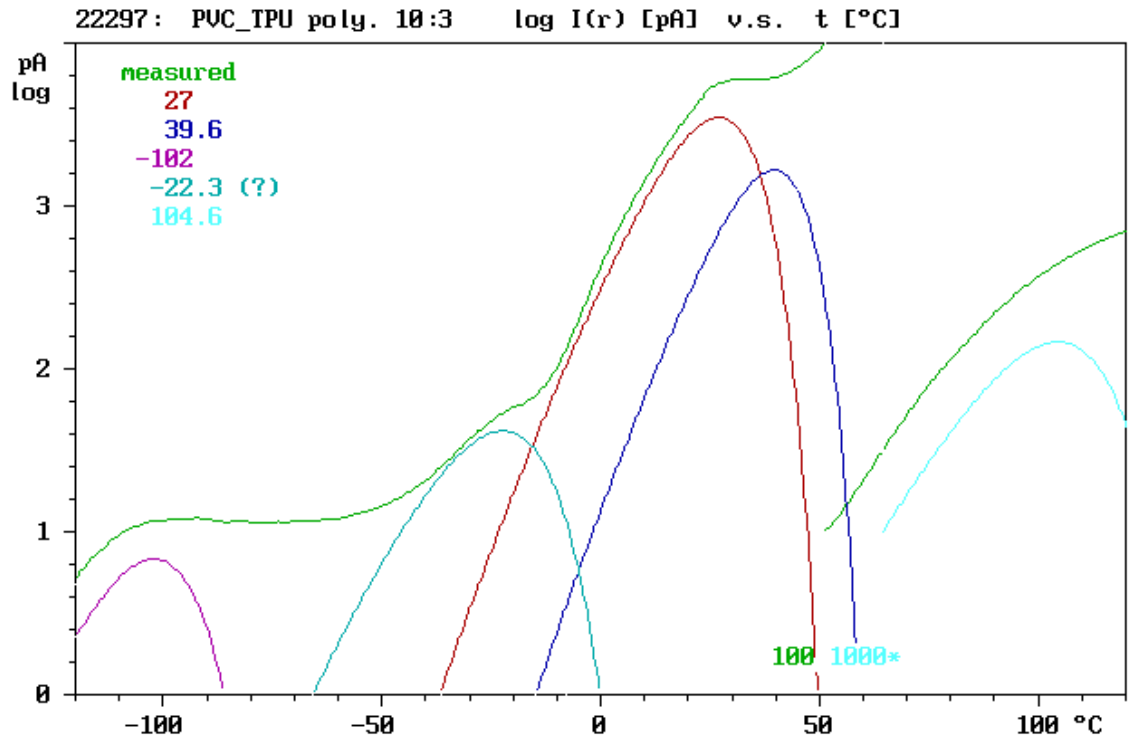

const=	23.576		
A=	35.11938		
B=	-8.509133	A_e=70.7	kJ/mol

ϑ_{max}	27	°C		τ_0	2.576e-13	s	B	
I_{max}	3500	pA		Q_0	963855	pAs	C	
A_e	84	kJ/mol		$\Delta\varepsilon$	36.3	-	n/col	2/**4**
ϑ_{max}	39.6	°C		τ_0	5.939e-16	s	B	
I_{max}	1660	pA		Q_0	407896	pAs	C	
A_e	103	kJ/mol		$\Delta\varepsilon$	15.4	-	n/col	3/**1**
ϑ_{max}	-102	°C		τ_0	2.215e-5	s	B	
I_{max}	6.8	pA		Q_0	1900	pAs	C	
A_e	23	kJ/mol		$\Delta\varepsilon$	0.072	-	n/col	4/**5**
ϑ_{max}	-22.3	°C		τ_0	3.6025e-8	s	B	
I_{max}	41.5	pA		Q_0	14206	pAs	C	
A_e	46	kJ/mol		$\Delta\varepsilon$	0.53	-	n/col	5/**3**
ϑ_{max}	104.6	°C		τ_0	1.094e-11	s	B	
I_{max}	146250	pA		Q_0	5.42e7	pAs	C	
A_e	95	kJ/mol		$\Delta\varepsilon$	2040	-	n/col	6/**B**
ϑ_{max}		°C		τ_0	e-	s	B	
I_{max}		pA		Q_0		pAs	C	
A_e		kJ/mol		$\Delta\varepsilon$		-	n/col	4/D

∫

■ **PVC/TPU (10/5)** 5K/min ↓ 5K/min ↑

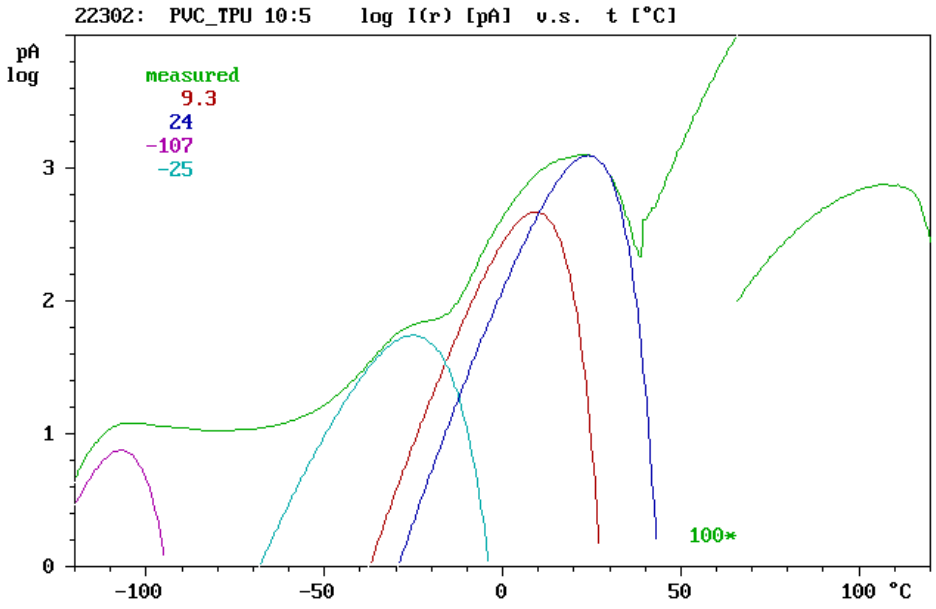

const=	23.576	
A=	33.07349	
B=	-7.70952	A_e=64.1 kJ/mol

ϑ_{max}	9.3	°C		τ_0	2.768e-14	s	B	
I_{max}	468	pA		Q_0	119472	pAs	C	
A_e	84	kJ/mol		$\Delta\varepsilon$	4.3	-	n/col	2/**4**
ϑ_{max}	24	°C		τ_0	9.759e-15	s	B	
I_{max}	1245	pA		Q_0	311553	pAs	C	
A_e	91	kJ/mol		$\Delta\varepsilon$	11.7	-	n/col	3/**1**
ϑ_{max}	-107	°C		τ_0	1.550e-7	s	B	
I_{max}	7.5	pA		Q_0	1606	pAs	C	
A_e	28	kJ/mol		$\Delta\varepsilon$	0.060	-	n/col	4/**5**
ϑ_{max}	-25	°C		τ_0	1.008e-8	s	B	
I_{max}	55	pA		Q_0	17723	pAs	C	
A_e	48	kJ/mol		$\Delta\varepsilon$	0.67	-	n/col	5/**3**
ϑ_{max}		°C		τ_0		s	B	
I_{max}		pA		Q_0		pAs	C	
A_e		kJ/mol		$\Delta\varepsilon$		-	n/col	6/**B**
ϑ_{max}		°C		τ_0	e-	s	B	
I_{max}		pA		Q_0		pAs	C	
A_e		kJ/mol		$\Delta\varepsilon$		-	n/col	4/D

$\int$ -110 - -60 =703pAs $\Delta\varepsilon$=0.026

■ **TPU**

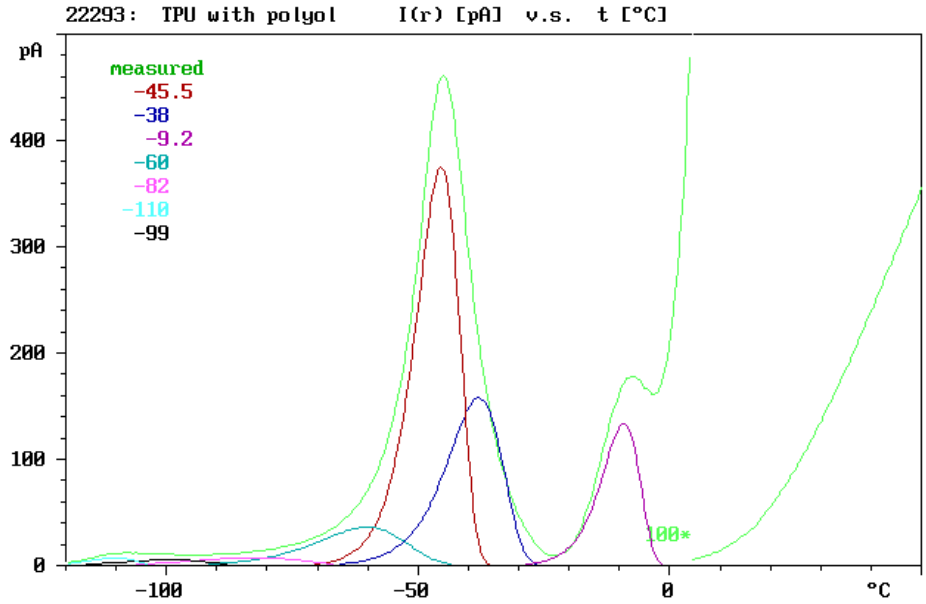

const=	39.293	
A=	31.02126	
B=	-6.618414	A_e=55 kJ/mol

J_{max}	-45.5	°C		t_0	5.689e-22	s	B	
I_{max}	375	pA		Q_0	50852	pAs	C	
A_e	100	kJ/mol		De	1.91	-	n/col	2/**4**
J_{max}	-38	°C		t_0	2.431e-17	s	B	
I_{max}	158	pA		Q_0	27317	pAs	C	
A_e	83	kJ/mol		De	1.01	-	n/col	3/**1**
J_{max}	-9.2	°C		t_0	1.509e-29	s	B	
I_{max}	134	pA		Q_0	15998	pAs	C	
A_e	154	kJ/mol		De	0.60	-	n/col	4/**5**
J_{max}	-60	°C		t_0	5.505e-9	s	B	
I_{max}	36	pA		Q_0	9794	pAs	C	
A_e	42	kJ/mol		De	0.369	-	n/col	5/**3**
J_{max}	-82	°C		t_0	2.906e-6	s	B	
I_{max}	7.6	pA		Q_0	2420	pAs	C	
A_e	28	kJ/mol		De	9.11e-2	-	n/col	5/D
J_{max}	-110	°C		t_0	5.218e-15	s	B	
I_{max}	7.5	pA		Q_0	959	pAs	C	
A_e	50	kJ/mol		De	3.6e-2	-	n/col	4/**B**

J_{max}	-99	°C		t_0	1.891e-7	s	B	
I_{max}	5.4	pA		Q_0	1342	pAs	C	
A_e	29	kJ/mol		De	5.05e-2	-	n/col	8/**F**

■ **TPU/Bio (50/5)** 5K/min ↓ 5K/min ↑

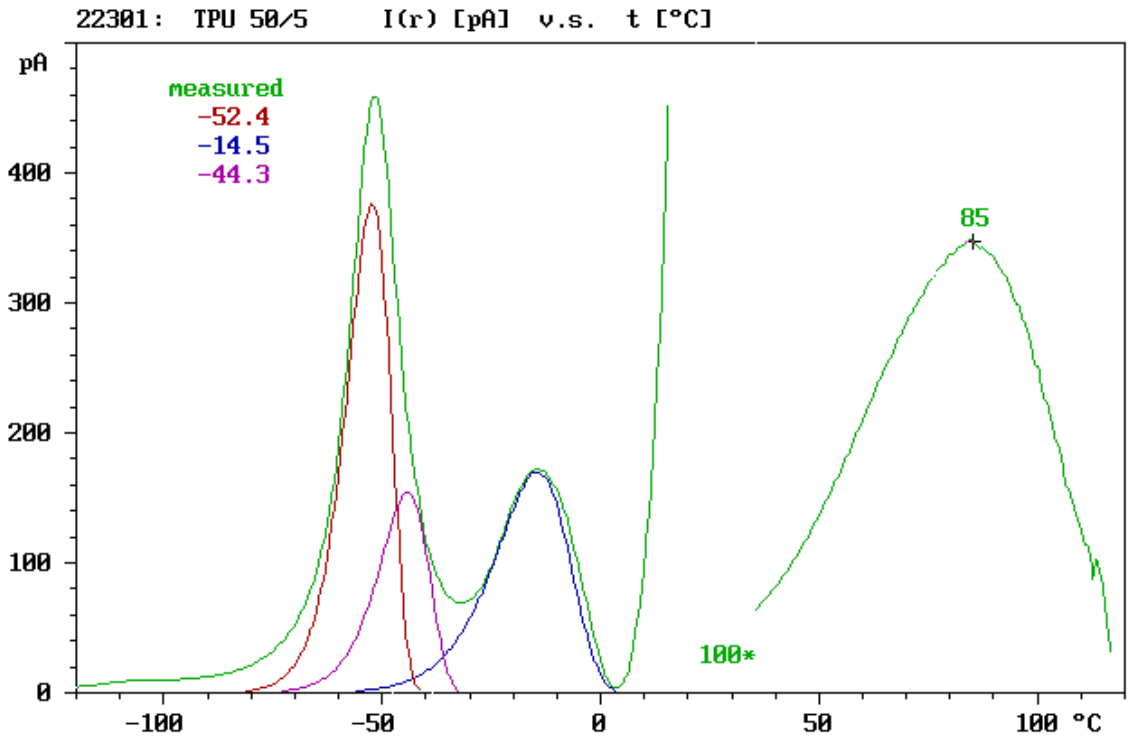

const=	23.576		
A=	30.58903		
B=	-6.83461	A_e= 56.8	kJ/mol

ϑ_{max}	-52.4	°C		τ_0	7.146e-18	s	B	
I_{max}	376	pA		Q_0	59504	pAs	C	
A_e	80	kJ/mol		$\Delta\varepsilon$	2.24	-	n/col	2/4
ϑ_{max}	-14.5	°C		τ_0	1.240e-11	s	B	
I_{max}	170	pA		Q_0	45300	pAs	C	
A_e	64	kJ/mol		$\Delta\varepsilon$	1.7	-	n/col	3/1
ϑ_{max}	-44.3	°C		τ_0	5.304e-16	s	B	
I_{max}	154	pA		Q_0	27820	pAs	C	
A_e	75	kJ/mol		$\Delta\varepsilon$	1.05	-	n/col	4/5
ϑ_{max}		°C		τ_0		s	B	
I_{max}		pA		Q_0		pAs	C	
A_e		kJ/mol		$\Delta\varepsilon$		-	n/col	5/3
ϑ_{max}		°C		τ_0		s	B	
I_{max}		pA		Q_0		pAs	C	
A_e		kJ/mol		$\Delta\varepsilon$		-	n/col	6/C

ϑ_{max}		°C		τ_0		s	B	
I_{max}		pA		Q_0		pAs	C	
A_e		kJ/mol		$\Delta\varepsilon$		-	n/col	7/ D

■ TPU/Bio (50/10)

5K/min ↓ 5K/min ↑

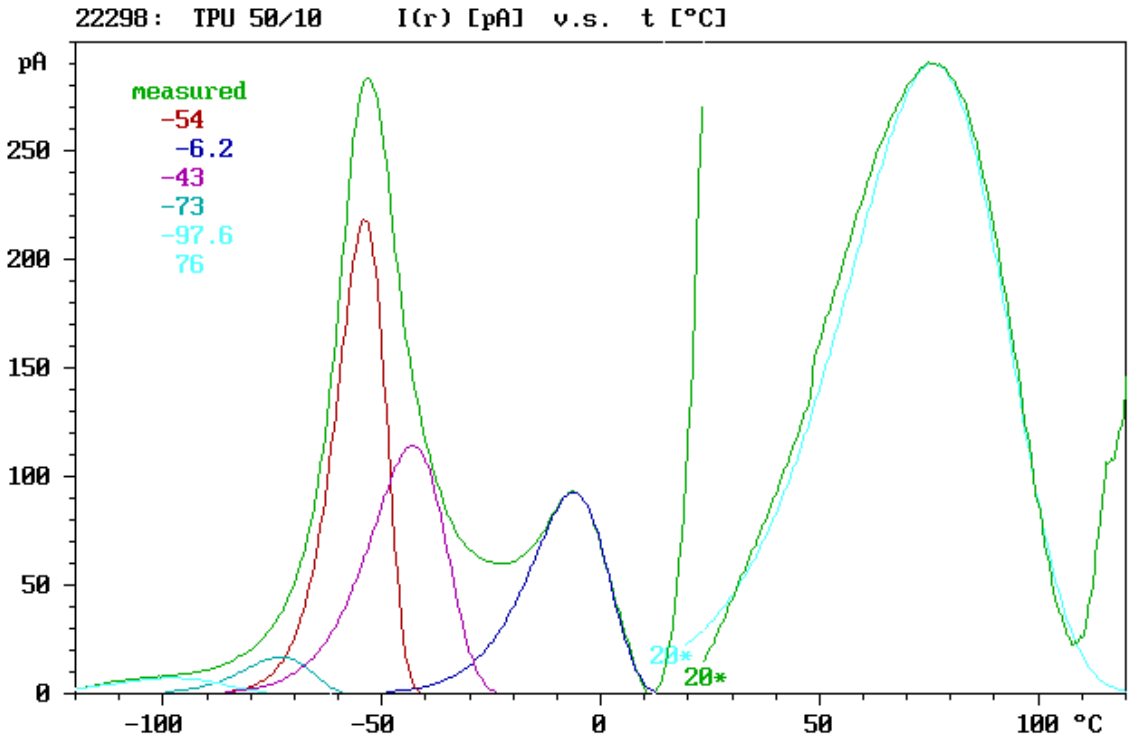

const=	23.576		
A=	27.37451		
B=	-6.398739	A_e=53.2	kJ/mol

ϑ_{max}	-54	°C		τ_0	1.416e-15	s	B	
I_{max}	218	pA		Q_0	38649	pAs	C	
A_e	8470	kJ/mol		$\Delta\varepsilon$	1.455	-	n/col	2/4
ϑ_{max}	-6.2	°C		τ_0	2.091e-11	s	B	
I_{max}	92.5	pA		Q_0	25845	pAs	C	
A_e	65	kJ/mol		$\Delta\varepsilon$	0.97	-	n/col	3/1
ϑ_{max}	-43	°C		τ_0	8.165e-10	s	B	
I_{max}	114	pA		Q_0	31153	pAs	C	
A_e	49	kJ/mol		$\Delta\varepsilon$	1.17	-	n/col	4/5
ϑ_{max}	-73	°C		τ_0	1.041e-9	s	B	
I_{max}	17	pA		Q_0	4094	pAs	C	
A_e	42	kJ/mol		$\Delta\varepsilon$	0.15	-	n/col	5/3

ϑ_{max}	-97.6	°C		τ_0	3.596e-4	s	B	
I_{max}	7.2	pA		Q_0	2523	pAs	C	
A_e	19	kJ/mol		$\Delta\varepsilon$	0.095	-	n/col	6/**B**
ϑ_{max}	76	°C		τ_0	3.886e-6	s	B	
I_{max}	5800	pA		Q_0	3346465	pAs	C	
A_e	52	kJ/mol		$\Delta\varepsilon$	126	-	n/col	7/ **B**

■ **PVC/TPU/Bio (10/1/5)** 5K/min ↓ 5K/min ↑

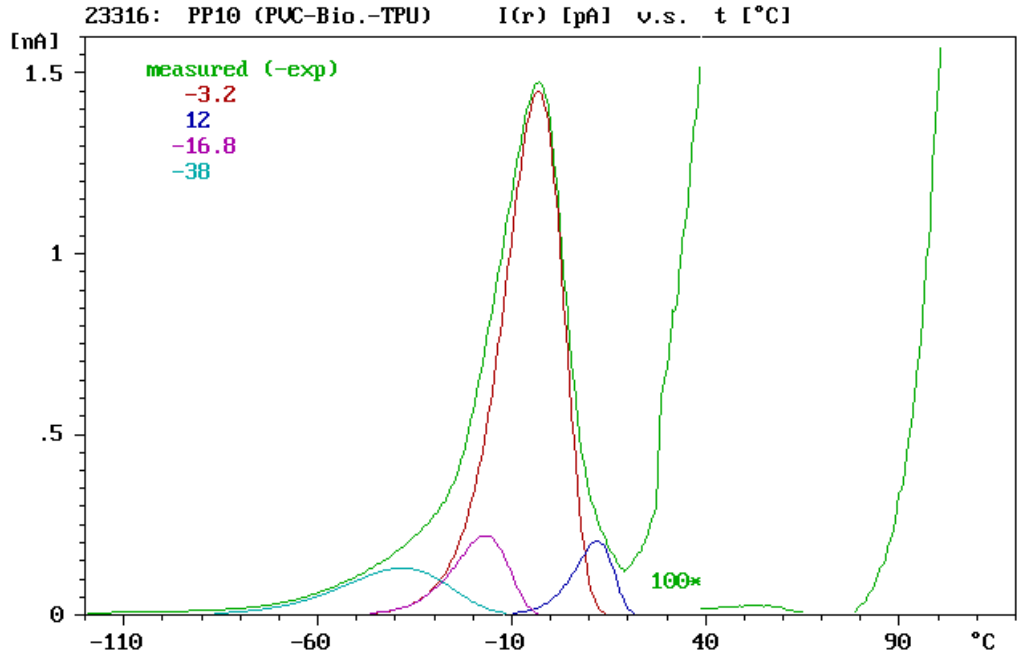

const=	23.576		
A=	35.92974		
B=	-8.289648	A_e= 68.9	kJ/mol

ϑ_{max}	-3.2	°C		τ_0	4.761e-14	s	B	
I_{max}	1450	pA		Q_0	344207	pAs	C	
A_e	79	kJ/mol		$\Delta\varepsilon$	13.0	-	n/col	2/**4**
ϑ_{max}	12	°C		τ_0	4.746e-24	s	B	
I_{max}	204	pA		Q_0	31773	pAs	C	
A_e	137	kJ/mol		$\Delta\varepsilon$	1.2	-	n/col	3/**1**
ϑ_{max}	-16.8	°C		τ_0	1.074e-14	s	B	
I_{max}	220	pA		Q_0	47788	pAs	C	

A_e	78	kJ/mol		$\Delta\varepsilon$	1.8	-	n/col	4/5
ϑ_{max}	-38	°C		τ_0	1.344e-5	s	B	
I_{max}	130	pA		Q_0	54851	pAs	C	
A_e	32	kJ/mol		$\Delta\varepsilon$	2.07	-	n/col	5/3
ϑ_{max}		°C		τ_0		s	B	
I_{max}		pA		Q_0		pAs	C	
A_e		kJ/mol		$\Delta\varepsilon$		-	n/col	6/C
ϑ_{max}		°C		τ_0		s	B	
I_{max}		pA		Q_0		pAs	C	
A_e		kJ/mol		$\Delta\varepsilon$		-	n/col	7/D

■ **PVC/TPU/Bio (10/2/5)** 5K/min ↓ 5K/min ↑

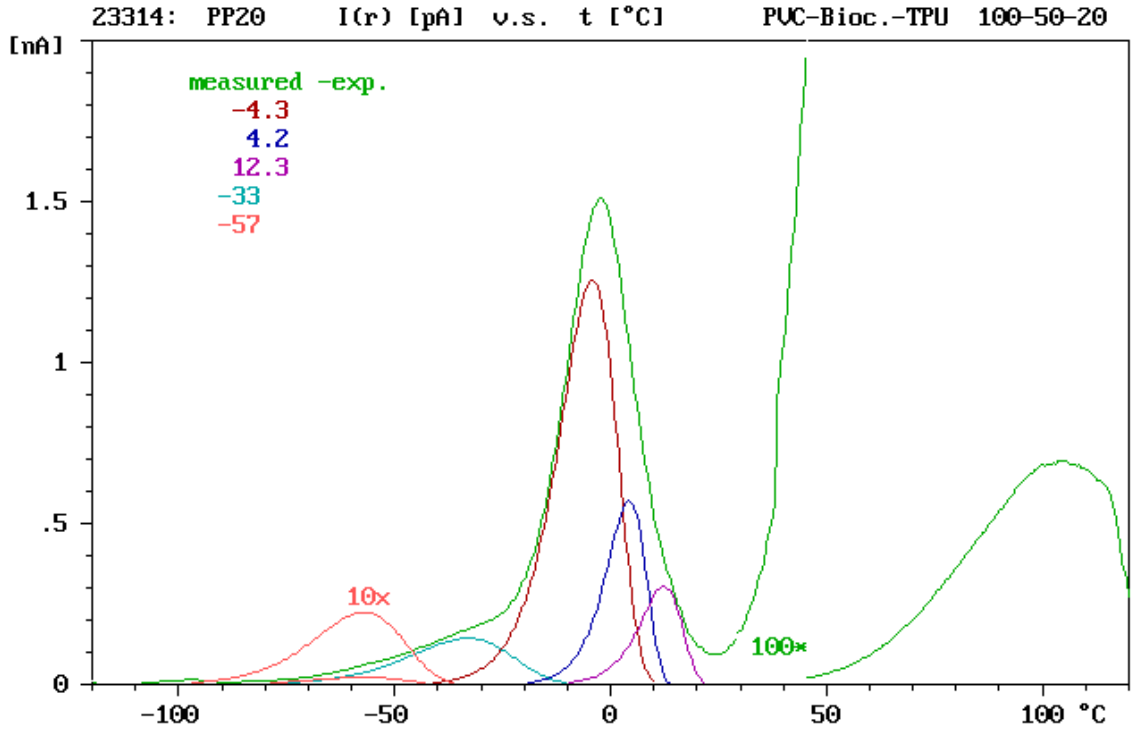

const=	23.576		
A=	32.88958		
B=	-7.652	A_e= 63.6	kJ/mol

ϑ_{max}	-4,.3	°C		τ_0	4.139e-16	s	B	
I_{max}	1256	pA		Q_0	264001	pAs	C	
A_e	158	kJ/mol		$\Delta\varepsilon$	9.94	-	n/col	2/4
ϑ_{max}	4.2	°C		τ_0	3.660e-25	s	B	
I_{max}	570	pA		Q_0	82888	pAs	C	

A_e	139	kJ/mol		$\Delta\varepsilon$	3.1	-	n/col	3/**1**
ϑ_{max}	12.3	°C		τ_0	1.397e-24	s	B	
I_{max}	306	pA		Q_0	46767	pAs	C	
A_e	140	kJ/mol		$\Delta\varepsilon$	1.76	-	n/col	4/**5**
ϑ_{max}	-33	°C		τ_0	4.885e-7	s	B	
I_{max}	143	pA		Q_0	52430	pAs	C	
A_e	39	kJ/mol		$\Delta\varepsilon$	1.97	-	n/col	5/**3**
ϑ_{max}	-57	°C		τ_0	2.856e-7	s	B	
I_{max}	22.5	pA		Q_0	7253	pAs	C	
A_e	36	kJ/mol		$\Delta\varepsilon$	0.27	-	n/col	6/**C**
ϑ_{max}		°C		τ_0		s	B	
I_{max}		pA		Q_0		pAs	C	
A_e		kJ/mol		$\Delta\varepsilon$		-	n/col	7/**D**
ϑ_{max}		°C		τ_0		s	B	
I_{max}		pA		Q_0		pAs	C	
A_e		kJ/mol		$\Delta\varepsilon$		-	n/col	8/**B**

■ **Bio-plasticizer** 5K/min ↓ 5K/min ↑

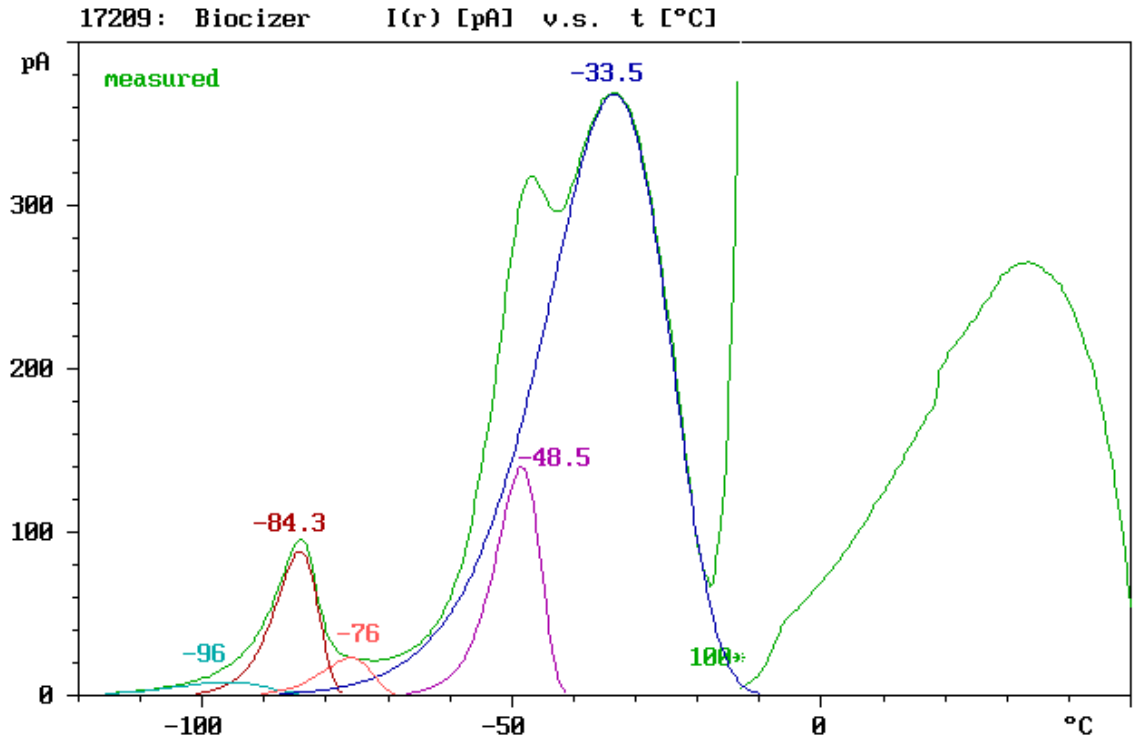

const= 180.723

A=	28.74688		
B=	-5.546991	A_e= 46	kJ/mol

ϑ_{max}	-84.3	°C		τ_0	1.294e-22	s	B	
I_{max}	88	pA		Q_0	9669	pAs	C	
A_e	85	kJ/mol		$\Delta\varepsilon$	0.36	-	n/col	2/**4**
ϑ_{max}	-33.5	°C		τ_0	1.173e-8	s	B	
I_{max}	368	pA		Q_0	115351	pAs	C	
A_e	46	kJ/mol		$\Delta\varepsilon$	4	-	n/col	3/**1**
ϑ_{max}	-48.5	°C		τ_0	1.562e-26	s	B	
I_{max}	140	pA		Q_0	15756	pAs	C	
A_e	118	kJ/mol		$\Delta\varepsilon$	0.59	-	n/col	4/**5**
ϑ_{max}	-96	°C		τ_0	8.693e-9	s	B	
I_{max}	8.3	pA		Q_0	1889	pAs	C	
A_e	34	kJ/mol		$\Delta\varepsilon$	0.071	-	n/col	5/**3**
ϑ_{max}	-76	°C		τ_0	3.090e-20	s	B	
I_{max}	23	pA		Q_0	2915	pAs	C	
A_e	80	kJ/mol		$\Delta\varepsilon$	0.11	-	n/col	6/**C**
ϑ_{max}		°C		τ_0		s	B	
I_{max}		pA		Q_0		pAs	C	
A_e		kJ/mol		$\Delta\varepsilon$		-	n/col	7/ **D**